PARTICLE PRODUCTION AT HIGH ENERGIES

By

AHPISIT UNG-KITCHANUKIT

A thesis presented for the degree of
Doctor of Philosophy
of the University of London

Department of Mathematics,
Royal Holloway College,
Egham, Surrey, TW20 OEX

September, 1976

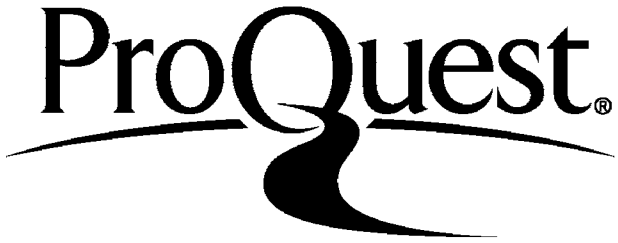

To
the Memories
of
my parents
and
youngest sister

ABSTRACT

An explicit Mueller-Regge model is constructed for the investigations of one-particle-inclusive processes in the fixed-M^2 and triple-Regge region. The model is then applied in the studies of Δ production and vector and tensor meson productions. The inclusive cross sections and density matrices of the decaying produced resonances are considered and compared with the available data. The qualitative behaviour of the cross section data can be approximately accounted for by the model, but the model is not satisfactory in details. By analogy with two-body processes absorption is introduced and the resultant model with cuts is used in the reinvestigations of the data. There is some improvement in the agreement between the model and the data with the introduction of absorption.

PREFACE

The work described in this thesis was carried out under the supervision of Dr. K.J.M. Moriarty in the Department of Mathematics, Royal Holloway College, London University between October, 1972 and September, 1976. Except where stated, the work described is original and has not been submitted to this or any other university for any degree.

The advice, help and encouragement of Dr. K.J.M. Moriarty throughout the author's postgraduate career is most gratefully acknowledged. The author wishes to thank his colleagues J.P. Rad, J.H. Tabor and in particular P. Choudhury for fruitful discussions and collaborations as well as for their friendship.

The help and encouragement of the late Professor S. Tolansky and Emeritus Professor E.H. Hutten during the author's transition from an undergraduate to a postgraduate are much appreciated. The financial support of Royal Holloway College is most gratefully received.

The hospitality of the Physics Department, Imperial College for the D.I.C. course in particle physics during 1972-1973 is much appreciated. The author is most indebted

to Mrs. Rowley and her family for hospitality during his long stay as a student in England. Finally, the author wishes to express his thanks to Mr. C.A. Scott for helping with the preparation of the manuscript and Mrs. S. Murdock for her typing.

CONTENTS

	Page
Abstract	1
Preface	2
Chapter 1 GENERAL INTRODUCTION	6
I. Introduction.	6
II. One Particle Inclusive Reactions.	8
III. The Generalized Optical Theorem.	10
IV. Mueller-Regge Limits and Scaling.	15
References.	21
Chapter 2 A MUELLER-REGGE MODEL	23
I. Introduction.	23
II. Formalism.	24
III. General Characteristics of the Model.	29
IV. A Study of Inclusive Δ Production.	31
V. A Study of Inclusive Vector and Tensor Meson Production in the Triple-Regge Region.	37
VI. Conclusion.	43
Appendix.	45
References.	50
Figures Captions and Figures.	53
Chapter 3 ABSORPTIVE CORRECTIONS IN A MUELLER-REGGE MODEL	65
I. Introduction.	65
II. Formalism.	67
III. Inclusive Vector Meson Production.	71
IV. Inclusive Δ Production.	73
V. Discussion and Conclusions.	75
Appendix.	79
Table of Integrals.	86
References.	88
Figures Captions and Figures.	92

Page

Appendices: 102

I. Notations, Conventions and Normalizations. 102

II. Kinematics and Wave Functions for the Evaluation of the Mueller-Regge Helicity Amplitudes. 107

III. The Vector Structure Functions. 111

IV. Normalization of One Particle Inclusive Cross Section. 114

References. 116

Tables: 117

I. Regge Parameters.

II. Regge Exchanges and Clebsch-Gordan coefficients for $0^- \xrightarrow{P} 1^-$.

III. Regge Exchanges and Clebsch-Gordan coefficients for $0^- \xrightarrow{P} 2^+$.

IV. Regge Exchanges and Clebsch-Gordan coefficients for $1/2^+ \xrightarrow{P} 3/2^+$.

CHAPTER 1

GENERAL INTRODUCTION

I. INTRODUCTION

The past few years have seen a great deal of interest in the study of particle production processes[1]. From the experimental point of view this development may seem only natural since production already accounts for 75-85% of the total cross sections at presently available energies[2]. However, because of the great complexity of multiparticle processes, parallel advances in both experimental and theoretical outlooks have been indispensable in providing the impetus to awaken and sustain this interest.

The adoption of the inclusive approach has been particularly fruitful in the investigation of production processes[3]. Theoretically, the inclusive approach is just a convenient way of extracting selective information from an otherwise unmanageably complicated system. Consequently, inclusive experiments are comparatively simple compared to the multibody exclusive experiments and the collection of data becomes a practical reality[4].

Further stimuli for the interest in production processes were provided by the scaling hypothesis of Feynman[5], and the limiting fragmentation hypothesis of Yang et al[6]. In fact, scaling in production processes had been predicted by AFS[7] in their studies of the multiperipheral model. Finally, the introduction of the generalised optical theorem by Mueller[8] made accessible inclusive reactions to Regge analyses[9] and gave rise to a fast developing inclusive phenomenology [10,11].

In this thesis we present the construction of an explicit Mueller-Regge model for use as a basis of inclusive phenomenology. The model was applied in the studies of inclusive resonance productions as a preliminary test of its suitability for more detailed investigations of the data. Subsequently absorptive corrections were prescribed and the inclusive resonance productions reinvestigated.

II. ONE PARTICLE INCLUSIVE REACTIONS

Inclusive reactions[3] are processes of the type $a+b \longrightarrow c+d+\ldots+n+X$, where c, d, ..., n are the n detected particles and X denotes the summation over all the undetected particles in the final state. For the one particle inclusive reaction $a+b \longrightarrow c+X$ (see Figure a) the inclusive cross section $f(ab \longrightarrow c)$ is given by:

$$f(ab \longrightarrow c) \equiv 2E_c \frac{d^3\sigma}{d^3p_c}(ab \longrightarrow c)$$

$$= \frac{1}{F}\sum_{n=1}^{\infty}\left(\prod_t \frac{1}{n_t!}\right)\int \prod_{i=1}^{n}\frac{d^3p_i}{2E_i}\,\delta^4\left(P_a+P_b-P_c-\sum_i P_i\right)$$

$$\cdot\cdot\left|\langle P_c,P_i,\ldots,P_n|A|P_a,P_b\rangle\right|^2,$$

where F is the initial flux factor given by:

$$F = 2\,\Delta^{\frac{1}{2}}(s,m_a^2,m_b^2)$$

with $\Delta(x,y,z) = x^2+y^2+z^2-2xy-2yz-2xz$ and $\delta^4(x-y) = (2\pi)^4\delta(x-y)$,

$$d^3p = \frac{d^3p}{(2\pi)^3},$$

and finally $\frac{1}{n_t!}$ is the statistical factor for n identical particles of type t.

The one particle inclusive process is a function of three independent invariants. A convenient set is given by:

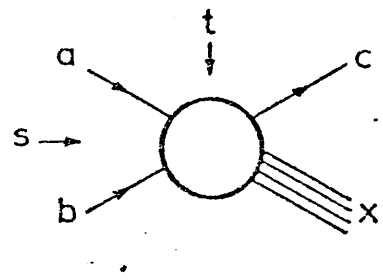

Figure a The one particle inclusive reaction $a+b \longrightarrow c+X$.

$$s = (P_a+P_b)^2,$$

$$t = (P_a-P_b)^2,$$

$$M^2 = (P_a+P_b-P_c)^2.$$

In terms of these invariants the inclusive cross section is given by:

$$2E_c \frac{d^3\sigma}{d^3P_c} \equiv 16\pi^2 \Delta^{\frac{1}{2}}(s,m_a^2,m_b^2) \frac{d^2\sigma}{dtdM^2}.$$

For a given s the physical region of the process in the tM^2 plane is the Chew-Low plot defined by[12]:

$$G(s,t,M^2,m_a^2,m_b^2,m_c^2) \leqslant 0,$$

with $M^2 \geqslant M^2_{min}$, where G is the tetrahedron function given by:

$$\begin{aligned} G(x,y,z,u,v,w) = {} & x^2y + xy^2 + z^2u + zu^2 + v^2w + vw^2 \\ & + xzw + xuv + yzv + yuw \\ & - xy(z+u+v+w) - zu(x+y+v+w) \\ & - vw(x+y+z+u). \end{aligned}$$

The total inclusive cross section is given by:

$$\sigma_{tot}(ab \longrightarrow c) = \frac{1}{F}\sum_{n=1}^{\infty}\frac{1}{n!}\int\frac{d^3p_c}{2E_c}\int\prod_{i=1}^{n}\frac{d^3p_i}{2E_i}\,\delta_4(P_a+P_b-P_c-\sum_i P_i)$$

$$\cdot|\langle P_c,P_i,\ldots,P_n|A|P_a,P_b\rangle|^2,$$

where for simplicity we are considering only one type of particle. Comparing this with the total cross section $\sigma_{tot}(ab)$ we can see that a factor $(n+1)^{-1}$ is missing in the final phase space for the total inclusive cross section. In fact, $\sigma_{tot}(ab\longrightarrow c)$ gives a measure of the average number of identical particles of type c in the final state ,

$$\sigma_{tot}(ab\longrightarrow c) = \langle m\rangle\ \sigma_{tot}(ab).$$

III. THE GENERALIZED OPTICAL THEOREM

The generalized optical theorem of Mueller's[8] relates the inclusive cross section to the forward discontinuity in M^2 of the $3 \longrightarrow 3$ amplitude (see Figure b).

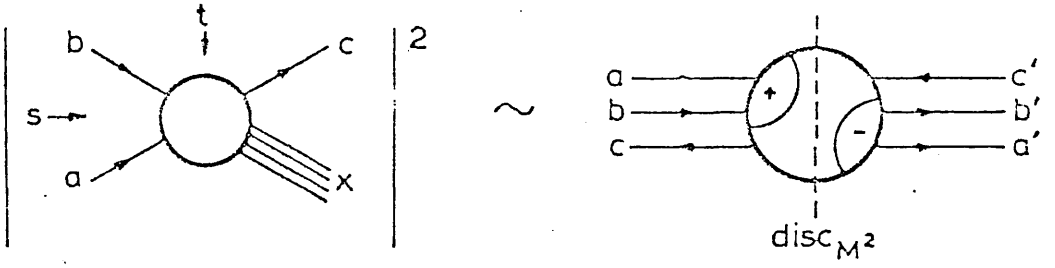

Figure b The Mueller optical theorem.

The Mueller theorem can be expressed in the form,

$$f(ab\longrightarrow c) \sim \underset{M^2}{\text{disc}} \langle a'b'\bar{c}'|A|ab\bar{c}\rangle$$

with $P_a=P_{a'}$, $P_b=P_{b'}$ and $P_{\bar{c}} = P_{\bar{c}'}$. The required six-particle amplitude in the Mueller theorem is in fact not the physical $3\longrightarrow 3$ amplitude but one that has been analytically continued so that the subenergy invariants s_{ab} and $s_{a'b'}$ are above and below their respective cuts[13] ($s_{ab} = s+i\varepsilon$ and $s_{a'b'} = s-i\varepsilon$) as illustrated in Figure b. Writing the $3\longrightarrow 3$ amplitude with the subenergy dependence explicitly shown we have:

$$\underset{M^2}{\text{disc}}\, A(\text{physical } 3\longrightarrow 3) = \underset{M^2}{\text{disc}}\, A(s+i\varepsilon, M^2, s+i\varepsilon),$$

whereas for the Mueller amplitude we require

$$\underset{M^2}{\text{disc}}\, A(s-i\varepsilon, M^2, s+i\varepsilon).$$

For the consideration of spin effects in inclusive processes the incorporation of helicity dependence into the generalized optical theorem is required. This is achieved through the use of the six-particle helicity amplitudes with the freedom of having different final and initial helicities[14]. The Mueller theorem then takes the form:

$$\langle \lambda_a', \lambda_b' | A^+ | \lambda_c', K\rangle \langle \lambda_c, K | A | \lambda_a, \lambda_b\rangle \sim$$

$$\underset{M^2}{\text{disc}} \langle \lambda_a', \lambda_b', \lambda_{\bar{c}}' | A | \lambda_a, \lambda_b, \lambda_{\bar{c}}\rangle ,$$

where λ_i are the helicities of particle i (i = a,b,c) and K denotes the summation of the helicities of the missing mass X.

We now consider the constraints imposed on the Mueller amplitudes by parity and time reversal[15] invariance. The parity relation for the Mueller amplitudes is given by:

$$\text{disc}_{M^2}\langle\lambda_a,\lambda_b,\lambda_{\bar{c}}|A|\lambda_a',\lambda_b',\lambda_{\bar{c}}'\rangle =$$

$$(-1)^{(\lambda_a-\lambda_a')+(\lambda_b-\lambda_b')+(\lambda_c-\lambda_c')}$$

$$\text{disc}_{M^2}\langle-\lambda_a,-\lambda_b,-\lambda_{\bar{c}}|A|-\lambda_a',-\lambda_b',-\lambda_{\bar{c}}'\rangle$$

The above expression can be obtained by considering the parity relation for the pseudo-two-body amplitude

$$\langle-\lambda_c,-K|A(-\phi_j)|-\lambda_a,-\lambda_b\rangle =$$

$$\frac{\eta_c\eta_x}{\eta_a\eta_b}(-1)^{S_c+S_x-S_a-S_b+(K-\lambda_c)-(\lambda_a-\lambda_b)}\langle\lambda_c,K|A(\phi_j)|\lambda_a,\lambda_b\rangle$$

where S denotes the spins of the particles and ϕ_j are the angles of the momenta in the composite state X. After taking the appropriate bilinear combinations of the pseudo-two-body amplitudes and integrating over all ϕ_j we can apply the Mueller theorem to obtain the parity relation for the Mueller amplitudes.

On applying time reversal to the Mueller amplitude we find that the time reversed Mueller amplitude is not a Mueller amplitude. This can be seen through the relation

$$T\,\mathrm{disc}_{M^2} A(s_{a'b'}(-), M^2, s_{ab}(+)) = e^{i\psi}\,\mathrm{disc}_{M^2} A(s_{ab}(+), M^2, s_{a'b'}(-1))$$

where T is the time reversal operator, ψ is the phase factor and (+),(-) refer to the $\pm i\varepsilon$ prescription. (See also Figure c.)

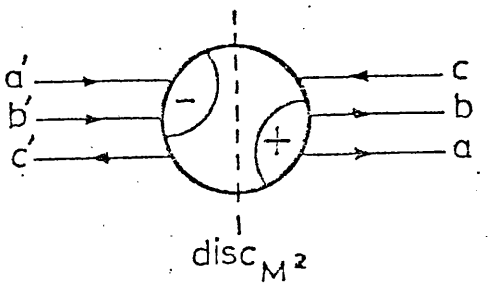

Figure c The time reversed Mueller amplitude.

The difficulty with time reversal invariance of the Mueller amplitudes is due to the fact that these are not the physical 3⟶3 amplitudes. The boundary conditions of the Mueller amplitudes (which are reached through a particular analytic continuation of the 3→3 amplitudes) are violated under time reversal. However, the Mueller amplitudes satisfy the Hermiticity condition[15]:

$$\langle \lambda_a', \lambda_b', \lambda_c' | A | \lambda_a, \lambda_b, \lambda_c \rangle = \langle \lambda_a, \lambda_b, \lambda_c | A^+ | \lambda_a', \lambda_b', \lambda_c' \rangle^*.$$

This can be seen by writing the Hermiticity of the Mueller amplitudes showing the subenergy dependence:

$$A(s_{a'b'}(-),M^2,s_{ab}(+)) = A^*(s_{ab}(-),M^2,s_{a'b'}(+)),$$

this relation is diagrammatically presented in Figure d.

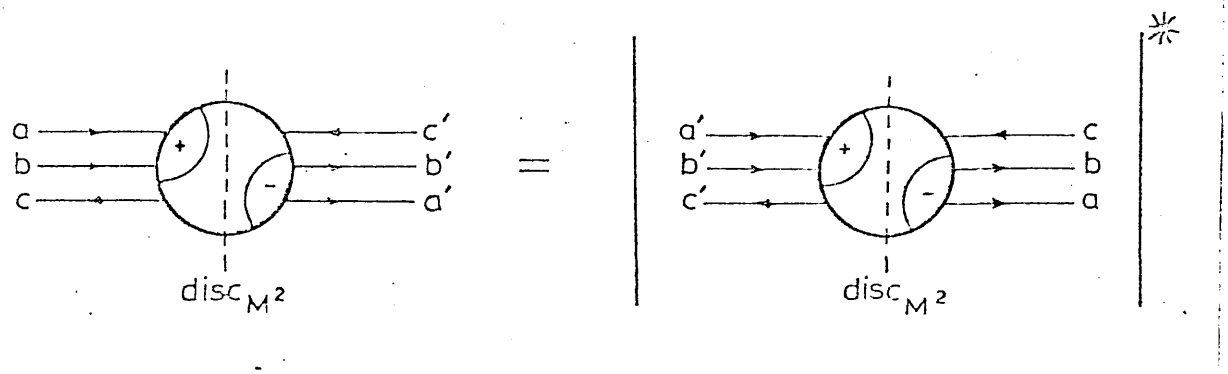

Figure d Hermiticity of the Mueller amplitudes.

The number of Mueller helicity amplitudes is given by $N_a^2 \times N_b^2 \times N_c^2$ where $N_i = 2S_i+1$ are the number of the helicity states of the particles. Parity invariance reduces the number of amplitudes by half, and in contrast to the two-body case no further constraint is gained from time reversal invariance (as discussed above). However, Hermiticity further reduces the number of amplitudes by a factor of two. The number of independent Mueller amplitudes is then:

$$\tfrac{1}{4} N_a^2 \times N_b^2 \times N_c^2.$$

The inclusive cross section in terms of the Mueller helicity amplitudes is given by

$$f(ab \longrightarrow c) \sim \sum_{\lambda_a,\lambda_b,\lambda_{\bar{c}}} \text{disc}_{M^2} < \lambda_a,\lambda_b,\lambda_{\bar{c}} |A| \lambda_a,\lambda_b,\lambda_{\bar{c}} >$$

and the density matrix element of the detected particle is :

$$\rho^{\lambda_c',\lambda_c} = \frac{\sum_{\lambda_a,\lambda_b} \text{disc}_{M^2} \langle \lambda_a,\lambda_b,\lambda_c' |A| \lambda_a,\lambda_b,\lambda_c \rangle}{\sum_{\lambda_a,\lambda_b,\lambda_c} \text{disc}_{M^2} \langle \lambda_a,\lambda_b,\lambda_c |A| \lambda_a,\lambda_b,\lambda_c \rangle}$$

Finally, from parity invariance we obtain the relation

$$\rho^{mm'} = (-1)^{m-m'} \rho^{-m-m'}.$$

IV. MUELLER-REGGE LIMITS AND SCALING

With the introduction of the Mueller theorem Regge analyses of inclusive processes become viable. The six-particle amplitudes can be partial wave analyzed in the appropriate channels and the Regge limits established[16,17].

For the purposes of Mueller-Regge analyses it is convenient to distinguish three regions of phase space:

(i) The beam fragmentation region:

For the beam fragmentation region the square of the 4-momentum transfer between the beam particle and the produced particle, t, is fixed and finite. The Feynman variable x defined by

$$x = \frac{p_{\parallel}}{\sqrt{s}} \sim 1 - \frac{M^2}{s},$$

where $p_{\parallel}$ is the cm. longitudinal momentum of the produced particle, is a convenient variable in this region.

The fragmentation region gives rise to three Regge limits. Moving inwards from the edge of the phase space where $x \sim 1$ we have:

(a) The fixed-M^2 limit where t and M^2 are fixed and small, and $\frac{s}{M^2} \longrightarrow \infty$,

(b) The triple-Regge limit where t is fixed and small, and $\frac{s}{M^2} \longrightarrow \infty$ and $M^2 \longrightarrow \infty$,

(c) The single-Regge limit where t and $\frac{s}{M^2}$ are fixed and finite. Note that sometimes in the literature the fragmentation region refers specifically to the single-Regge limit.

The corresponding Mueller-Regge diagrams for the above limits are shown in Figure e.

(ii) The target fragmentation region:

The target fragmentation region is simply the other end of the phase space where the momentum transfer squared between the target particle and the produced particle, u, is fixed and finite. The discussion for the

beam fragmentation region applies here with the change $t \longrightarrow u$ and $x \longrightarrow -x$.

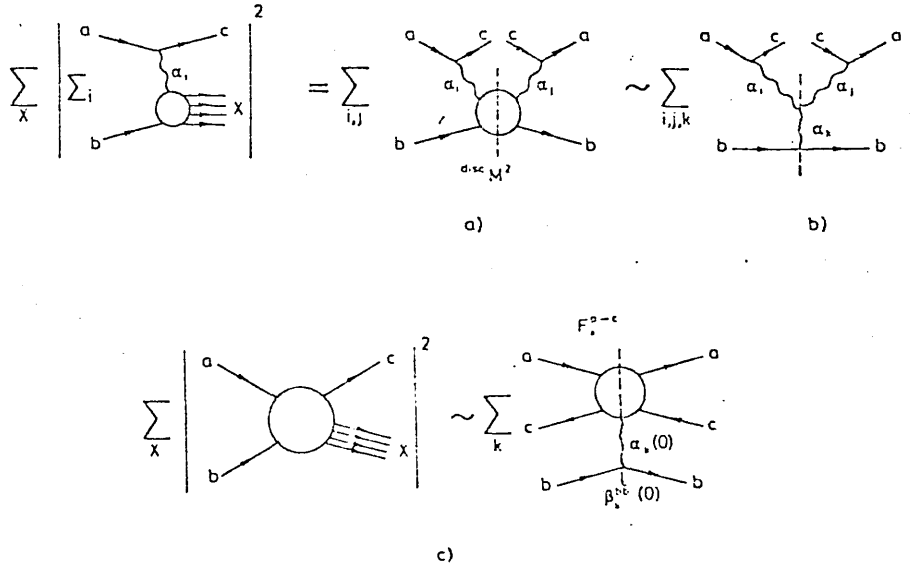

Figure e Regge limits of $a+b \longrightarrow c+X$ for: a) fixed-M^2, b) $s \gg M^2 \gg 1$ (triple-Regge), and c) fixed $\frac{s}{M^2}$ (single-Regge).

(iii) The central region or the double-Regge limit:

As its name implies, the central region is in the centre of phase space where $x \sim 0$ and $tu \sim s$ with $\frac{tu}{s}$ fixed and finite, where u is given by $u = (P_b - P_c)^2$. The rapidity variable defined by

$$y = \tfrac{1}{2} \ln \left(\frac{E+p_{''}}{E-p_{''}} \right)$$

is a convenient variable for use in this region. The corresponding Mueller-Regge diagram for this region is given in Figure f.

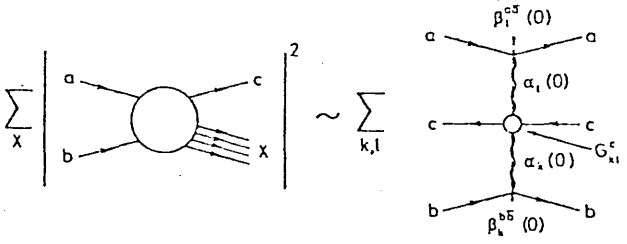

Figure f Double-Regge limit for a+b⟶c+X in the central region.

The division of the phase space can be conveniently displayed in the rapidity space and is shown in Figure g below.

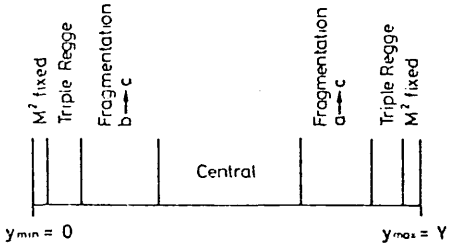

Figure g Phase space regions in rapidity for a+b⟶c+X.

The asymptotic behaviours of the single particle inclusive cross sections are governed by the above Mueller-Regge limits. In the fragmentation region the inclusive cross sections are given by:

i) In the fixed-M^2 and triple-Regge limit (Figure e):

$$f(a\xrightarrow{b}c)\sim \frac{1}{s}\sum_{i,j}\beta_i^{\bar{ac}}(t)(s)^{\alpha_i(t)+\alpha_j(t)}\beta_j^{\bar{ac}}(t)f^{ib\to jb}(M^2,t),$$

where β denotes the Reggeon-particle-particle coupling, α denotes the Regge trajectory functions, and $f^{ib\to jb}(M^2,t)$ is the forward Reggeon-particle scattering amplitude.

$$f^{ib\to jb}(M^2,t) \underset{M^2\to\infty}{\sim} \sum_k \beta_k^{b\bar{b}}(0)(M^2)^{\alpha_k(0)-\alpha_i(t)-\alpha_j(t)} g_{ijk}(t,t,0)$$

gives the asymptotic form of $f^{ib\to jb}$ with g_{ijk} denoting the triple-Regge coupling.

ii) In the single-Regge limit (Figure e)

$$f(a\xrightarrow{b}c)\sim \frac{1}{s}\sum_k \beta_k^{b\bar{b}}(0)(M^2)^{\alpha_k(0)} F_k^{a\to c}(x,t)$$

where $F_k^{a\to c}$ is the coupling of the Reggeon k to the 4-particle $(a\bar{c}\text{-}a\bar{c})$ system.

For the central region, the relevant Mueller-Regge limit is the double-Regge limit (Figure f) and the inclusive cross section is given by:

$$f(a|c|b)\sim \frac{1}{s}\sum_{k,\ell} \beta_\ell^{a\bar{a}}(0)(t)^{\alpha_\ell(0)} G_{\ell k}^{c}(\tfrac{ut}{s})(u)^{\alpha_k(0)} \beta_k^{b\bar{b}}(0)$$

where $G_{\ell k}^{c}(\frac{ut}{s})$ is the coupling of the Reggeons ℓ,k to $c\bar{c}$.

The leading asymptotic behaviours of the inclusive cross sections are provided by the Pomeron exchange with an intercept of unity $\alpha_p(0) = 1$. Then the leading behaviours of the inclusive cross sections are given by:

$$f(a\xrightarrow{b}c)(s,x,t) \longrightarrow f(a\xrightarrow{b}c)(x,t) \qquad (A)$$

for the fragmentation region and

$$f(a|c|b)(s,t,u) \longrightarrow f(a|c|b)(\frac{ut}{s}) \qquad (B)$$

for the central region. The expressions (A) and (B) are simply statements of Feynman scaling[5] of the inclusive cross sections. (A) is also a statement of limiting fragmentation[6] and it is seen that the limiting fragmentation hypothesis and Feynman scaling postulate are equivalent in the fragmentation region. Noting that for the double-Regge limit $\frac{ut}{s}$ is fixed and finite and can be written

$$\frac{ut}{s} = m_c^2 + p_{c_\perp}^2$$

it is seen that Feynman scaling in the central region given by (B) is simply the AFS scaling[7].

The next-to-leading contributions given by the intercept-half meson trajectories provide the scaling breaking terms and control the approach to scaling.

REFERENCES

1. For a review of multiparticle production see, e.g.
   L. Van Hove, Phys. Reports, 1C, 347 (1971);
   D. Horn, Phys. Reports, 4C, 1 (1972);
   W.R. Fraser et al., Rev. Mod. Phys., 44, 284 (1972).

2. G. Giacomelli, Phys. Reports, 23C, 123 (1976).

3. For a review of inclusive approach see, e.g.
   S. Humble, Introduction to Particle Production in Hadron Physics, Academic Press (1974).

4. For a review of inclusive data see, e.g.
   K. Zalewski, I-93, Proc. 17th Int. Conf. on High Energy Physics, London (1974), Ed. J.R. Smith;
   J. Whitmore, Phys. Reports, 10C, 273 (1974);
   R. Stroynowski, 67, Proc. 6th Int. Colloq. on Multiparticle Reactions, Oxford (1975), Rutherford Preprint RL 75-143;
   G. Giacomelli, A.F. Greene and J.R. Sandford, Phys. Reports, 19C, 169 (1975).

5. R.P. Feynman, Phys. Rev. Letters, 23, 1415 (1969).

6. J. Benecke, T.T. Chou, C.N. Yang and E. Yen, Phys. Rev., 188, 2159 (1969).

7. D. Amati, A. Stanghellini and S. Fubini, Nuovo Cimento, 26, 896 (1962).

8. A.H. Mueller, Phys. Rev., D2, 2963 (1970).

9. P.D.B. Collins and E.J. Squires, Regge poles in particle physics (Springer, Berlin, 1968).

10. H.M. Chan, C.S. Hsue, C. Quigg and J.M. Wong, Phys. Rev. Lett., 26, 672 (1971).

11. For a review see, e.g.
   R. Slansky, Phys. Reports, 11C, 99 (1974);
   R.G. Roberts, 201, Proc. 14th Scottish Summer School (1973);
   R.L. Crawford and R. Jennings, Academic Press (1974).

12. E. Byckling and K. Kajantie, Particle Kinematics, John Wiley and Son (1973).

13. C.I. Tan, Phys. Rev., D4, 2412 (1972);

K.E. Cahill and H.P. Stapp, Phys. Rev., D6, 1007 (1972);

J.C. Polkinghorne, Nuovo Cimento, 7A, 555 (1972).

14. H.D.I. Abarbanel and D.J. Gross, Phys. Rev. Letters, 26, 732 (1971);

G.A. Ringland, R.J.N. Phillips and R. Worden, Phys. Letters, 408, 239 (1972),

15. J.P. Ader, C. Meyers and Ph. Salin, Nucl. Phys., B47, 397 (1972); Nucl. Phys., B82, 237 (1974);

J. Randa and A Donnachie, Nucl. Phys., B109, 495 (1976).

16. For a review see, e.g.

J.E. Young, Rivista del Nuovo Cim., 2, 88 (1972);

R.C. Brower, C.E. De Tar and J.H. Weis, Phys. Reports, 14C, 257 (1974).

17. H.D.I. Abarbanel and A. Schwimmer, Phys. Rev., D6, 3018 (1972);

C.E. De Tar and J.H. Weis, Phys. Rev., D4, 3141 (1971);

C.E. Jones, F.E. Low and J.E. Young, Phys. Rev., D4, 2358 (1971);

P. Goddard and A.R. White, Nuovo Cimento, 1A, 645 (1971);

N.S. Craigie and G. Kramer, Nucl. Phys., B82, 69 (1974).

CHAPTER 2

A MUELLER-REGGE MODEL

I. INTRODUCTION

A Mueller-Regge model has been developed for the studies of one particle inclusive processes in the fixed-M^2 and triple-Regge regions. Basically the model is a triple Regge model with the assumption of duality for the M^2- channel.

The model has been developed to exploit the apparatus of Regge phenomenology in one particle inclusive reactions. The advent of the Mueller optical theorem[1] has made accessible inclusive reactions to Regge analyses and given birth to several Mueller-Regge models[2]. Utilizing the Regge parameters derived from a Regge model[3] which has met with reasonable successes in exclusive processes, a Mueller-Regge model has evolved. The couplings required for the evaluation of the Mueller-Regge diagrams are determined from the relevant decay widths and symmetries. Finally, the forward M^2-discontinuity of the Reggeon-particle amplitude is related to the corresponding particle-particle cross section allowing for the off-mass shell effect. The resultant model is then essentially parameter-free with all input clearly specified.

II. FORMALISM

The one particle inclusive cross section in the kinematic region of our interest (fixed-M^2 and triple-Regge region) is related, through the Mueller optical theorem, to the Mueller-Regge diagram of Fig. a.

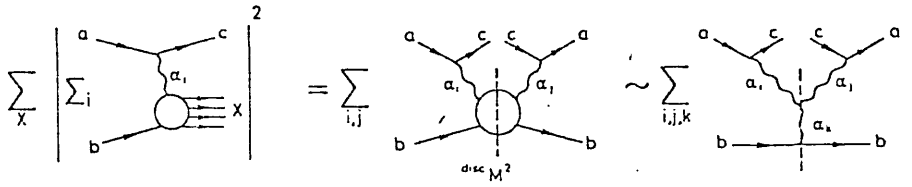

Fig. a The Mueller-Regge diagram in the fixed-M^2 and triple-Regge regions.

The Mueller-Regge amplitudes corresponding to the diagram are given by:

$$H^{\lambda_c'\lambda_b'\lambda_a'}_{\lambda_c\lambda_b\lambda_a} = \sum_{\mathcal{R}} J_5^{\lambda_c\lambda_a} \Delta\Gamma_5^{\lambda_b\mathcal{R}} (J_5^{\lambda_c'\lambda_a'} \Delta\Gamma_5^{\lambda_b'\mathcal{R}})^+,$$

for pseudoscalar exchange, and

$$H^{\lambda_c'\lambda_b'\lambda_a'}_{\lambda_c\lambda_b\lambda_a} = \sum_{\mathcal{R}} J^{\lambda_c\lambda_a} \Delta_{\mu\nu} \Gamma_\nu^{\lambda_b\mathcal{R}} (J_{\mu'}^{\lambda_c'\lambda_a'} \Delta_{\mu'\nu'} P_{\nu'}^{\lambda_b'\mathcal{R}})^+,$$

for vector exchanges, where J is the current at the particle-particle-Reggeon vertex (a,c,R). Δ and Γ are, respectively, the Reggeized propagator and structure function at the inclusive vertex.

For boson exchange processes the Reggeized propagators are obtained through the replacement[3]:

$$\frac{1}{t-m^2} \longrightarrow \alpha' \frac{(1+\xi \exp - i\pi\alpha(t))}{2} \Gamma[f(t)] \left(\frac{s}{M^2}\right)^{\alpha(t)-J}$$

where conventional Regge notations have been adopted, J is the spin of the exchange and $\Gamma[f(t)]$ is the Euler gamma function given by:

$$\Gamma[f(t)] = \begin{cases} -\Gamma(-\alpha(t)) & \text{for unnatural parity exchange,} \\ \Gamma(1-\alpha(t)) & \text{for natural parity exchange.} \end{cases}$$

Strong exchange degeneracy is assumed for the particle pairs π-B, ρ-A_2 and w-f and the Regge trajectories are determined from the requirement that they pass through the appropriate particles on the Chew-Frautschi plot. The trajectories are presented in Table I.

The couplings of a strong exchange degenerate pair are identical and to the leading order the Reggeized higher spin exchange amplitudes are given by those of the lower spin with appropriate changes in the signature[3].

The currents, J, are standard field theoretic currents[4] with all the particles a, c, R put on their mass shells. They are given for the various processes under investigation.

The structure functions Γ are related to the forward Reggeon-particle scattering amplitudes in the M^2-

channel. For the pseudoscalar case we have:

$$\sum_{\lambda_b,\mathcal{N}}^{-} \Gamma_s^{\lambda_b \mathcal{N}} (\Gamma_s^{\lambda_b \mathcal{N}})^* = \text{disc}_{M^2} A(\pi b)$$

$$= 2\,\Delta^{\frac{1}{2}}(M^2, t, m_b^2)\,\sigma_{tot}(\pi b).$$

The vector structure functions are more complicated but we adopt the form[5]:

$$\sum_{\lambda_b,\mathcal{N}}^{-} \Gamma_V^{\lambda_b \mathcal{N}} (\Gamma_{V'}^{\lambda_b \mathcal{N}})^* = (P_b)_V\,(P_b)_{V'}\,V,$$

where: $V = \frac{8m_v^2}{M^2}\,\sigma_{tot}(vb)$,

with v denoting the exchange vector meson. The form of the vector structure functions is discussed in Appendix III.

With the assumption of two-component duality in the M^2-channel[6], the Regge-particle cross section in the kinematic region of interest assumes the Regge form:

$$\sigma_{tot}(Rb) \sim A + \frac{B}{M}$$

The criterion for exoticity of Chan et al.[7] is adopted so that when Rb is exotic, only the M independent term in $\sigma_{tot}(Rb)$ arising from the pomeron contribution is retained, giving:

$$\sigma_{tot}(Rb) \sim A \qquad \text{for exotic Rb.}$$

The physical πp cross section is adopted for the

Rp cross section when R is a π-Reggeon; due to the small mass of the π this assumption is reasonable. However, when R is a ρ-Reggeon, a t dependence is introduced for off-mass-shell scattering[8]. The required cross sections are:

$$\sigma_{tot}(\pi p) = 23.4 + \frac{8.3}{M} \quad (9) \quad \text{mb},$$

for pseudoscalar exchange, and:

$$\sigma_{tot}(\rho p) = 0.27(98.6 + \frac{64.9}{M}) \frac{0.65}{(1 - \frac{t}{m_\rho^2})^2} \quad (10) \quad \text{mb},$$

for vector exchanges.

In the case where particle b is a meson M we invoke simple quark counting rules[11] to obtain $\sigma_{tot}(RM)$ from $\sigma_{tot}(Rp)$ through the relation:

$$\sigma_{tot}(RM) = \frac{2}{3} \sigma_{tot}(Rp)$$

In the inclusive production of resonances, the most readily accessible measurables are the inclusive cross sections and the decay density matrices of the produced resonances. The averaging and summing over helicities λ_a, λ_b are required, giving:

$$\frac{1}{2S_a+1} H^{\lambda_c'\lambda_c} = \frac{1}{2S_a+1} \sum_{\lambda_a} H^{\lambda_c'\lambda_a}_{\lambda_c\lambda_a}$$

where $H^{\lambda_c'\lambda_a'}_{\lambda_c\lambda_a}$ is the Mueller-Regge amplitude after the summing and averaging over λ_b', λ_b in the structure functions.

The inclusive cross section is given by:

$$\frac{s}{\pi}\frac{d^2\sigma}{dtdM^2} = \frac{1}{64\pi^2 k^2}\frac{1}{2S_a+1}\sum_{i,\lambda_c} H^{\lambda_c\lambda_c}$$

where the summation over i implies the summation over all possible exchanges, and k is the initial state c.m. 3-momentum. For the normalization of the inclusive cross section see Appendix IV.

The density matrix elements of the produced resonance c are given by[12]:

$$\rho^{\lambda_c'\lambda_c}_{c.m.} = \frac{\sum_i H^{\lambda_c'\lambda_c}}{\sum_{i,\lambda_c} H^{\lambda_c\lambda_c}}$$

Since we have evaluated the Mueller-Regge amplitudes in the centre of mass frame to obtain the density matrix elements in the Gottfried-Jackson frame we require a Wigner rotation, giving:

$$\rho^{\mu'\mu}_{G.J.} = \sum_{\lambda_c',\lambda_c} d^{J_c}_{\mu'\lambda_c'}(\chi)\,\rho^{\lambda_c'\lambda_c}_{c.m.}\,d^{J_c}_{\mu\lambda_c}(\chi)$$

Here χ is the angle between the directions of particle a and the M^2 cluster, as seen in the rest frame of particle c and is given by:

$$\tan\chi = \frac{m_c\, k \sin\theta}{E_c\, k\cos\theta - E_a\, q}$$

III. GENERAL CHARACTERISTICS OF THE MODEL

The Mueller-Regge model outlined above, apart from being essentially parameter-free, exhibits the general desirable features of Mueller-Regge type models[13] such as Feynman scaling[14] and factorization.

The inclusive cross section for $a+b \longrightarrow c+X$ in the present kinematic region is notated $f(a \xrightarrow{b} c)(s,M^2,t)$ and behaves like

$$f(a \xrightarrow{b} c)(s, M^2, t) \sim \frac{1}{s} H(s, M^2, t)$$

where the factor $\frac{1}{s}$ derives from the initial flux factor and H is the Mueller-Regge amplitude after summation of all the helicities:

$$H = \sum_{\lambda_c,\lambda_b,\lambda_a} H^{\lambda_c\lambda_b\lambda_a}_{\lambda_c\lambda_b\lambda_a}$$

To consider the s and M^2 dependence of H we discuss the pseudoscalar and vector exchanges separately.

(a) Pseudoscalar exchange

The Reggeized propagators give a factor of $(\frac{s}{M^2})^{2\alpha(t)}$ and from the discontinuity of the forward Reggeon-particle amplitude in the M^2-channel we obtain a factor $M^2\,\sigma_{tot}(Rb)$.

(b) Vector exchange

Here the s and M^2 dependence of H are given by three terms. The Reggeized propagators contribute the term $(\frac{s}{M^2})^{2\alpha(t)-2}$, the contraction of the currents to the vector structure functions give a factor s^2 and the structure function V gives a term $\frac{1}{M^2}\sigma_{tot}(Rb)$.

From (a) and (b) it can be seen that for both pseudoscalar and vector exchanges the inclusive cross section behaves like:

$$f(a \xrightarrow{b} c)(s, M^2, t) \sim (\frac{s}{M^2})^{2\alpha(t)-1} \sigma_{tot}(Rb)$$

The Reggeon-particle cross-section behaves like:

$$\sigma_{tot}(Rb) \sim A + \frac{B}{M}$$

and for large M^2 we obtain Feynman scaling for the inclusive cross section,

$$f(a \xrightarrow{b} c)(s, M^2, t) \longrightarrow f(a \xrightarrow{b} c)(\frac{s}{M^2}, t).$$

For the case of exotic Rb channel no M dependence is expected for $\sigma_{tot}(Rb)$ and early scaling is obtained. This criterion for early scaling is essentially that given by Chan et al.[7].

The model is factorizable and using this property we obtain:

$$\frac{f(a \xrightarrow{b} c)(s, M^2, t)}{f(a \xrightarrow{d} c)(s, M^2, t)} \simeq \frac{\sigma_{tot}(Rb)(M^2)}{\sigma_{tot}(Rd)(M^2)}$$

where we have factorized out the common particle-particle-Reggeon vertices, a-c-R. This relation holds when there is only one exchange R. However, in the case where several exchanges contribute to the process the above relation is a good approximation provided R is the dominant contribution in the region of our interest.

Further, factorization implies that for large M^2 $\frac{f(a \xrightarrow{b} c)}{\sigma^{\infty}_{tot}(ab)}$ is independent of b[15], where $\sigma^{\infty}_{tot}(ab)$ is the high energy cross section for ab scattering. The result follows from the factorization of the pomeron-b-b vertex at large scattering energy for $\sigma_{tot}(Rb)$ and $\sigma_{tot}(ab)$.

IV. A STUDY OF INCLUSIVE Δ PRODUCTION

The model is applied to study the inclusive production of $\Delta(1236)$ resonance. In this process most of the Δ's are produced in the fixed-M^2 and triple-Regge subspace of the target fragmentation region. The relevant Mueller-Regge diagram is shown in Fig. b on the following page.

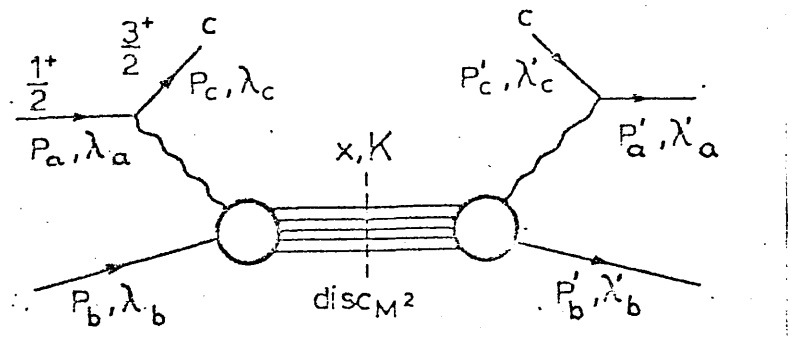

Fig. b The Mueller-Regge diagram for Δ production.

The currents at the particle-particle-Reggeon vertex, $(a(\frac{1}{2}^+)) - c(\frac{3}{2}^+) - R)$, are, respectively, for pseudo-scalar exchange:

$$J_5^{\lambda_c \lambda_a} = \frac{g}{m_B} G\, Q_\eta \bar{\chi}_\eta(P_c, \lambda_c)\, u(P_a, \lambda_a)$$

and for vector exchange

$$J_\mu^{\lambda_c \lambda_a} = -\frac{g}{2m_B^2} G\, \varepsilon_{\mu\nu k\eta}\, P_\nu\, Q_k\, \bar{\chi}_\eta(P_c, \lambda_c)\, u(P_a, \lambda_a)$$

The notations are such that χ_η and u denote, respectively, the spin $\frac{3}{2}$ and spin $\frac{1}{2}$ wave functions, P and Q are, respectively, the sum and difference of the incoming and outgoing 4-momenta of the external particles a and c at the vertex, $\varepsilon_{\mu\nu k\eta}$ is the antisymmetric Levi-Civita tensor, m_B is the average of the a and c masses. The coupling g is obtained from the $\Delta \longrightarrow \pi p$ decay width[16] and G is the appropriate Clebsch-Gordan coefficient.

With the above currents, the required Mueller-Regge amplitudes are evaluated and given in Section (iii)

of the Appendix. The Regge exchanges contributing to the process, together with the values of the Clebsch-Gordan coefficients, are given in Table IV.

Discussion and Results:

For the inclusive production of Δ in the target fragmentation end of the phase space we can exploit the availability of a variety of beam particles. Experiments can be performed utilizing the different beams and through a suitable series of beams the concepts of factorization and M^2 - duality with the question of exoticity can be investigated. The phenomenological importance of such data together with the comparative ease with which the Δ is produced have resulted in several reports of the process in the last few years [17-25]. The emerging picture, as indicated by the data, tends to support the qualitative validity of the triple-Regge model at least as far as the inclusive cross section is concerned.

The Regge exchanges contributing to the inclusive production of Δ are the unnatural parity exchange, π, and the natural parity exchanges, ρ and A_2. The results of the model calculations are presented in Figures 1-5 together with the corresponding data. For the inclusive cross

sections (Figures 1-4) the separate contributions from the different naturality exchanges are shown together with their total contribution. Note that the theoretical curves have been normalized by a factor of 1/6 for the pion and kaon beams (Figures 1, 2) and a factor of 1/8 for the antiproton and proton beams (Figures 3, 4).

The general features of the data[17-19] (Figures 1-3) are the sharp kinematic cut offs in M^2/s and the pronounced resonance structures at small M^2. However, in Figure 2 for the K^- and π^- beams [18] (where the M^2 channel is exotic) the absence of resonance structure is very noticeable. Qualitatively it can be seen in Figures 1-3 that the model gives a reasonable account of the data. The predominance of the unnatural parity exchange, π, is predicted by the model for small values of $|t|$.

Factorization is already hinted at by the data. For a factorizable system the structures in the inclusive cross sections can be understood as due to the Rb scattering at small M^2. The absence of structures for exotic Rb affirms this view. Further confirmation is provided in Figure 3c where the physical $\pi^+ p$ cross sections[26] at the various M^2 values corresponding to those in the M^2-channel of the Rb scattering have been used in the calculation of

the $p \xrightarrow{\bar{p}} \Delta^{++}$ cross section. The structures of the inclusive cross sections are clearly reproduced. Note that we also adopted the $\pi^+ p$ cross section for the vector structure function in this particular calculation but it is not a really crucial point since the π is the dominant exchange. From this investigation it seems that the structures of the Reggeon-particle cross section are similar to those of the corresponding particle-particle cross section for the Reggeized pion.

For the test of factorization we consider the relation:

$$\frac{f(a \xrightarrow{b} c)(s, M^2, t)}{\sigma_{tot}(Rb)\,(M^2)}$$

If factorization holds, then this ratio should be independent of the particle b. For the present process the available data satisfy this condition with $\sigma(Rb)$ approximated by $\sigma(\pi b)$. The asymptotic condition

$$\frac{f(a \xrightarrow{b} c)}{\sigma^{\infty}_{tot}(pb)}$$

independent of b is not yet satisfied by the available data[25] except for the cases where $ab\bar{c}$ is exotic[18]. It has been reported that the suppression of the inclusive cross section for the K^- and π^- beams (exotic M^2-channel)

relative to the cross section for the K^+ and π^+ are of the order of 3[27]. This factor can be understood from the experimental data for the ratio of $K^-\pi^-$ and $K^+\pi^-$ cross sections[28]. It is precisely $\frac{1}{3}$ in the energy range corresponding to the M^2 range of the above inclusive processes.

The data for the proton beams at various energies in the FNAL range show Feynman scaling[24]. However, experiments with pion and kaon beams are still at too low an energy for scaling to set in. The exceptions are the K^- and π^- beam where early scaling is expected from Chan et al.'s criterion[7]. In Figure 2 early scaling can be seen.

So far, we have obtained a picture where the model, apart from the normalization, is successful in describing the data. In particular when full use is made of the experimental information for the cross section corresponding to the Rb scattering in the M^2-channel, the agreement is very remarkable.

We next consider the decay density matrices of the Δ in the Gottfried-Jackson frame. Because the produced particles are resonances they subsequently decay and the decay distributions supply extra information on the production mechanism. The model predicts the values of $\rho_{33} = 3/8$, $\mathrm{Re}\ \rho_{3-1} = \sqrt{3}/8$ and $\mathrm{Re}\ \rho_{31} = 0$ for ρ and A_2

exchanges and $\rho_{33} = \text{Re}\ \rho_{3-1} = \text{Re}\ \rho_{31} = 0$ for π exchange. These values are independent of s, t and M^2. The total contribution of all the exchanges to the density matrices are given in Figure 5. Although the result is given for $p \xrightarrow{K^+} \Delta^{++}$ at 16 Gev/c it is not expected to depend on the beam particle or the energy. Dao et al.[20] and Barish et al.[24] in the process $p \xrightarrow{p} \Delta^{++}$ at 303 and 205 Gev/c obtain the values $\rho_{33} \sim 0.1$ and $\text{Re}\ \rho_{31} \sim \text{Re}\ \rho_{3-1} \sim 0$, in reasonable agreement with the model prediction in Figure 5. However, due to the extremely low quality of the above data (no t and M^2 dependence) no significance can be attached to the finding. On comparing the prediction with the more detailed data of Chliapnikov et al.[25] and M. Bardadin-Otwinowska et al.[23] it can be seen that the model is not satisfactory in the t and M^2 dependence.

V. A STUDY OF INCLUSIVE VECTOR AND TENSOR MESON PRODUCTION IN THE TRIPLE-REGGE REGION

In the investigations of single particle inclusive production of vector and tensor mesons, the Mueller-Regge diagram in the near forward section of the bean fragmentation region is presented in Figure c.

For vector meson production the currents at the patticle-particle-Reggeon vertex, $a(0^-)$-$c(1^-)$-R, are given by:

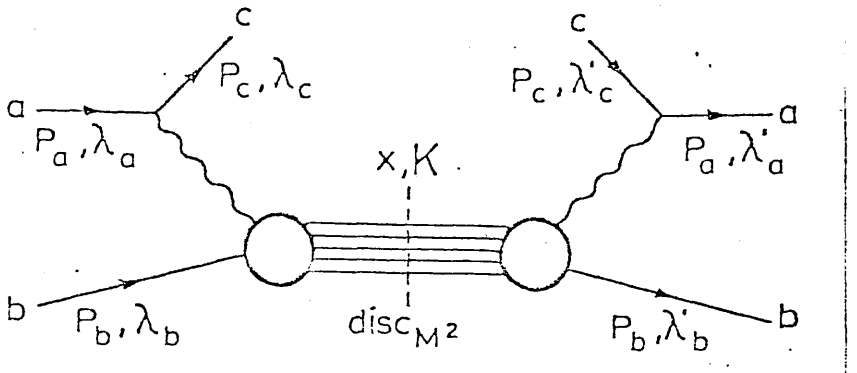

Figure c The Mueller-Regge diagram for vector and tensor meson production in the fixed M^2 and triple-Regge region.

$$J_5^{\lambda_c} = -3\,h\,F\,Q_\eta \bar{\phi}_\eta(P_c,\lambda_c)\phi_5(P_a),$$

for pseudoscalar exchange and,

$$J_\mu^{\lambda_c} = \frac{3h}{m_M}(D+2S)\,\varepsilon_{\mu\nu\kappa\eta}\,P_\nu Q_\kappa \bar{\phi}_\eta(P_c,\lambda_c)\phi_5(P_a),$$

for vector exchange, where ϕ_η and ϕ_5 are, respectively, the vector and pseudoscalar wave functions, P and Q are the sum and difference of the incoming and outgoing meson momenta at the vertex, h is the coupling evaluated from the $\rho \longrightarrow 2\pi$ decay width[16], F and D+2S are the Clebsch-Gordan coefficients, finally m_M is the sum of the two meson masses.

In the case of tensor meson production, the currents at the $a(0^-)$-$c(2^+)$-R vertex are of the form :

$$J_5^{\lambda_c} = -h_f(D+2S)P_\kappa Q_\eta\, \bar{\phi}_{\kappa\eta}(P_c,\lambda_c)\phi_5(P_a)$$

for pseudoscalar exchange, and

$$J_{\mu}^{\lambda_c} = \frac{\mu_o}{2m_M^2} h_f F P_\eta \varepsilon_{\mu\nu\rho\nu} P_\rho Q_\nu \phi_{\lambda\eta}(P_c,\lambda_c)\phi_5(P_a)$$

for vector exchange, where ϕ is the tensor wave function and the coupling h_f is estimated from the $f \longrightarrow 2\pi$ decay width[16], μ_o is taken to be 0.63 Gev/c^2.

The Mueller-Regge amplitudes are evaluated using the above currents and are given in Sections (i) and (ii) of the Appendix for vector and tensor meson production, respectively. Tables II and III, respectively, give the Regge exchanges contributing to the vector and tensor meson production together with the Clebsch-Gordan coefficients.

Discussion and Results:

The production of meson resonances is a rich source of information for the study of high energy production mechanisms. Due to their subsequent decays, they are highly relevant to the observed meson spectra and the question of correlations. Furthermore, polarization measurements obtained from the decay distributions provide valuable additional variables for the study of such processes. In the last few years several inclusive vector meson production experiments have been reported[29] including a recent report on inclusive f production[30].

The model calculations are presented in Figures 6-11 for various inclusive vector and tensor meson productions. For other processes not discussed, Tables II and III provide the relevant Regge exchanges and Clebsch-Gordan coefficients required for their analyses. The comparative difficulty of meson resonance experiments, together with the observed predominance of central production at high energies, leave us only qualitative data for comparison with the model.

None of the inclusive vector and tensor mesons produced from pion and kaon beams are expected to show early scaling. However, approximate scaling (with a scaling breaking term proportional to M^{-1}) is predicted. The prediction is consistent with the $\pi^- \xrightarrow{p} \rho^o$ data in the P_{LAB} range of 8-205 Gev/c[31] for the kinematic region under investigation. The prediction for the ρ^o inclusive cross section is given in Figure 6. Of the two exchanges, π and A_2, contributing to this process, the predominance of π is given by the model.

Figures 7 and 8 show the process $K^- \xrightarrow{p} \overline{K^{*o}}$ with the available high quality data at 14.3 Gev/c[32]. The Regge exchanges taking part in this process are the unnatural parity pair π and B, and the natural parity pair

ρ and A_2. The unnatural parity exchanges provide the major contribution to this process. It can be seen that on a qualitative level the model is not too unreasonable in accounting for the data. The observed over-estimate in normalization is expected from our previous study of inclusive Δ production in this model. The turnovers in the inclusive distributions at small $|t|$ is a threshold effect and can be seen to get more pronounced with increasing M^2 (Figure 7). On close scrutiny the model is found not to be very satisfactory in accounting for the t and M^2 dependence of the data.

The spin density matrices of the observed vector mesons are given by:

$$\rho_{oo} = 1, \quad \rho_{1-1} = 0, \quad \text{Re } \rho_{10} = 0,$$

for production from π and B (unnatural parity) exchanges, and:

$$\rho_{oo} = 0, \quad \rho_{1-1} = 0.5, \quad \text{Re } \rho_{10} = 0,$$

for production from ρ and A_2 (natural parity) exchanges. The density matrices for ρ^o are given in Figure 9 for the π and A_2 contribution at 205 Gev/c. Note that the density matrices are expected to scale and show very little s dependence in the model. In the dual model calculations with B_8 functions, ρ_{oo} is found to be important for π

exchange[33], but for A_2 exchange[34] ρ_{11} is the dominant density matrix element. Note that in these dual model calculations all the possible exchanges are not considered together. In the dual model the inclusive prediction tends to the exclusive prediction with decreasing M^2/s and $\rho_{oo} \longrightarrow 1$ as M^2/s falls; however, in the present model $\rho_{oo} \longrightarrow 1$ as M^2/s increases, as can be seen in Figure 9. The density matrix data for $K^- \xrightarrow{p} \overline{K^{*o}}$, (where ρ and B also contribute) at 14.3 Gev/c indicate slightly negative Re ρ_{10}, zero ρ_{1-1} and $0.2 \leqslant \rho_{oo} \leqslant 0.8$ with perhaps a small rise of ρ_{oo} with M^2/s.

The predictions of the model are given for the inclusive production of f and A_2^o (Figures 10-11). The Regge exchange contributing to the f production is taken to be the π. For the inclusive A_2^o production the ρ and B contribute with the unnatural parity term B dominating. For f production, $\rho_{oo} = 1$ is the only non-vanishing decay density matrix element. In A_2^o decay, the non-vanishing density matrix elements are ρ_{11} and ρ_{1-1} for production through ρ exchange, and ρ_{oo} for production through B exchange. With the recent report on inclusive f production[30] data will soon be available for comparison with the model. It is expected that the findings for the vector meson case will hold true.

VI. CONCLUSION

An explicit Mueller-Regge model has been constructed for use as a basis for the studies of inclusive reactions in the triple-Regge and fixed-M^2 regions. The model is essentially parameter-free and provides a suitable framework for the investigations of one-particle-inclusive processes using the Regge concepts derived from two-body phenomenology.

Exploratory applications of the model in the study of inclusive resonance production have met with surprising qualitative success, as discussed in Sections IV and V. However, no special significance need be attached to the findings. Experience in two-body phenomenology has taught us caution in the interpretation of such successes. We shall adopt the attitude that the qualitative successes of the model are merely indications of its viability as a basic framework for more detailed investigations of the data.

From theoretical and phenomenological considerations the model is expected to be too naive to provide a realistic description of the world. Even with the scarcity of high quality data, there are already glimpses in our study of inclusive resonance production of the inadequacy of the model to account for details. Similar findings are arrived

at in the applications of the model to charge-exchange inclusive meson and nucleon production processes[35,36].

From the studies of exclusive processes, it is known that apart from Regge poles, Regge cuts[37] are an essential ingredient of any realistic model of high energy interactions. The inadequacy of the model for details may then be seen as being due to the neglect of cuts and by analogy with two-body reactions may be remedied to a large extent by their inclusion[38]. With this point of view we can see that we have in our model a very reasonable framework for further investigations of inclusive processes. In particular, we shall adopt the absorption prescription for the incorporation of cuts and apply the absorbed model in the investigations of inclusive resonance productions. The polarization information in such processes can then be exploited to the full to determine the forms of the cut corrections. This programme is carried out in the next chapter.

APPENDIX

The Mueller-Regge amplitudes $H^{\lambda_c' \lambda_a', \lambda_c \lambda_a}$ can be written in the form:

$$H_i^{\lambda_c'\lambda_a', \lambda_c\lambda_a} = (\chi_i^{\lambda_c'\lambda_a'})^* \; W_i \; \chi_i^{\lambda_c\lambda_a}$$

where i denotes the exchange and

$$\chi_i^{\lambda_c\lambda_a} = \alpha_i' \frac{[1 + \xi \exp(-i\pi\alpha_i(t)]}{2} \Gamma_i[f(t)] \left(\frac{s}{M^2}\right)^{\alpha_i(t)-J_i} {}_{a_i}^{\lambda_c\lambda_a}.$$

The structure function W is given by:

$$W_i = \begin{cases} G_s^2 \; 2\,\Delta^{\frac{1}{2}}(M^2, m_b^2, t)\; \sigma_{tot}(\pi p) & \text{for } i = \pi \text{ exchange,} \\ G_v^2 V & \text{for } i = \text{vector exchange,} \end{cases}$$

where G_s and G_v are, respectively, the pseudoscalar and vector couplings containing the appropriate Clebsch-Gordon coefficients.

The G and $a^{\lambda_c\lambda_a}$ are given below for the processes under investigation. We work in the centre of mass system defined in Appendix II.

i) <u>Vector meson production ($0^- \xrightarrow{b} 1^-$)</u>:

For this process particle a is spinless and the label λ_a is redundant. We have simply a^{λ_c} and in this beam fragmentation region we take $P_a = P_1$, $P_b = P_2$ and $P_c = P_3$.

a) We then obtain for pseudoscalar exchange:

$$a_s^o = \frac{qE_1 - kE_3\cos\theta}{m_3}$$

$$a_s^{\pm 1} = \mp \frac{k\sin\theta}{\sqrt{2}}$$

b) For vector exchange we have:

$$a_v^o = 0,$$

$$a_v^{\pm 1} = -\sqrt{2}\, q\, k(E_1 + E_2)\sin\theta$$

The two couplings are, respectively:

$$G_s = -3hF,$$

$$G_v = \frac{3h}{m_1+m_3}(D+2S).$$

ii) Tensor meson production ($0^- \xrightarrow{b} 2^+$):

The tensor meson is in the beam fragmentation region and we adopt the same four-momenta label as in the vector meson case. With the spinless beam particle we have a^{λ_c} given by:

a) For pseudoscalar exchange:

$$a_s^o = \frac{2}{\sqrt{6}\, m_3^2}(q^2E_1^2 - 2qkE_1E_3\cos\theta + k^2E_3^2\cos^2\theta - \frac{m_3^2}{2}k^2\sin^2\theta),$$

$$a_s^{\pm 1} = \mp \frac{k}{m_3}\sin\theta\,(qE_1 - kE_3\cos\theta),$$

$$a_s^{\pm 2} = \frac{k^2}{2}\sin^2\theta.$$

b) For vector exchange:

$$a_v^{o} = 0,$$

$$a_v^{\pm 1} = \frac{1}{m_3} q\, k \sin\theta (E_1 + E_2)(qE_1 - kE_3\cos\theta),$$

$$a_v^{\pm 2} = \mp q\, k^2 \sin^2\theta (E_1 + E_2).$$

The pseudoscalar and vector couplings are, respectively:

$$G_s = -h_f(D + 2S),$$

$$G_v = \frac{\mu_o}{2m_M^2} h_f F.$$

iii) <u>Δ production $(\frac{1}{2}^+ \xrightarrow{b} \frac{3}{2}^+)$</u>:

Here both particles a and c contain spins and both the helicity indices λ_a and λ_c are retained. The upper half of the indices only will be shown explicitly; it is to be understood that the factor $\frac{1}{2}$ is implicitly present. The process takes place in the target fragmentation region and we write $P_a = P_2$, $P_b = P_1$, $P_c = P_4$.

We introduce the variables:

$$E = \sqrt{(m_2 + E_2)(E_4 + m_4)},$$

$$C_{\pm} = E^2 \pm kq,$$

$$D = \frac{k \sin\theta}{E}$$

$$F = \frac{2kq(E_1 + E_2)\sin\theta}{E}$$

a) For pseudoscalar exchange we have:

$$a_s^{3,1} = -\frac{1}{\sqrt{2}} D C_- \cos\theta/2,$$

$$a_s^{1,1} = \frac{1}{\sqrt{6}} D C_+ \sin\theta/2 + \frac{\sqrt{2}(qE_2 - kE_4\cos\theta)C_-}{\sqrt{3}m_4 E} \cos\theta/2,$$

$$a_s^{-1,1} = \frac{1}{\sqrt{6}} D C_- \cos\theta/2 - \frac{\sqrt{2}(qE_2 - kE_4\cos\theta)C_+}{\sqrt{3}m_4 E} \sin\theta/2$$

$$a_s^{-3,1} = \frac{1}{\sqrt{2}} D C_+ \sin\theta/2,$$

together with:

$$a_s^{3,-1} = a_s^{-3,1}, \qquad a_s^{1,-1} = -a_s^{-1,1}$$

$$a_s^{-1,-1} = a_s^{1,1}, \qquad a_s^{-3,-1} = -a_s^{3,1}.$$

b) For vector exchange we obtain:

$$a_v^{3,1} = -\frac{1}{\sqrt{2}} F C_- \cos\theta/2,$$

$$a_v^{1,1} = \frac{1}{\sqrt{6}} F C_+ \sin\theta/2,$$

$$a_v^{-1,1} = -\frac{1}{\sqrt{6}} F C_- \cos\theta/2,$$

$$a_v^{-3,1} = \frac{1}{\sqrt{2}} F C_+ \sin\theta/2,$$

together with,

$$a_v^{3,-1} = -a_v^{-3,1}, \qquad a_v^{1,-1} = a_v^{-1,1}$$
$$a_v^{-1,-1} = -a_v^{1,1}, \qquad a_v^{-3,-1} = a_v^{3,1}.$$

The two couplings are given by:

$$G_s = \frac{g}{m_B} G,$$
$$G_v = -\frac{gG}{2m_B^2}.$$

REFERENCES

1. A.H. Mueller, Phys. Rev., D2, 2963 (1970).

2. See, e.g.

   D. Horn and F. Zachariasen, Hadron Physics at Very High Energies, Benjamin (1973).

3. S.A. Adjei, P.A. Collins, B.J. Hartley, K.J.M. Moriarty and R.W. Moore, Ann. of Phys. (N.Y.), 75, 405 (1973);

   P.A. Collins, B.J. Hartley, R.W. Moore and K.J.M. Moriarty, J. Phys., A6, 506 (1973).

4. See e.g.

   R. Delbourgo, Elementary Particle Symmetries, D.I.C. Lecture Notes (1972).

5. N.S. Craigie, G. Kramer and J. Körner, Nucl. Phys., B68, 509 (1974).

6. H.M. Chan and P. Hoyer, Phys. Letters, 36B, 79 (1971);

   P.G.O. Freund, Phys. Rev. Letters, 20, 235 (1968);

   H. Harari, Phys. Rev. Letters, 20, 1395 (1968).

7. H.M. Chan, C.S. Hsue, C. Quigg and J.M. Wang, Phys. Rev. Letters, 26, 672 (1971).

8. A. Dar, K.J.M. Moriarty and J. Tran Thanh Van, Acta Phys. Austr., 43, 99 (1975).

9. V.S. Barashenkov, "Interaction Cross Sections of Elementary Particles", Israel Program for Scientific Translations Ltd., 1968.

10. J.J. Sakurai and D. Schildknecht, Phys. Letters, 40B, 121 (1972).

11. H.J. Lipkin and F. Scheck, Phys. Rev. Letters, 16, 71 (1966).

12. G.A. Ringland, R.J.N. Phillips and R. Worden, Phys. Letters, 40B, 239 (1972).

13. See, e.g.

   R.G. Roberts, Phenomenology of inclusive reactions, Proc. 14th Scottish Universities Summer School (1973), Eds. R.L. Crawford and R. Jennings, Academic Press (1974).

14. R.P. Feynman, Phys. Rev. Letters, 23, 1415 (1969);
J. Benecke, T.T. Chou, C.N. Yang and E. Yen, Phys. Rev., 188, 2159 (1969).

15. H.I. Miettinen, Phys. Letters, 38B, 431 (1972).

16. Particle data group, N. Barash-Schmidt et al., Rev. Mod. Phys., 48 (1976).

17. J.V. Beaupre et al., Nucl. Phys., B67, 413 (1973);
K.W.J. Barnham, private communication.

18. P. Bosetti et al., Nucl. Phys., B81, 61 (1974);
K.W.J. Barnham, private communication.

19. P. Gregory et al., Paper submitted to the 2nd Aix-en-Provence International Conference on Elementary Particles, September 1973;
P. Gregory and H. Muirhead, private communication.

20. F.T. Dao et al., Phys. Rev. Letters, 30, 34 (1973).

21. D. Brick et al., Phys. Rev. Letters, 31, 488 (1973).

22. J.P. De Brion et al., Phys. Rev. Letters, 34, 910 (1975).

23. M. Bardadin-Otwinowska et al., paper presented at the International Conference on Elementary Particles, Palermo, June 1975.

24. S.J. Barish et al., Phys. Rev., D12, 1260 (1975).

25. P.C. Chliapnikov et al., Nucl. Phys., B105, 510 (1976).

26. E. Bracci et al., Compilation of cross sections, CERN/HERA 72-1 (1972).

27. M.J. Counihan, private communication.

28. M. Bardadin-Otwinowska et al., Nucl. Phys., B72, 1 (1974);
P.V. Chliapnikov et al., Phys. Letters, 55B, 237 (1975).

29. F.C. Winkelmann, "Inclusive Meson Resonance Production", L.B.L. Report LBL-3045, April 1974;

K. Böchmann, "Single Particle and Multiplicity Distributions", Rapporteur Talk at the International Conference on High Energy Physics, Palermo, Sicily, June 1975. (Bonn University Preprint, BONN-HE-75-12, August 1975.)

30. J. Bartke et al., Nucl. Phys., B107, 93 (1976).

31. F.C. Winkelmann et al., Phys. Letters, 56B, 101 (1975);
D. Fong et al., Phys. Letters, 60B, 124 (1975);
J. Brau et al., Nucl. Phys., B99, 232 (1975);
M. Deutschmann et al., Nucl. Phys., B103, 426 (1976);
See also Ref. 29.

32. K. Paler et al., Nucl. Phys., B96, 1 (1975).

33. K. Kang and P. Shen, Phys. Rev., D7, 164 (1973);
J. Randa, Phys. Rev., D7, 2236 (1973).

34. J. Randa, Phys. Rev., D9, 2612 (1974).

35. K.J.M. Moriarty, J.H. Tabor and A. Ungkitchanukit, Acta Phys. Austr., 45, 325 (1976).

36. K.J.M. Moriarty, J.P. Rad, J.H. Tabor and A. Ungkitchanukit, Acta Phys. Austr., 46 (1976).

37. P.D.B. Collins and E.J. Squires, Regge Poles in Particle Physics, (Springer, Berlin, 1968);
P.D.B. Collins, Phys. Reports, 1C, 103 (1971).

38. R.W.B. Ardill, P. Choudhury, K.J.M. Moriarty and A. Ungkitchanukit, Acta Phys. Austr., 46 (1976).

FIGURE CAPTIONS

Fig. 1 The inclusive cross sections for $p \xrightarrow{\pi^+} \Delta^{++}_2$ for $s = 16.00, 30.31, 45.55$ and 94.73 $(\text{Gev})^2$. Data from Ref. 17.

Fig. 2 The inclusive cross sections for exotic M^2-channels a) and b) $p \xrightarrow{K^-} \Delta^{++}$ at $s = 19.91$ and 31.15 $(\text{Gev})^2$, c) and d) $p \xrightarrow{\pi^-} \Delta^{++}$ at $s = 30.93$ and 94.73 $(\text{Gev})^2$. Data from Ref. 18.

Fig. 3 The inclusive cross sections for $p \xrightarrow{\bar{p}} \Delta^{++}_2$, a) and b) at $s = 18.74$ and 24.33 $(\text{Gev})^2$, and c) at $s = 18.74$ $(\text{Gev})^2$ where the theoretical curve contains the physical $\sigma_{tot}(\pi^+ p)(M^2)$ as input. Data from Ref. 19.

Fig. 4 The inclusive cross sections for $p \xrightarrow{p} \Delta^{++}$ for $s = 131.26$ and 570.37 $(\text{Gev})^2$.

Fig. 5 The density matrix elements for the decay of the Δ^{++} produced from $p \xrightarrow{K^+} \Delta^{++}$ at $P_{LAB} = 16$ Gev/c.

Fig. 6 The inclusive cross sections for $\pi^- p \xrightarrow{} \rho^o$ at $s = 385.6$ $(\text{Gev})^2$.

Fig. 7 The inclusive cross sections for $K^- p \xrightarrow{} \overline{K^{*o}}$ at 14.3 Gev/c at fixed M^2 plotted vs. t. Data from Ref. 32.

Fig. 8 The inclusive cross sections for $K^- p \xrightarrow{} \overline{K^{*o}}$ at 14.3 Gev/c at fixed t plotted vs. M^2/s. Data from Ref. 32.

Fig. 9 The density matrix elements for the decay of the ρ^o produced in $\pi^- p \xrightarrow{} \rho^o$ at 205 Gev/c.

Fig. 10 The inclusive cross section for $\pi^\pm p \xrightarrow{} f$ at $s = 385.6$ $(\text{Gev})^2$.

Fig. 11 The inclusive cross sections for $\pi^\pm p \xrightarrow{} A^o_2$ at $s = 385.6$ $(\text{Gev})^2$.

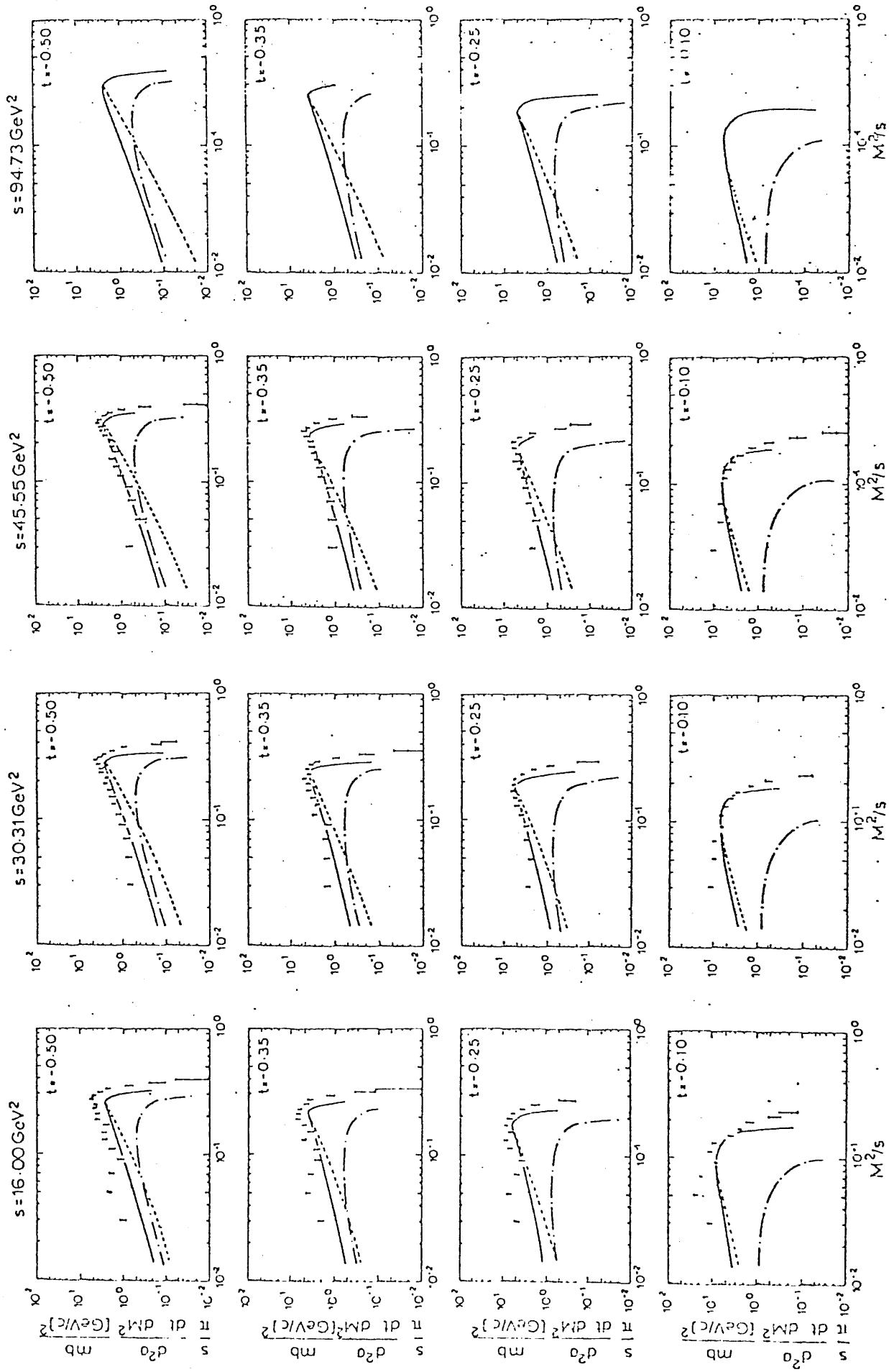
π⁺+p — Δ⁺⁺+X
s=16.00 GeV²
s=30.31 GeV²
s=45.55 GeV²
s=94.73 GeV²
t=-0.50
t=-0.35
t=-0.25
t=-0.10
s/π d²σ/dt dM² mb/(GeV/c)²
M²/s
a. ..... Unnatural parity
b. – – – – Natural parity
c ——— Total
d

Fig. 1

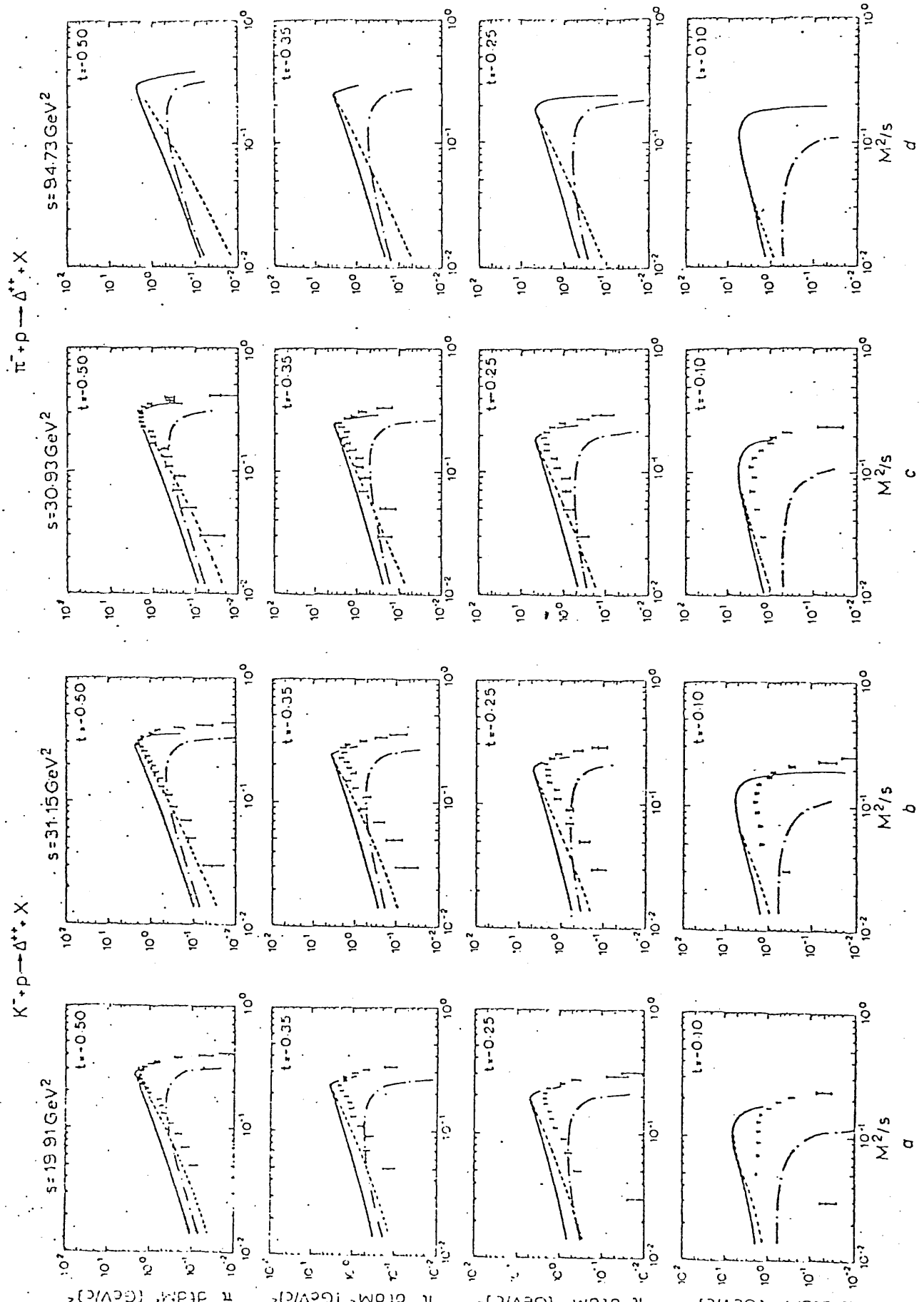
K⁻+p→Δ⁺⁺+X
π⁻+p→Δ⁺⁺+X
s=19.91GeV²
s=31.15GeV²
s=30.93GeV²
s=94.73GeV²
t=-0.50
t=-0.35
t=-0.25
t=-0.10
M²/s
a
b
c
d
Unnatural parity
Natural parity
Total

Fig. 2

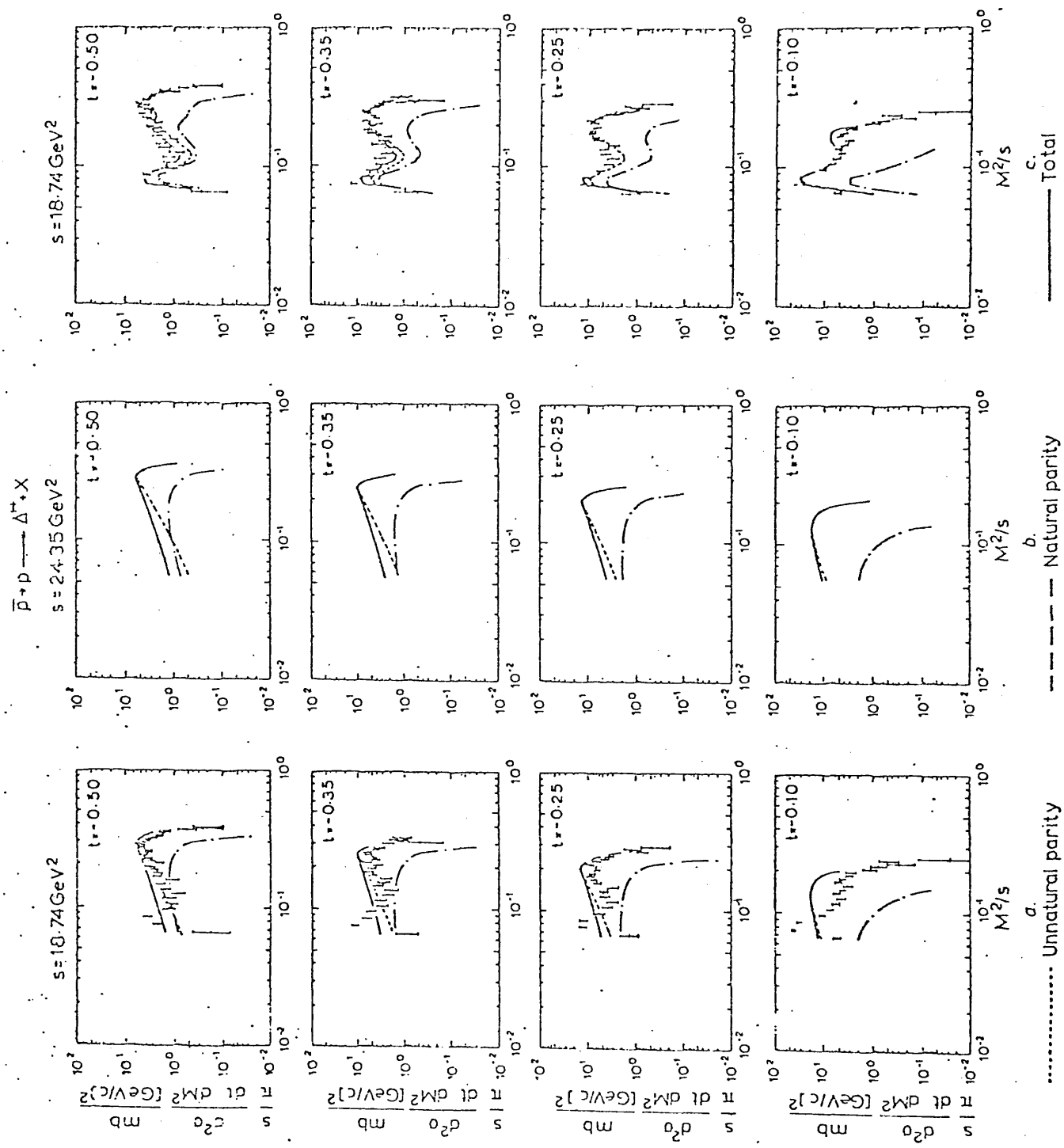
$\bar{p}+p \longrightarrow \Delta^{++}X$
s = 18.74 GeV2
s = 24.35 GeV2
s = 18.74 GeV2
t = -0.50
t = -0.35
t = -0.25
t = -0.10
$\frac{s}{\pi}\frac{d^2\sigma}{dt\,dM^2}$ mb [GeV/c]^2
M^2/s
a. ..... Unnatural parity
b. — — — — Natural parity
c. —— Total

Fig. 3

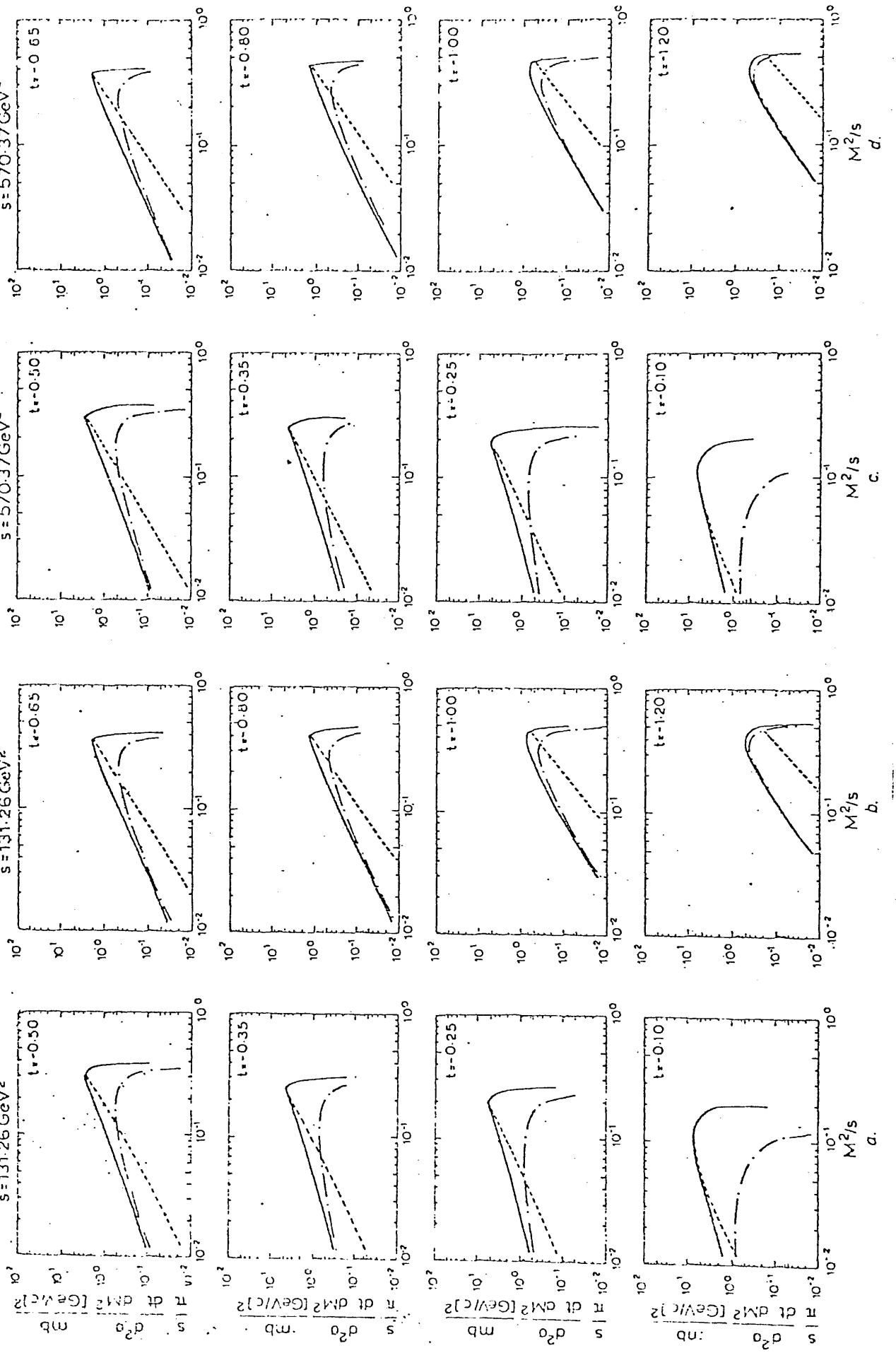
p+p → Δ++X
s = 131.26 GeV²
s = 570.37 GeV²
t = -0.50
t = -0.65
t = -0.35
t = -0.80
t = -0.25
t = -1.00
t = -0.10
t = -1.20
t = -0.65
t = -0.80
t = -1.00
t = -1.20
M²/s
a.
b.
c.
d.
Unnatural parity
Natural parity
Total

Fig. 4

$K^+ + p \longrightarrow \Delta^{++} + X$

$P_{LAB} = 16\,GeV/c$

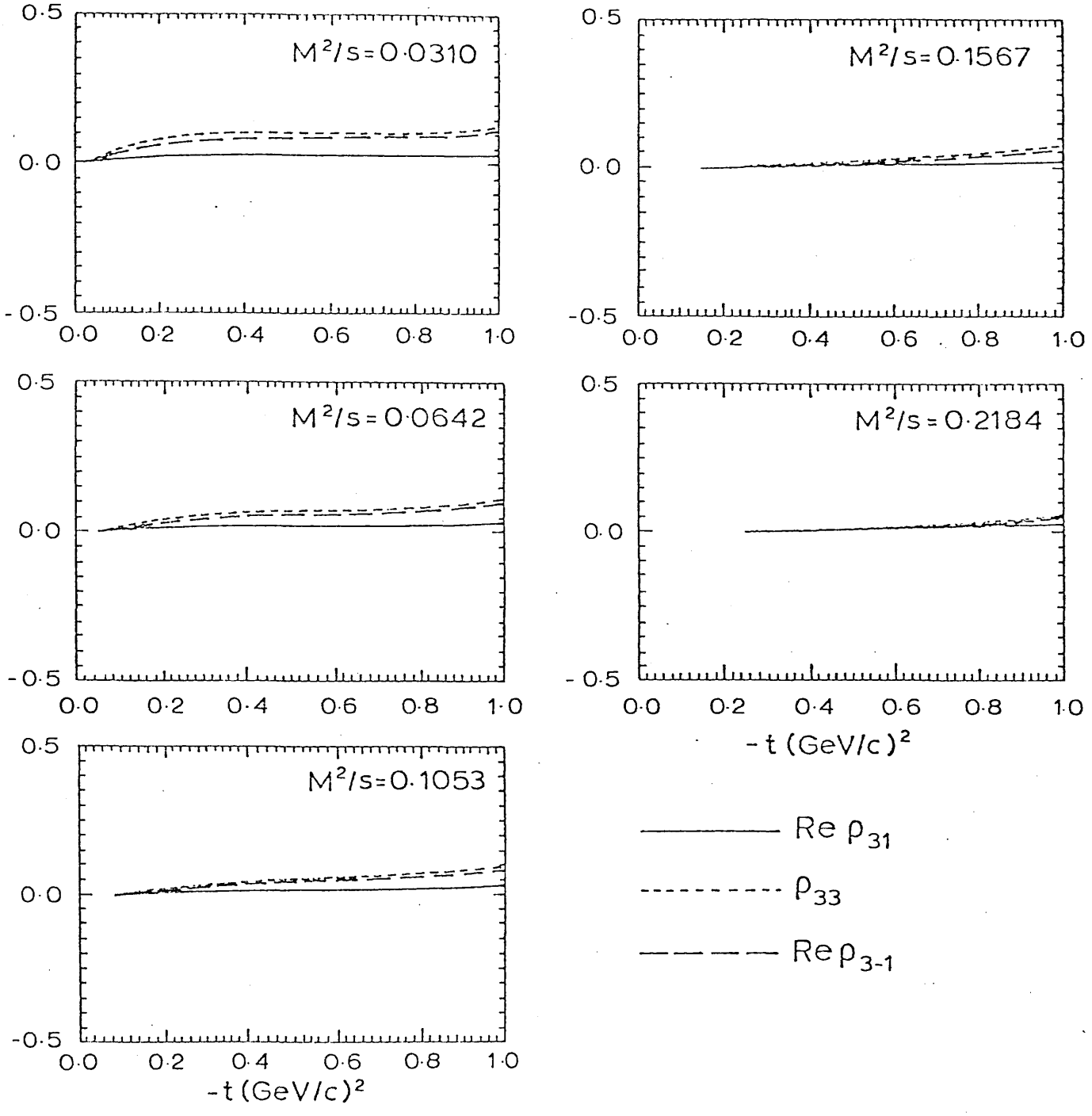

Fig. 5

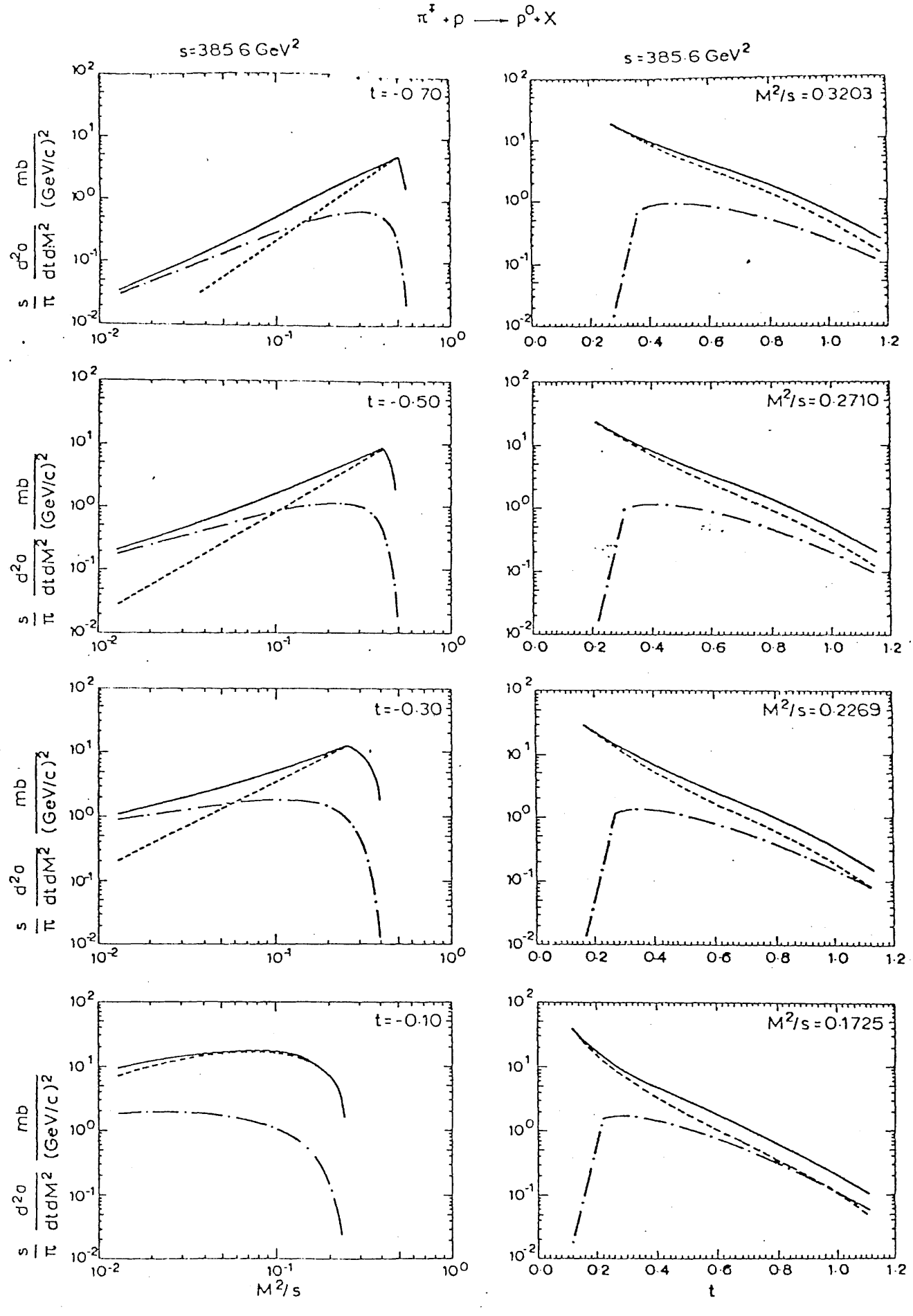
$\pi^{\mp} + p \longrightarrow \rho^0 + X$
s=385 6 GeV^2
s = 385·6 GeV^2
t = -0 70
M^2/s = 0 3203
t = -0·50
M^2/s = 0·2710
t = -0·30
M^2/s = 0·2269
t = -0·10
M^2/s = 0·1725
$\frac{s}{\pi}\frac{d^2\sigma}{dt\,dM^2}$ $\frac{mb}{(GeV/c)^2}$
M^2/s
t
Unnatural parity
Natural parity
Total

Fig. 6

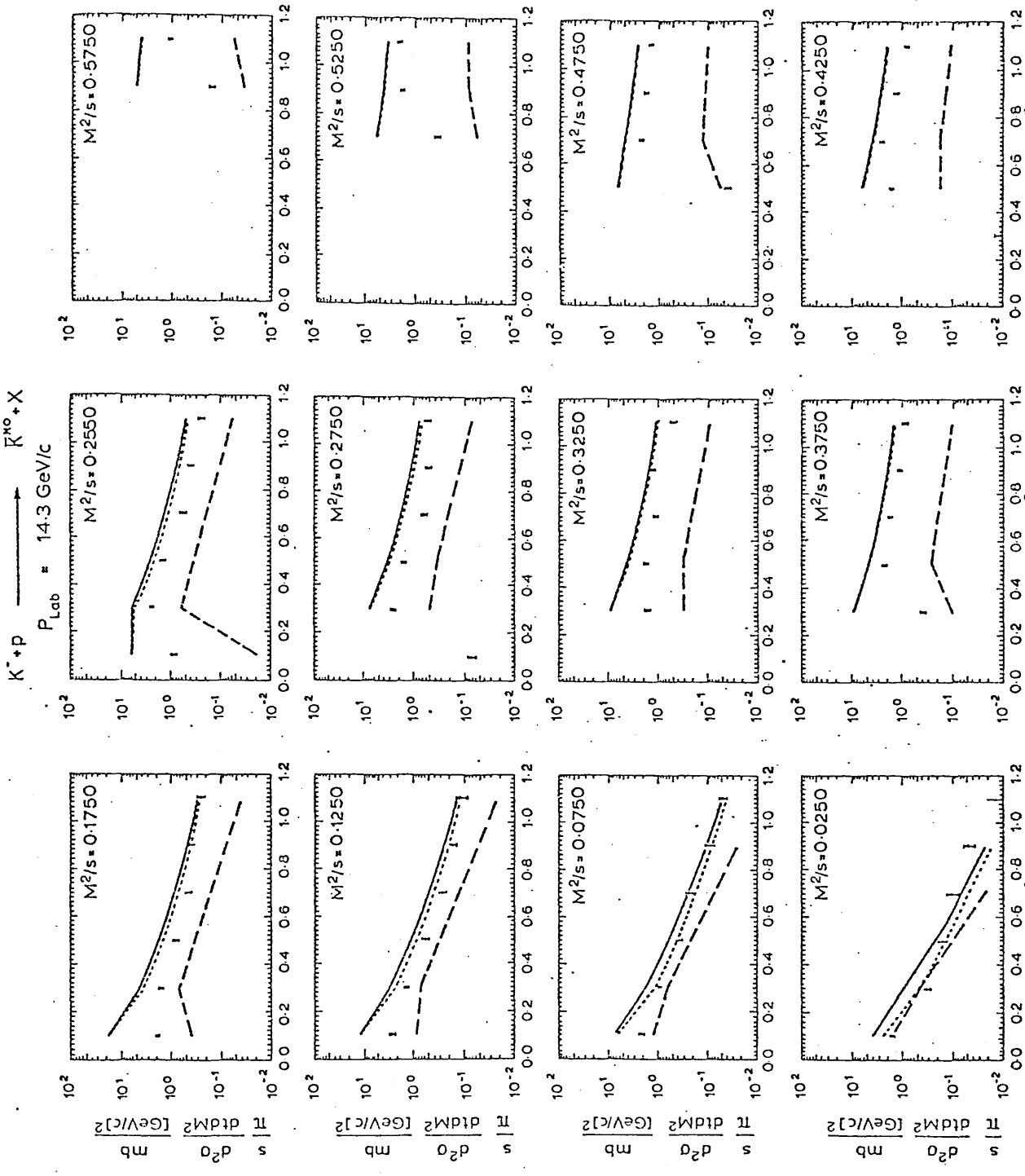
K⁻+p → K̄⁰+X
P_Lab = 14.3 GeV/c
M²/s = 0.2550
M²/s = 0.2750
M²/s = 0.3250
M²/s = 0.3750
M²/s = 0.4250
M²/s = 0.4750
M²/s = 0.5250
M²/s = 0.5750
M²/s = 0.1750
M²/s = 0.1250
M²/s = 0.0750
M²/s = 0.0250
s/π d²σ/dtdM² mb/[GeV/c]²
-t [GeV/c]²
Unnatural parity
Natural parity
Total

Fig. 7

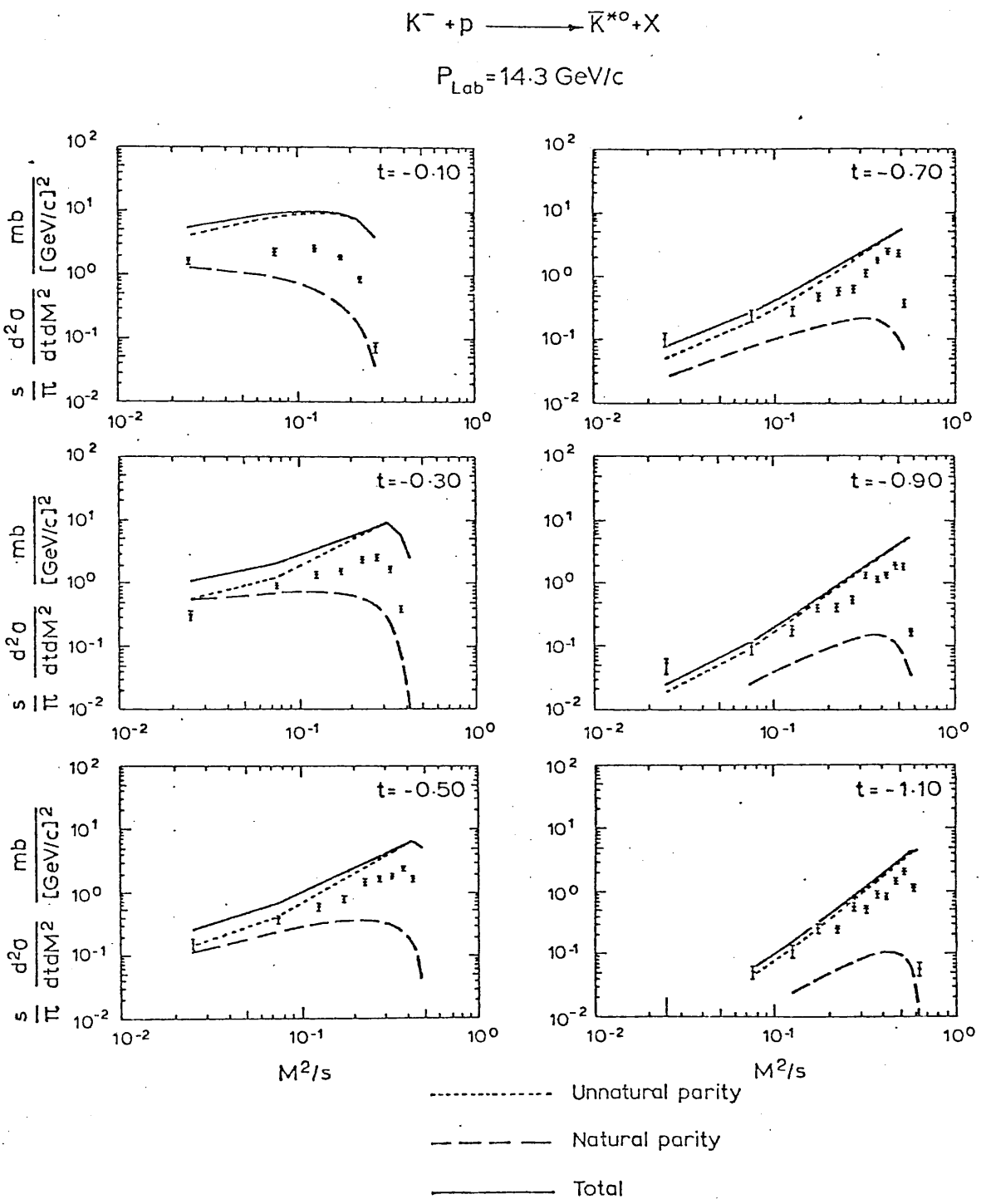
K⁻ + p ⟶ K̄*⁰ + X
P_Lab = 14.3 GeV/c
t = -0.10
t = -0.70
t = -0.30
t = -0.90
t = -0.50
t = -1.10
s/π d²σ/dtdM² mb/[GeV/c]²
M²/s
Unnatural parity
Natural parity
Total

Fig. 8

$$\pi^- + p \longrightarrow \rho^0 + X$$

$$P_{Lab} = 205\ \text{GeV/c}$$

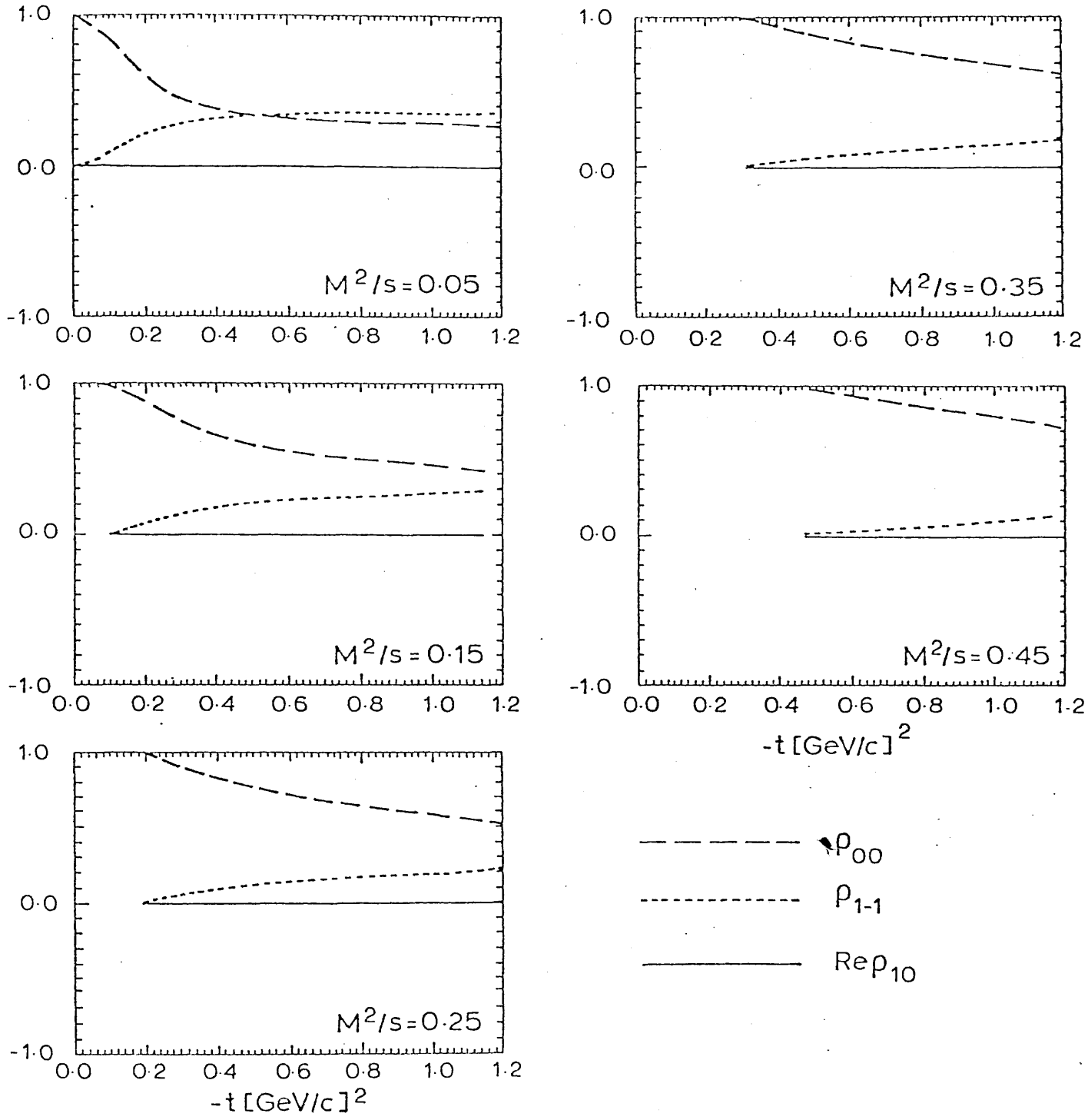

Fig. 9

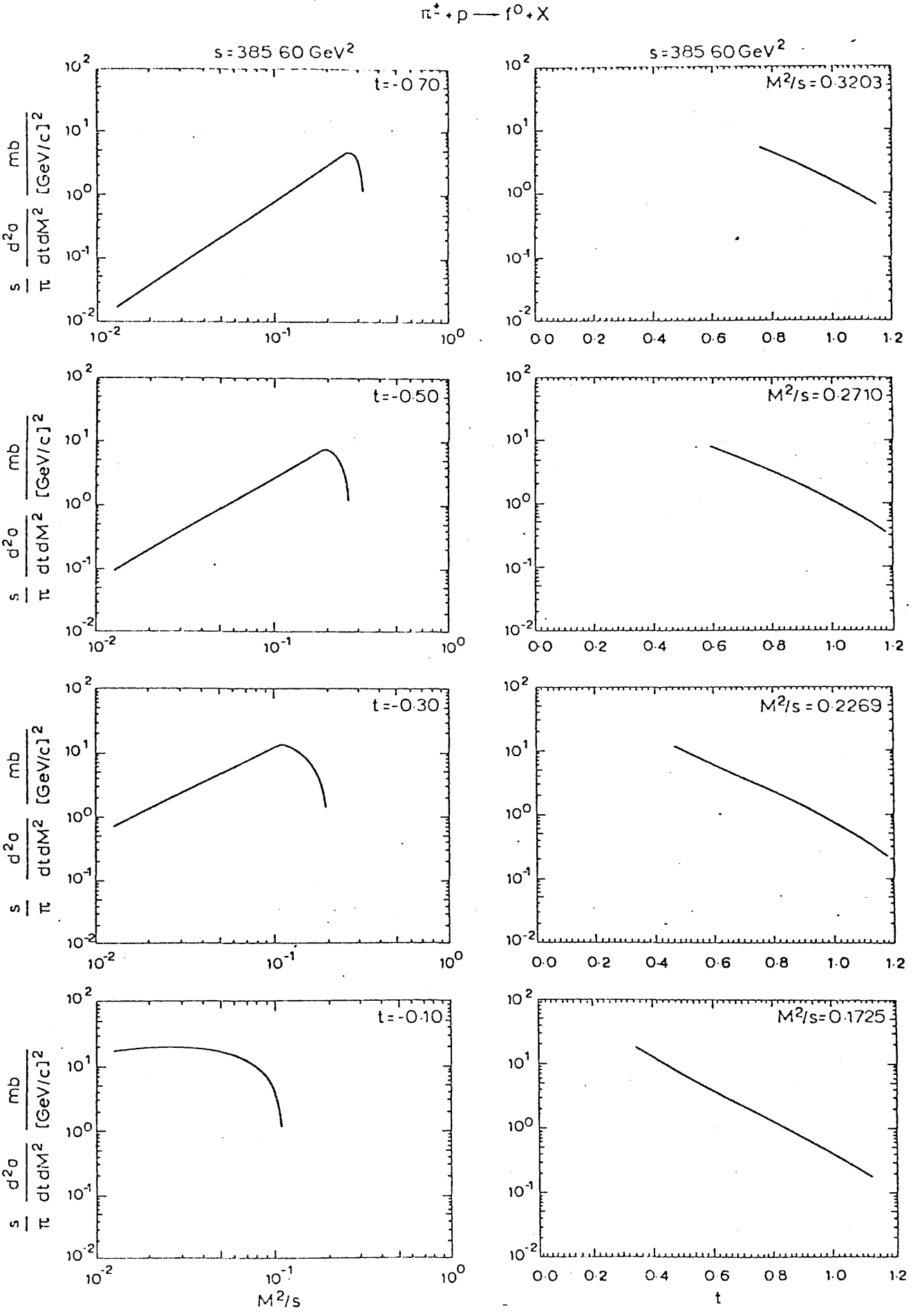
$\pi^{\pm} + p \rightarrow f^0 + X$
s = 385 60 GeV²
t = -0 70
t = -0·50
t = -0·30
t = -0·10
M²/s = 0·3203
M²/s = 0·2710
M²/s = 0·2269
M²/s = 0·1725
$\frac{s}{\pi} \frac{d^2\sigma}{dt\,dM^2}$ mb / [GeV/c]²
M²/s
t

Fig.10

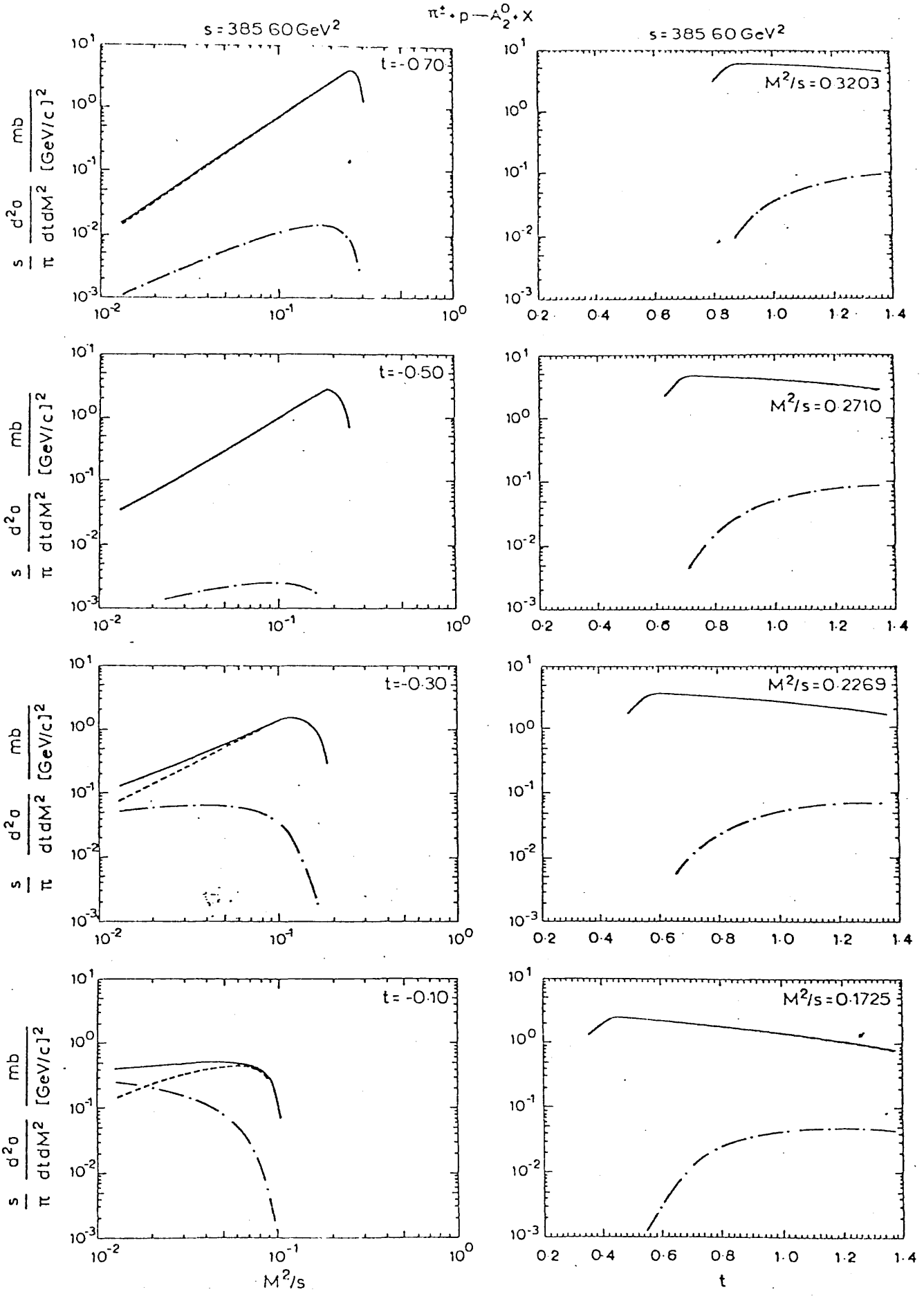
$\pi^{\pm} + p \rightarrow A_2^0 + X$
s = 385 60 GeV²
s = 385 60 GeV²
t = -0 70
M²/s = 0 3203
t = -0·50
M²/s = 0·2710
t = -0·30
M²/s = 0·2269
t = -0·10
M²/s = 0·1725
$\frac{s}{\pi}\frac{d^2\sigma}{dt\,dM^2}\frac{mb}{[GeV/c]^2}$
M²/s
t
Unnatural parity
Natural parity
Total

Fig.11

CHAPTER 3

ABSORPTIVE CORRECTIONS IN A MUELLER-REGGE MODEL

I. INTRODUCTION

Since the introduction of the generalized optical theorem[1] the Mueller-Regge model has established itself as a useful framework for inclusive phenomenology[2]. In particular the triple-Regge model has met with considerable success in qualitatively accounting for the data[3]. However, the improving quality (and quantity) of the data are increasingly pointing towards the importance of cuts in inclusive processes.

In the investigations into the inclusive production of Δ[4], vector and tensor mesons[5] within a Mueller-Regge model of the last chapter, it was found that although qualitatively quite satisfactory in accounting for the inclusive cross sections, in details the model failed. Further, there were some difficulties with the normalization. Craigie et al[6] in studying the inclusive photoproduction of pions found that the Mueller-Regge pole model would give a normality dip in the forward direction ($k_\perp^2 \longrightarrow 0$) in contradiction with the data which show a peak[7]. Subsequent work with the model including cuts resolved the problem[8].

The data on target asymmetry for the processes $\gamma + p\uparrow \longrightarrow \pi^{\pm} + X$ [9] and $\pi^{\pm} + p\uparrow \longrightarrow \pi^{\pm} + X$ [10] provide further evidence for the importance of cuts in inclusive processes. The triple-Regge limit for factorizing poles and Pomeron predicts no target asymmetry to leading order in s in the beam fragmentation region and the main contribution to the target asymmetry is expected to arise from cuts[11]. Soffer and Wray[12] and Ahmed et al[13] correctly predicted the target asymmetry in $(\pi^{\pm} \xrightarrow{p\uparrow} \pi^{\pm})$ and $(\gamma \xrightarrow{p\uparrow} \pi^{\pm})$, respectively, using the Mueller-Regge model with cut corrections.

From the theoretical viewpoint cuts are required for consistency with s-channel unitarity[14]; the existence of Regge poles implies the existence of Regge cuts which are generated from the poles through unitarity. In inclusive processes cuts are expected to be important and have been discussed by several authors[15], and they are also required to remove inconsistencies caused by decoupling theorems[16].

In the last chapter we constructed an explicit Mueller-Regge model which was found to be a reasonable basis for phenomenology. We now introduce cuts into the model through the Gottfried-Jackson-Sopkovich absorption formalism[17].

In the absorption framework the impact parameter amplitudes are modified to take into account absorptive (unitarity) effects due to elastic rescatterings in the initial and final states.

II. FORMALISM

The incorporation of cuts in the Mueller-Regge model will be considered in the absorption formalism. The effects of elastic scatterings in the ab and a'b' channels shown in Figure a are taken into account through absorption in the impact parameter space. The impact parameter space Mueller-Regge amplitudes acquire the absorptive corrections:

$$H_{abs}^{\lambda_c'\lambda_a',\lambda_c\lambda_a}(b',b) = (S^{\frac{1}{2}}(b'))^* \, H^{\lambda_c'\lambda_a',\lambda_c\lambda_a}(b',b) S^{\frac{1}{2}}(b)$$

through the rescatterings[17], where $H(b',b)$ and $H_{abs}(b',b)$ are respectively the unmodified and modified impact parameter space Mueller-Regge amplitudes, b' and b are the impact parameter spaces corresponding to the a'b' and ab channels and $S(b')$ and $S(b)$ are the elastic scattering matrices.

It is expected that rescatterings in the $b'\bar{c}'$ and $b\bar{c}$ channels shown in Figure b will also provide significant absorptive corrections to the Mueller-Regge amplitudes. However, for simplicity we shall not explicitly

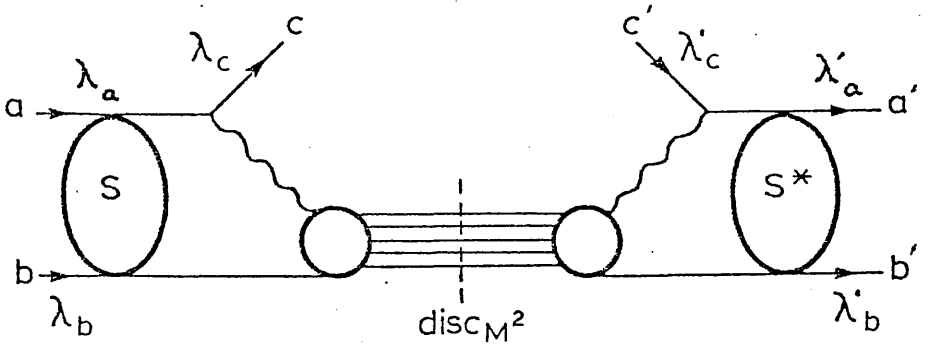

Figure a Rescatterings in the ab and a'b' channels for a+b $\longrightarrow$c+X in the fixed-M^2 and triple-Regge regions.

consider these channels but instead work in the a'b' and ab channels using S in place of $S^{\frac{1}{2}}$ in the absorption prescription given above. The absorbed impact parameter space Mueller-Regge amplitudes are then given by:

$$H^{\lambda'_c\lambda'_a,\lambda_c\lambda_a}_{abs}(b',b) = S^*(b')H^{\lambda'_c\lambda'_a,\lambda_c\lambda_a}(b',b)S(b)$$

with the elastic scattering matrices given by:

$$S(b) = 1 - C\, e^{-\lambda b^2}$$

and a similar expression for S(b'), where C is the opacity and $\lambda = R^{-2}$, with R denoting the interaction radius of the target.

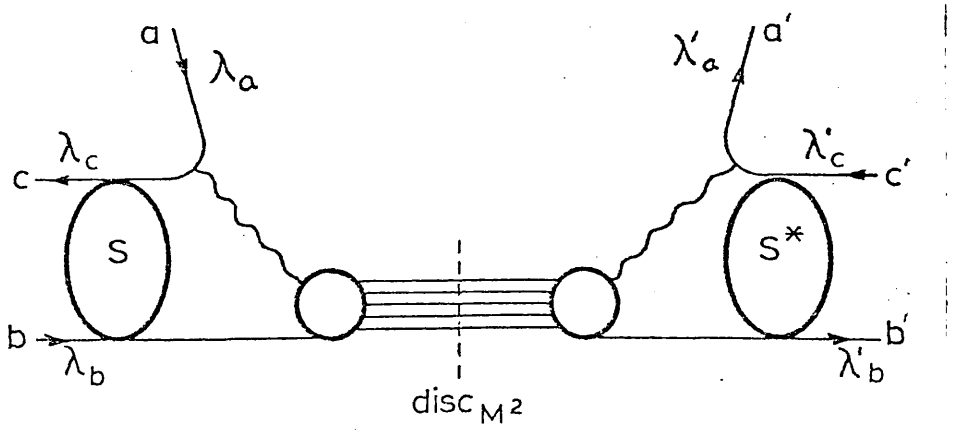

Figure b Rescatterings in the b'$\bar{c}$' and b$\bar{c}$ channels for a+b $\longrightarrow$ c+X in the fixed M^2 and triple-Regge region.

The Mueller-Regge model constructed in the last chapter will be employed as the basis for the absorptive corrections. We work in the cm. frame with the Mueller-Regge amplitudes of the last chapter given in terms of the variables s_{ab}, τ, M^2, $s_{a'b'}$, and τ'. The variables τ and τ' are related to the invariants t_{ac} and $t_{a'c'}$ and are defined in the Appendix; physically they correspond to the transverse momenta of the system. The impact parameter space representations of the Mueller-Regge amplitudes are obtained through the Fourier-Bessel transform:

$$H^{\lambda_c'\lambda_a',\lambda_c\lambda_a}(b',b) = \int_0^\infty \tau_1' d\tau_1' \int_0^\infty \tau_1 d\tau_1 J_{\nu'}(b'\tau_1') J_\nu(b\tau_1) H^{\lambda_c'\lambda_a',\lambda_c\lambda_a}(\tau_1',\tau_1)$$

where b and τ are the conjugate variables in the transform.

The absorbed Mueller-Regge amplitudes in the impact parameter space is then given by:

$$H_{abs}^{\lambda_c'\lambda_a',\lambda_c\lambda_a}(b',b) = \int_0^\infty \tau_1' d\tau_1' \int_0^\infty \tau_1 d\tau_1 J_{\nu'}(b'\tau_1') J_\nu(b\tau_1) \cdot S^*(b') H^{\lambda_c'\lambda_a',\lambda_c\lambda_a}(\tau_1',\tau_1) S(b)$$

To recover the absorbed Mueller-Regge amplitudes we perform the inverse Fourier-Bessel transform:

$$H_{abs}^{\lambda_c'\lambda_a',\lambda_c\lambda_a}(\tau',\tau) = \int_0^\infty \tau_1' d\tau_1' \int_0^\infty \tau_1 d\tau_1 \int_0^\infty b' db' \int_0^\infty b db J_{\nu'}(b'\tau_1') J_\nu(b\tau_1) \cdot J_{\nu'}(b'\tau') J_\nu(b\tau) S^*(b') H^{\lambda_c'\lambda_a',\lambda_c\lambda_a}(\tau_1',\tau_1) S(b)$$

The b' and b integrations can be performed straight away using

the orthogonality of the Bessel functions and the relation given in the table at the end of this chapter once the expressions for S(b') and S(b) are substituted into the above equation. We obtain:

$$H_{abs}^{\lambda_c'\lambda_a',\lambda_c\lambda_a}(\tau',\tau) = \int_0^\infty \tau_1' d\tau_1' \int_0^\infty \tau_1 d\tau_1 \, H^{\lambda_c'\lambda_a',\lambda_c\lambda_a}(\tau_1',\tau_1) \cdot$$

$$\cdot\left\{\frac{1}{\tau'}\,\delta(\tau'-\tau_1') - \frac{C}{2\lambda}\exp\left(-\frac{\tau'^2+\tau_1'^2}{4\lambda}\right) I_{\nu'}\left(\frac{\tau'\tau_1'}{2\lambda}\right)\right\} \cdot$$

$$\cdot\left\{\frac{1}{\tau}\,\delta(\tau-\tau_1) - \frac{C}{2\lambda}\exp\left(-\frac{\tau^2+\tau_1^2}{4\lambda}\right) I_{\nu}\left(\frac{\tau\tau_1}{2\lambda}\right)\right\},$$

where ν' and ν are the total helicity flips on each side of disc M^2. The simplifying assumption that the inclusive vertex is primarily non-flip[8,18,19] is made, since spin non-flip seems to be the dominant mechanism at this vertex. Then ν' and ν are given by:

$$\nu' = |\lambda_c' - \lambda_a'| \quad \text{and} \quad \nu = |\lambda_c - \lambda_a| .$$

The evaluations of the absorbed Mueller-Regge amplitudes are given in the Appendix.

In the absorption prescription the terms $C\,e^{-\lambda b^2}$ in the elastic scattering matrices can be considered as the impact parameter space projection of the Pomeron pole contribution[8]. The absorption then corresponds to the inclusion of the correction terms due to the Mueller-Regge

diagrams of Figure c to the standard Mueller-Regge diagram of the last chapter.

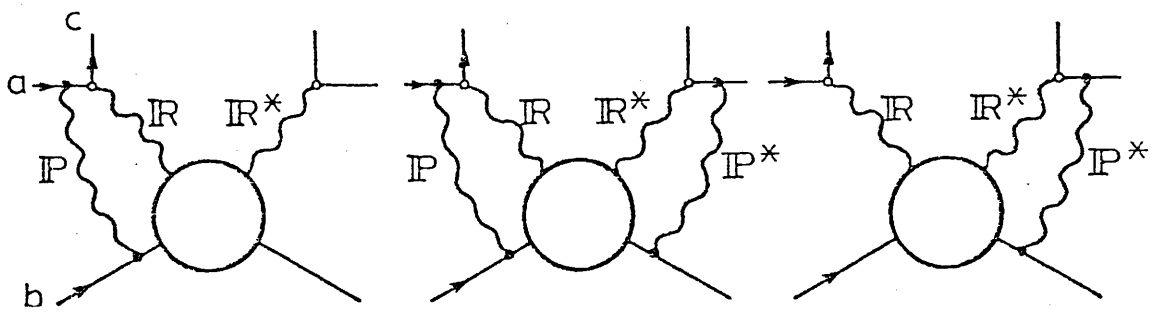

Figure c The Mueller-Regge diagrams corresponding to the absorptive corrections.

The values of the absorption parameters C and λ are obtained from two-body exclusive phenomenology and taken to be C = 0.7 and $\lambda = 0.068$ $(\text{Gev/c})^2$ [20]. The inclusive cross sections and density matrices are then calculated using the expressions given in Chapter 2 with H_{abs} in place of H.

III. INCLUSIVE VECTOR MESON PRODUCTION

The inclusive vector meson production in the fixed-M^2 and triple-Regge region is considered with absorptive corrections[21]. The Mueller-Regge (pole) amplitudes of the last chapter are modified to account for

rescatterings and the absorbed Mueller-Regge amplitudes are given at the end of this chapter.

The results of the study of the processes $K^- p \to \overline{K^{*o}}$ and $\pi^- p \to \rho^o$ are presented in Figures 1-5. The Regge pole exchanges are π, B, ρ and A_2 for $K^- p \to \overline{K^{*o}}$ and π and A_2 for $\pi^- p \to \rho^o$. The cuts are obtained through the absorption prescription. Various experiments have been reported for inclusive vector meson production[22], however, apart from $K^- p \to \overline{K^{*o}}$ at 14.3 Gev/c[23], the data are only qualitative.

In Figures 1-3 the model is compared with the $K^- p \to \overline{K^{*o}}$ data at 14.3 Gev/c. It can be seen that the inclusive cross sections are well described by the model both qualitatively and quantitatively except at small $|t|$. The suppression of the inclusive cross sections seen in the data at small $|t|$ is due to the kinematic boundary and can be seen to get more noticeable with increasing M^2. In contrast to the unabsorbed Mueller-Regge model where the normalisation is over-estimated in the absorbed version the normalisation is in reasonable agreement with the data.

The decay density matrix elements of the produced $\overline{K^{*o}}$ are given in the Gottfried-Jackson frame in Figure 3. The values given for Re ρ_{10} and ρ_{1-1} from the data are

compatible with zero. For ρ_{oo} the model predicts that ρ_{oo} increases with M^2/s as the absorption falls with increasing M^2 and ρ_{oo} approaches the unabsorbed value of the previous chapter. Although there is some improvement in the absorbed model to account for the data the situation is not entirely satisfactory. The ρ_{oo} data show only a slight increase with M^2/s. Note that the dual models[24] mentioned in the last chapter are also not compatible with the data.

In Figures 4-5 the predictions for $\pi^- \longrightarrow \rho^o$ are given at 15 and 205 Gev/c. The prediction for $K^- \xrightarrow{p} K^{*o}$ are also given at 205 Gev/c in Figures 2, 3 and 5. It can be seen that the fixed t vs, M^2/s plots show approximate scaling, this is compatible with the experimental evidence[22]. The density matrix elements also show very little s dependence.

IV. INCLUSIVE Δ PRODUCTION

The inclusive production of Δ is studied in the absorbed Mueller-Regge model[25]. The results of the investigation are presented in Figs. 6-8. From previous studies of the available data[26-30] it has been found that some forms of absorption are required in the triple-Regge model[25,26,31]. In Figs. 6-7 where the unabsorbed

calculations are also shown it can be seen that absorptive corrections go a long way in improving the agreement between the model and the data. Apart from a great improvement in the normalization the t and M^2/s dependences are also improved. At small $|t|$ the suppression of the inclusive cross sections is a kinematic effect and has been discussed. For $p\xrightarrow{K^-}\Delta^{++}$ where the M^2 channel is exotic the model gives a large estimate due to the relatively large ratio of $K^-\pi^-$ to $K^+\pi^-$ cross sections as discussed in the previous chapter.

The density matrix elements for the decaying Δ^{++} produced in $p\xrightarrow{K^-}\Delta^{++}$ at 14.3 Gev/c[29] are shown in Fig. 8. Chliapnikov et al[30] have given compatible density matrices for $p\xrightarrow{K^+}\Delta^{++}$ at 16 Gev/c. The values of Re ρ_{3-1} and Re ρ_{31} at around zero are reasonably accounted for by the model. For ρ_{33} the agreement between the model and the data is satisfactory at small M^2 but the model gives decreasing ρ_{33} with increasing M^2/s not seen in the data. Dao et al[30] and Barish et al[26] have presented the density matrices for $p\xrightarrow{p}\Delta^{++}$ at, respectively, 303 and 205 Gev/c with the values $\rho_{33} \sim 0.1$, Re $\rho_{31} \sim$ Re $\rho_{3-1} \sim 0$. Taking these data into account the situation is slightly improved. However, these data are very qualitative with no M^2 and t dependence given and no conclusion can be made on such

bases. Further data are required for useful tests of the model.

Predictions of the model are given for the inclusive cross sections and density matrices in Figs. 6-7 at 205 Gev/c.

V. DISCUSSION AND CONCLUSION

From the applications of the absorbed Mueller-Regge model it is evident that absorptive corrections are relevant to inclusive processes. The agreement between the absorbed model and the data compared to the unabsorbed model presents a significant improvement. In particular the normalization shows a marked improvement and the M^2 and t dependence of the inclusive cross sections are somewhat improved. When the density matrices are considered, the situation is less than totally satisfactory. Although the absorption improves the density matrices there seems to be some difficulties with the M^2 dependence. Further high quality data are required for the M^2 dependence of the density matrices before the situation can be clarified.

Note that the kinks observed in the theoretical curves near the edges of the plots are due to the computer-

graph-plotting package[32]. Near the kinematic cutoffs at the boundary of the phase space the plotter requires a very dense set of points to give smooth curves in the regions where the slopes are changing rapidly. In practice it is more convenient to plot a convenient number of points giving the resultant kinks. Throughout this work the numerical calculations have been performed in the framework of a computer programme developed for this purpose[33].

In our present study we have considered the inclusive production of resonances of the type $a \xrightarrow{b} c\uparrow$, where the polarization of the produced resonance c is taken into account. For such processes we average and sum over the helicities of a and b leaving the nonflip M^2-channel amplitudes. We then approximate the Rb amplitudes by the spin independent total cross sections and the Mueller-Regge amplitudes can then be factorized and absorption effected as shown in the appendix. The polarizations are expected to scale for this type of processes and can be seen in the Figs. However, for polarization of the type $a \xrightarrow{b\uparrow} c$ the spin flip Rb amplitudes are required. The M^2-channel scattering is dominated by meson exchange in the non-forward direction and absorption is necessary for this type of polarization effects which behave like $(M^2)^{-\frac{1}{2}}$ (12,13).

The absorption prescription we have adopted is based on a heuristic footing and is perhaps over-simple since absorptions in multiparticle amplitudes can be arbitrarily complicated. However, in adopting this simple form only two parameters C and λ (which are fixed in the present work) are introduced. With the eventual availability of high quality inclusive polarization data the model can be used in studying the magnitude and forms of cuts in inclusive processes. In two body phenomenology polarizations have played an important role in our understanding of cuts and the situation is expected to be similar in inclusive processes. The study of inclusive resonance production should provide the basis of our understanding of cuts in inclusive processes and good quality polarization data are required.

It is interesting to note that the polarization data we have considered are well accounted for by the model in the small M^2/s region (within the range of the validity of the fixed M^2 and triple-Regge limit). The absorbed Mueller-Regge model has been applied in the studies of meson [34] and nucleon [35] productions with improvement in the normalization and t and M^2 dependence. For polarization the model has been reasonably successful in accounting for the Λ

polarization in the process $p \xrightarrow{p} \Lambda$[36].

Recently, Craigie et al[37] have developed a model where all the multi-Reggeon exchanges in the fragmentation region are considered and work is in progress in applying the model to charge exchange meson productions[38]. There is an indication that other forms of absorptive corrections apart from the forms we have considered may be significant. However, further data are required for the clarification of this point.

APPENDIX

Using the notations of the previous section we write the Mueller-Regge amplitudes in the form:

$$H_i^{\lambda_c'\lambda_a',\lambda_c\lambda_a} = (\chi_i^{\lambda_c'\lambda_a'})^* W_i \chi_i^{\lambda_c\lambda_a},$$

where i again denotes the exchange.

Introducing the variable τ, the conjugate variable to the impact parameter, b, in the Fourier-Bessel transform. We then write $H^{\lambda_c'\lambda_a',\lambda_c\lambda_a}$, $(\chi^{\lambda_c'\lambda_a'})^*$ and $\chi^{\lambda_c\lambda_a}$ in terms of the variable τ using the relations:

$$\tau = 2k \sin\theta/2,$$
$$\tau^2 = \frac{k}{q}(t_{min} - t).$$

We obtain:

$$H^{\lambda_c'\lambda_a',\lambda_c\lambda_a}(\tau', \tau_1') = (\chi^{\lambda_c'\lambda_a'}(\tau_1'))^* W \chi^{\lambda_c\lambda_a}(\tau'),$$

where we have left out the M^2 and S labels.

Substituting this in the absorption integral yields:

$$H_{abs}^{\lambda_c'\lambda_a',\lambda_c\lambda_a}(\tau) = \left\{(\chi^{\lambda_c'\lambda_a'}(\tau))^* - \frac{c}{2\lambda}\exp(-\frac{\tau^2}{4\lambda}) \int_0^{\tau_1'} d\tau_1' (\chi^{\lambda_c'\lambda_a'}(\tau_i'))^* \cdot \right.$$
$$\left. \cdot \exp(-\frac{\tau_1'^2}{4\lambda}) \; I_\nu(\frac{\tau\tau_1'}{2\lambda})\right\}$$
$$W \left\{\chi^{\lambda_c\lambda_a}(\tau) - \frac{c}{2\lambda}\exp(-\frac{\tau^2}{4\lambda})\int_0^\infty \tau' d\tau' \chi^{\lambda_c\lambda_a}(\tau')\exp(-\frac{\tau'^2}{4\lambda}) I_\nu(\frac{\tau\tau'}{2\lambda})\right\}$$

The absorbed Mueller-Regge amplitudes can then be cast in the form:

$$H_{abs}^{\lambda_c'\lambda_a',\lambda_c\lambda_a} = \left\{(\chi^{\lambda_c'\lambda_a'})^* - (\mathcal{C}^{\lambda_c'\lambda_a'})^*\right\} W\left\{\chi^{\lambda_c\lambda_a} - \mathcal{C}^{\lambda_c\lambda_a}\right\},$$

where we have introduced:

$$\mathcal{C}^{\lambda_c\lambda_a} = \frac{c}{2\lambda}\exp(-\frac{\tau^2}{2\lambda})\int_0^\infty \tau' d\tau' \chi^{\lambda_c\lambda_a}(\tau')\exp(-\frac{\tau'^2}{4\lambda}) I_\nu(\frac{\tau\tau'}{2\lambda})$$

Since χ have been evaluated for the unabsorbed amplitudes the only objects to be determined are $\mathcal{C}$. For the evaluation of $\mathcal{C}$ the gamma functions in χ are parametrized in the form:

$$\Gamma_i\left[f(t)\right] = \sum_{j=1}^{2} A_i^j \exp B_i^j t$$

for analytic solution of the integrals. The parameters A and B are fitted over the t range of interest and given in a table at the end of this Appendix.

We define the variables:

$$\phi_i = \sum_{j=1}^{2} A_i^j \exp\left[B_i^j t_{min}\right] (\frac{\alpha_i'}{2})(\frac{s}{M^2}) \quad (\alpha_{o_i} + \alpha_i' t_{min} - J_i),$$

$$\zeta_i = \sum_{j=1}^{2} \frac{1}{4\lambda} + (B_i^j + \alpha_i' \ln(\frac{s}{M^2}))\frac{q}{k},$$

$$\zeta_i' = \zeta_i - i\pi\alpha'(\frac{q}{k}),$$

$$\gamma_i = \frac{\tau^2}{16\lambda^2\zeta_i},$$

$$\gamma_i' = \frac{\tau^2}{16\lambda^2\zeta_i'},$$

$$\eta_i = \xi_i \exp\left[-i\pi(\alpha_{o_i} + \alpha_i' t_{min})\right],$$

$$\gamma = \frac{C}{2\lambda} \exp\left[-\frac{\tau^2}{2\lambda}\right].$$

Then χ is put in the form:

$$\chi_i^{\lambda_c\lambda_a}(\tau) = \sum_{j=1}^{2} \phi_i \exp\left[-\frac{q}{k}(B_i^j + \alpha' \ln\frac{s}{M^2})\tau^2\right](1+\eta_i \exp i\pi\alpha'\tau^2\frac{q}{k}).$$
$$a_i^{\lambda_c\lambda_a}(\tau).$$

Substituting this in the expression for $\mathcal{E}$ gives:

$$\mathcal{E}_i^{\lambda_c\lambda_a}(\tau) = \gamma\int_0^\infty \exp(-\zeta_i\tau'^2)\, I_\nu(\frac{\tau\tau'}{2\lambda})a^{\lambda_c\lambda_a}(\tau')\,\tau'\,d\tau'$$

$$+\gamma\eta_i\int_0^\infty \exp(-\zeta_i'\tau'^2)\, I_\nu(\frac{\tau\tau'}{2\lambda})a^{\lambda_c\lambda_a}(\tau')\,\tau'\,d\tau'.$$

A table of all relevant integrals necessary for the evaluation of the absorption integrals are presented at the end of this section.

Working in the cms. as described in Appendix II, we obtain:

i) <u>Vector meson production, $0^- \xrightarrow{b} 1^-$</u>:

The vector mesons are in the beam fragmentation region and we write $P_a = P_1$, $P_b = P_2$, $P_c = P_3$. The particle a is spinless and its helicity label, λ_a, is dropped.

a) For pseudo scalar exchange we obtain:

$$\mathcal{C}_s^o = \frac{\gamma\phi_i}{2m_3}\left\{\frac{e^{\gamma_i}}{\zeta_i}\left(\left(qE_1 - kE_3\right) + \frac{E_3(\gamma_i+1)}{2\zeta_i k}\right.\right.$$
$$\left.\left. + \eta_i \frac{e^{\gamma_i'}}{\zeta_i'}\left(\left(qE_1 - kE_3\right) + \frac{E_3(\gamma_i'+1)}{2\zeta_i' k}\right)\right\},\right.$$

$$\mathcal{C}_s^{\pm 1} = \mp \frac{\gamma\phi_i}{\sqrt{2}} \frac{\tau}{8\lambda}\left\{\frac{e^{\gamma_i}}{\zeta_i^2}\left(1 - \frac{(\gamma_i+2)}{8\zeta_i k^2}\right) + \eta_i\left(\frac{e^{\gamma_i'}}{\zeta_i'^2}\right)\left(1 - \frac{(\gamma_i'+2)}{8\zeta_i' k^2}\right)\right\},$$

b) For vector exchange we obtain:

$$\mathcal{C}_V^0 = 0,$$

$$\mathcal{C}_V^{\pm 1} = -\sqrt{2}\, q(E_1+E_2)\gamma\phi_i \frac{\tau}{8\lambda}\left\{\frac{e^{\gamma_i}}{\zeta_i^2}\left(1 - \frac{(\gamma_i-2)}{8\zeta_i k^2}\right) + \right.$$
$$\left. + \eta_i \frac{e^{\gamma_i'}}{\zeta_i'^2}\left(1 - \frac{(\gamma_i'-2)}{8\zeta_i' k^2}\right)\right\}.$$

The relevant couplings are:

$$G_s = -3hF,$$

$$G_v = \frac{3h(D+2S)}{m_1+m_3}$$

ii) <u>Δ production, $\frac{1}{2}^+ \xrightarrow{b} \frac{3}{2}^+$:</u>

The Δ are produced in the target fragmentation region and we use $P_a = P_2$, $P_b = P_1$, $P_c = P_4$.

We introduce the variables:

$$E = \sqrt{(E_2+m_2)(E_4+m_4)}$$

$$C_{\pm} = E^2 \pm kq$$

$$D = \frac{k \sin\theta}{E}$$

$$F = \frac{2k q(E_1+E_2)\sin\theta}{E}$$

Then the $\mathcal{E}^{\lambda_c\lambda_a}$ are given by:

a) For pseudoscalar exchange:

$$\mathcal{E}_s^{3,1} = -\frac{kC_-}{\sqrt{2}E}\gamma\phi_i \frac{\tau}{2k\lambda}\left\{\left[\frac{e^{\gamma_i}}{\zeta_i^2}\left(1-\frac{(\gamma_i+2)}{4k^2\zeta_i}\right)\right]+\eta_i\begin{bmatrix}\gamma_i\to\gamma_i'\\ \zeta_i\to\zeta_i'\end{bmatrix}\right\},$$

$$\mathcal{E}_s^{1,1} = \frac{1}{\sqrt{3}E}\gamma\phi_i\left[\frac{C_+}{\sqrt{2}}\frac{1}{4k}\left\{\left[\frac{e^{\gamma_i}}{\zeta_i^2}\left((\gamma_i+1)-\frac{[(\gamma_i+3)(\gamma_i+1)-1]}{8k^2\zeta_i}\right)\right]\right.\right.$$

$$\left.+\eta_i\begin{bmatrix}\gamma_i\to\gamma_i'\\ \zeta_i\to\zeta_i'\end{bmatrix}\right\}+\frac{\sqrt{2}}{2m_4}qE_2C_-\left\{\left[\frac{e^{\gamma_i}}{\zeta_i}\left(1-\frac{(\gamma_i+1)}{8k^2\zeta_i}\right)\right]+\eta_i\begin{bmatrix}\gamma_i\to\gamma_i'\\ \zeta_i\to\zeta_i'\end{bmatrix}\right.$$

$$\left.\left.-\frac{\sqrt{2}}{2m_4}kE_4C_-\left\{\left[\frac{e^{\gamma_i}}{\zeta_i}\left(1-\frac{(\gamma_i+1)}{16k^2\zeta_i}\right)\right]+\eta_i\begin{bmatrix}\gamma_i\to\gamma_i'\\ \zeta_i\to\zeta_i'\end{bmatrix}\right\}\right],$$

$$\mathcal{E}_s^{-1,1} = \frac{1}{\sqrt{3}E}\gamma\phi_i\frac{\tau}{8k\lambda}\left[\frac{C_-}{\sqrt{2}}k\left\{\left[\frac{e^{\gamma_i}}{\zeta_i^2}\left(1-\frac{(\gamma_i+2)}{4k^2\zeta_i}\right)\right]+\eta_i\begin{bmatrix}\gamma_i\to\gamma_i'\\ \zeta_i\to\zeta_i'\end{bmatrix}\right.\right.$$

$$-\frac{\sqrt{2}}{2m_4}qE_2C_+\left\{\frac{e^{\gamma_i}}{\zeta_i^2}+\eta_i\frac{e^{\gamma_i'}}{\zeta_i'^2}\right\}+\frac{\sqrt{2}}{2m_4}kE_4C_+\left\{\left[\frac{e^{\gamma_i}}{\zeta_i^2}\left(1-\frac{(\gamma_i+2)}{2k^2\zeta_i}\right)\right]\right.$$

$$\left.\left.\left.+\eta_i\begin{bmatrix}\gamma_i\to\gamma_i'\\ \zeta_i\to\zeta_i'\end{bmatrix}\right\}\right],$$

$$\mathcal{E}_s^{-3,1} = -\frac{kC_+}{\sqrt{2}E}\gamma\phi_i\frac{\tau^2}{64k^2\lambda^2}\left\{\left[\frac{e^{\gamma_i}}{\zeta_i^3}\left(1-\frac{(\gamma_i+3)}{8k^2\zeta_i}\right)\right]+\eta_i\begin{bmatrix}\gamma_i\to\gamma_i'\\ \zeta_i\to\zeta_i'\end{bmatrix}\right\},$$

with:

$$\mathcal{E}_s^{3,-1} = \mathcal{E}_s^{-3,1}, \qquad \mathcal{E}_s^{1,-1} = -\mathcal{E}_s^{-1,1}$$

$$\mathcal{E}_s^{-1,-1} = \mathcal{E}_s^{1,1}, \qquad \mathcal{E}_s^{-3,-1} = -\mathcal{E}_s^{3,1}.$$

b) For vector exchange we have:

$$\mathcal{E}_v^{3,1} = -\frac{\sqrt{2}\,k\,q(E_1+E_2)C_-}{E}\gamma_i\phi_i\frac{\tau}{8k\lambda}\left\{\left[\frac{e^{\gamma_i}}{\zeta_i^2}\left(1-\frac{(\gamma_i+2)}{4k^2\zeta_i}\right)\right]\right.$$

$$\left.+\eta_i\left[\begin{matrix}\gamma_i\to\gamma_i'\\ \zeta_i\to\zeta_i'\end{matrix}\right]\right\},$$

$$\mathcal{E}_v^{1,1} = \frac{2\,k\,q(E_1+E_2)}{\sqrt{6}E}C_+\gamma_i\phi_i\frac{1}{4k^2}\left\{\left[\frac{e^{\gamma_i}}{\zeta_i^2}\left((\gamma_i+1)-\right.\right.\right.$$

$$\left.\left.\left.-\frac{[(\gamma_i+3)(\gamma_i+1)-1]}{8k^2\zeta_i}\right)\right]+\eta_i\left[\begin{matrix}\gamma_i\to\gamma_i'\\ \zeta_i\to\zeta_i'\end{matrix}\right]\right\},$$

$$\mathcal{E}_v^{-1,1} = -\frac{2\,k\,q(E_1+E_2)}{\sqrt{6}E}C_-\gamma_i\phi_i\frac{\tau}{8k\lambda}\left\{\left[\frac{e^{\gamma_i}}{\zeta_i^2}\left(1-\frac{(\gamma_i+2)}{4k^2\zeta_i}\right)\right]\right.$$

$$\left.+\eta_i\left[\begin{matrix}\gamma_i\to\gamma_i'\\ \zeta_i\to\zeta_i'\end{matrix}\right]\right\},$$

$$\mathcal{E}_v^{-3,1} = \frac{\sqrt{2}\,k\,q(E_1+E_2)C_+}{E}\gamma_i\phi_i\frac{\tau^2}{64k^2\lambda^2}\left\{\left[\frac{e^{\gamma_i}}{\zeta_i^3}\left(1-\frac{(\gamma_i+3)}{8k^2\zeta_i}\right)\right]\right.$$

$$\left.+\eta_i\left[\begin{matrix}\gamma_i\to\gamma_i'\\ \zeta_i\to\zeta_i'\end{matrix}\right]\right\},$$

and

$$\mathcal{C}_v^{3,-1} = -\mathcal{C}_v^{-3,1}, \qquad \mathcal{C}_v^{1,-1} = \mathcal{C}_v^{-1,1},$$

$$\mathcal{C}_v^{-1,-1} = -\mathcal{C}_v^{1,1}, \qquad \mathcal{C}_v^{-3,-1} = \mathcal{C}_v^{3,1}.$$

The relevant couplings are, respectively:

$$G_s = \frac{g}{m_B} G, \quad \text{and}$$

$$G_v = -\frac{g}{2m_B^2} G.$$

TABLE

Parameters for the gamma function approximation

Exchange	A^1	B^1	A^2	B^2
π, B	-59.8910	41.12	-14.143	3.398
ρ, A_2	0.8914	2.96	0.778	-0.072
ω, f	0.8076	2.75	0.645	-0.266

The parameters are obtained by a fit in the range $0 \leqslant |t| \leqslant 2$.

TABLE OF INTEGRALS AND OTHER USEFUL MATHEMATICAL RELATIONS

1. Fourier-Bessel or Hankel transform[39]:

The Fourier-Bessel transform is given by:

$$F(b) = \int_0^\infty J_\nu(b\tau)\, Q(\tau)\tau\, d\tau,$$

and the inverse transform is:

$$Q(\tau) = \int_0^\infty J_\nu(b\tau)\, F(b)\, bdb,$$

where J_ν is the Bessel function of the first kind and $\nu > -1$.

2. Orthogonality conditions for $J_\nu(b\tau)$:

We have:

$$\int_0^\infty J_\nu(b\tau)\, J_\nu(b'\tau)\tau\, d\tau = \frac{1}{b}\,\delta(b' - b),$$

and

$$\int_0^\infty J_\nu(b\tau)\, J_\nu(b\tau')\, bdb = \frac{1}{\tau}\,\delta(\tau' - \tau).$$

3. We have the relation:

$$\int_0^\infty db\; b\; J_\nu(b\tau) J_\nu(b\tau')\, C \exp(-\lambda b^2)$$

$$= \frac{C}{2\lambda} \exp\left(-\frac{\tau^2 + \tau'^2}{4\lambda}\right) I_\nu\left(\frac{\tau\tau'}{2\lambda}\right),$$

where I_ν is the Bessel function of imaginary argument and related to $J_\nu(x)$ through:

$$I_\nu(x) = i^{-\nu} J_\nu(ix) \quad \text{for integral } \nu.$$

4. Integral for the evaluation of $\mathcal{E}^{(40)}$:

$$\int_0^\infty x^\mu \exp(-\alpha x^2) I_\nu(kx)dx \equiv \int_0^\infty x^\mu \exp(-\alpha x^2) i^{-\nu} I_\nu(ikx)dx$$

$$= \frac{k^\nu \Gamma(\frac{\nu+\mu+1}{2})}{2^{\nu+1}\alpha^{\frac{1}{2}(\mu+\nu+1)}\Gamma(\nu+1)} {}_1F_1\left(\frac{\nu+\mu+1}{2}, \nu+1; \frac{k^2}{4\alpha}\right),$$

for $\mathrm{Re}\,\alpha > 0$, $\mathrm{Re}\,\mu+\nu > -1$, where ${}_1F_1(\alpha,\gamma;z) \equiv \phi(\alpha,\gamma;z)$ is the degenerate hypergeometric function and $\Gamma(n)$ is the gamma function.

5. Functional relations for the degenerate hypergeometric function:

We have:

i) $\phi(\alpha,\alpha;z) = \exp(z).$

ii) $\alpha\phi(\alpha+1,\gamma;z) = (z+2\alpha-\gamma)\phi(\alpha,\gamma;z) + (\gamma-\alpha)\phi(\alpha-1,\gamma;z).$

For $\gamma = \alpha$ we obtain:

iii) $\phi(\alpha+1,\alpha;z) = \frac{z+\alpha}{\alpha}\exp(z).$

REFERENCES

1. A.H. Mueller, Phys. Rev., D2, 2963 (1970).

2. See e.g.

   D. Horn and F. Zachariasen, Hadron Physics at Very High Energies, Benjamin (1973);

   S. Humble, Introduction to Particle Production in Hadron Physics.

3. H.M. Chan, Lectures given at the GIFT Seminar, University of Barcelona, Spain (1973); Rutherford Laboratory Report, RL-73-062;

   R.G. Roberts, Proc. 14th Scottish Universities Summer School (1973), eds. R.L. Crawford and R. Jennings, Academic Press (1974).

4. P. Choudhury, K.J.M. Moriarty, J.H. Tabor and A. Ungkitchanukit, Acta Phys. Austr., 47 (1977).

5. P. Choudhury, K.J.M. Moriarty, J.H. Tabor and A. Ungkitchanukit, Acta Phys. Austr. (to be published).

6. N.S. Craigie, G. Kramer and J. Körner, Nucl. Phys., B68, 509 (1974).

7. F. Brasse, Proc. of Int. Symposium on Electron-Photon Interactions at High Energies, Bonn, 1973.

8. N.S. Craigie and G. Kramer, Nucl. Phys., B75, 509 (1974).

9. Private communication on the preliminary data to G. Kramer by H. Genzel.

10. L. Dick et al., Phys. Letters, 57B, 93 (1975).

11. H.D.I. Abarbanel and D.J. Gross, Phys. Rev. Letters, 26, 732 (1971);

    R.J.N. Phillips, G.A. Ringland and R.P. Worden, Phys. Letters, 40B, 239 (1972);

    P. Salin and J. Soffer, Nucl. Phys., B71, 125 (1974).

12. J. Soffer and D. Wray, Nucl. Phys., B73, 231 (1974).

13. K. Ahmed, N.S. Craigie, J. Körner and G. Kramer, Nucl. Phys., B106, 275 (1976).

14. P.D.B. Collins and E.J. Squires, Regge poles in particle physics, (Springer, Berlin, 1968);
P.D.B. Collins, Phys. Reports, 1C, 103 (1971).

15. J.L. Cardy and A. White, Phys. Letters, 47B, 445 (1973);
I. Halliday and C.T. Sachrajda, Phys. Rev., D8, 3598 (1973);
A.A. Migdal, A.M. Polyakov and K.A. Ter-Martirosyan, Phys. Letters, 48B, 239 (1974);
H.D.I. Abarbanel, J. Bartels, J.M. Bronzan and D. Sidhu, Phys. Rev., D12, 2496 (1975).

16. For a review of the decoupling problems see, e.g.
R.C. Brower, C.E. De Tar and J.H. Weis, Phys. Reports, 14C, 257 (1974).

17. J.D. Jackson, Rev. Mod. Phys., 37, 484 (1965).

18. J. Pumplin, Phys. Rev., D13, 1249 (1976); Phys. Rev., D13, 1261 (1976).

19. L. Caneschi and A. Schwimmer, Nucl. Phys., B44, 31 (1972); Nucl. Phys., B48, 519 (1972).

20. S.A. Adjei, P.A. Collins, B.J. Hartley, K.J.M. Moriarty and R.W. Moore, Ann. of Phys. (N.Y.), 75, 405 (1973).

21. P. Choudhury, K.J.M. Moriarty. J.H. Tabor and A. Ungkitchanukit, Absorption Corrections in the one-particle inclusive production of vector mesons in the triple-Regge region, R.H.C. Preprint, June 1976.

22. F.C. Winkelmann et al., Phys. Letters, 56B, 101 (1975);
D. Fong et al., Phys. Letters, 60B, 124 (1975);
M. Deutschmann et al., Nucl. Phys., B103, 426 (1976);
J. Brau et al., Nucl. Phys., B99, 232 (1975);
J. Bartke et al., Nucl. Phys., B107, 93 (1976).

23. K. Paler et al., Nucl. Phys., B96, 1 (1975).

24. K. Kang and P. Shen, Phys. Rev., D7, 164 (1973);
J. Randa, Phys. Rev., D7, 2236 (1973); Phys. Rev., D9, 2612 (1974).

25. P. Choudhury, K.J.M. Moriarty. J.H. Tabor and A. Ungkitchanukit, Absorptive corrections in the inclusive production of Δ in the triple-Regge region, R.H.C. Preprint, August 1976.

26. S.J. Barish et al., Phys. Rev., D12, 1260 (1975).

27. J.V. Beaupre et al., Nucl. Phys., B67, 413 (1973);
K.J.M. Barnham: private communication.

28. P. Bosetti et al., Nucl. Phys., B81, 61 (1974);
K.J.M. Barnham: private communication.

29. M. Bardadin-Otwinowska et al., Paper presented at the International Conference on Elementary Particles, Palermo, June 1975.

30. P. Gregory et al., Paper submitted to the 2nd Aix-en-Provence International Conference on Elementary Particles, September 1973; P. Gregory and H. Muirhead, private communication.
J.P. De Brion et al., Phys. Rev. Letters, 34, 910 (1975);
F.T. Dao et al., Phys. Rev. Letters, 30, 34 (1973);
D. Brick et al., Phys. Rev. Letters, 31, 488 (1973);
P.V. Chliapnikov et al., Nucl. Phys., B105, 510 (1976).

31. E. Gotsman, Phys. Rev., D9, 1575 (1974).

32. J. Anderson, K.J.M. Moriarty and R.C. Beckwith, Comp. Phys. Comm., 9, 85 (1975).

33. K.J.M. Moriarty and J.H. Tabor, A Program for calculating the observables for single-particle-inclusive production reactions, R.H.C. Preprint, July, 1976.

34. P. Choudhury, K.J.M. Moriarty, J.H. Tabor and A. Ungkitchanukit, Acta Phys. Austr., 47 (1977).

35. K.J.M. Moriarty, J.P. Rad, J.H. Tabor and A. Ungkitchanukit, Absorptive Corrections to single-particle-inclusive charge exchange nucleon reaction, R.H.C. Preprint, May 1976.

36. K.J.M. Moriarty, J.P. Rad, J.H. Tabor and A. Ungkitchanukit, Nuovo Cimento Letters, 17 (1976);

Proc. of AIP Conf., Particles and Fields subseries. ZGS Summer Symposium on High Energy Physics with Polarized Beams and Targets Argonne, Illinois, August 1976. Edited by M. Marshak.

37. N.S. Craigie, K.J.M. Moriarty and J.H. Tabor, A Closed Eikonal formula for summing all multiple Reggeon exchange contributions to the inclusive six-point function in the fragmentation region, CERN Preprint TH-2140 (1976).

38. N.S. Craigie, K.J.M. Moriarty, J.H. Tabor and H.N. Thompson, R.H.C. Preprint (in preparation).

39. See any standard mathematical text, e.g. G. Goertzel and N. Tralli, "Some Mathematical Methods of Physics", McGraw-Hill Book Co., Inc. (1960).

40. I.S. Gradsteyn and I.M. Ryzhik, "Tables of Integral Series and Products", Academic Press (1965).

FIGURE CAPTIONS

Fig. 1. The inclusive cross section for $K^- p \to \overline{K^{*o}}$ for fixed M^2/s plotted vs. t at 14.3 Gev/c. Data from Ref. 23.

Fig. 2. The inclusive cross section for $K^- p \to \overline{K^{*o}}$ for fixed t plotted vs. M^2/s at 14.3 and 205 Gev/c. Data at 14.3 Gev/c from Ref. 23.

Fig. 3 The density matrix elements for the decay of the $\overline{K^{*o}}$ produced in $K^- p \to \overline{K^{*o}}$ for fixed M^2/s plotted vs. t in the Gottfried-Jackson frame at 14.3 and 205 Gev/c. Data at 14.3 Gev/c from Ref. 23.

Fig. 4(a) The inclusive cross section for fixed M^2/s plotted vs. t for $\pi^- p \to \rho^o$ at 15 and 205 Gev/c.

(b) The density matrix elements for the decay of the ρ^o produced in $\pi^- p \to \rho^o$ for fixed M^2/s plotted vs. t in the Gottfried-Jackson frame at 15 and 205 Gev/c.

Fig. 5(a) The inclusive cross section for $K^- p \to \overline{K^{*o}}$ for fixed M^2/s plotted vs. t at 205 Gev/c.

(b) The inclusive cross section for $\pi^- p \to \rho^o$ for fixed t plotted vs. M^2/s at 205 Gev/c.

Fig. 6 The inclusive cross section at fixed t plotted vs. M^2/s for $p \xrightarrow{\pi^+} \Delta^{++}$ at $24^{(*)}$, 16 and 205 Gev/c and for $p \xrightarrow{K^-} \Delta^{++}$ at 16 Gev/c. Data at 24, 16 Gev/c for the π^+ beam from Ref. 27 and at 16 Gev/c for the K^- beam from Ref. 28.

* At 24 Gev/c pole contribution shown for comparison.

Fig. 7 The inclusive cross section at fixed M^2/s plotted vs. t (a), (b) for $p \xrightarrow{\pi^+} \Delta^{++}$ at 24(*) and 205(*) Gev/c and, (c) for $p \xrightarrow{K^-} \Delta^{++}$ at 14.3 Gev/c. Data at 24 Gev/c from Ref. 27.

(d) The density matrix elements for the decay of the Δ^{++} produced in $p \xrightarrow{\pi^+} \Delta^{++}$ for fixed M^2/s vs. t in the Gottfried-Jackson frame at 205 Gev/c.

* The prediction of the unabsorbed Mueller-Regge model is shown for comparison.

Fig. 8 The density matrix elements for the decay of the Δ^{++} produced in $p\xrightarrow{K^-}\Delta^{++}$ for fixed M^2/s plotted vs. t. in the Gottfried-Jackson frame at 14.3 Gev/c. Data from Ref. 29.

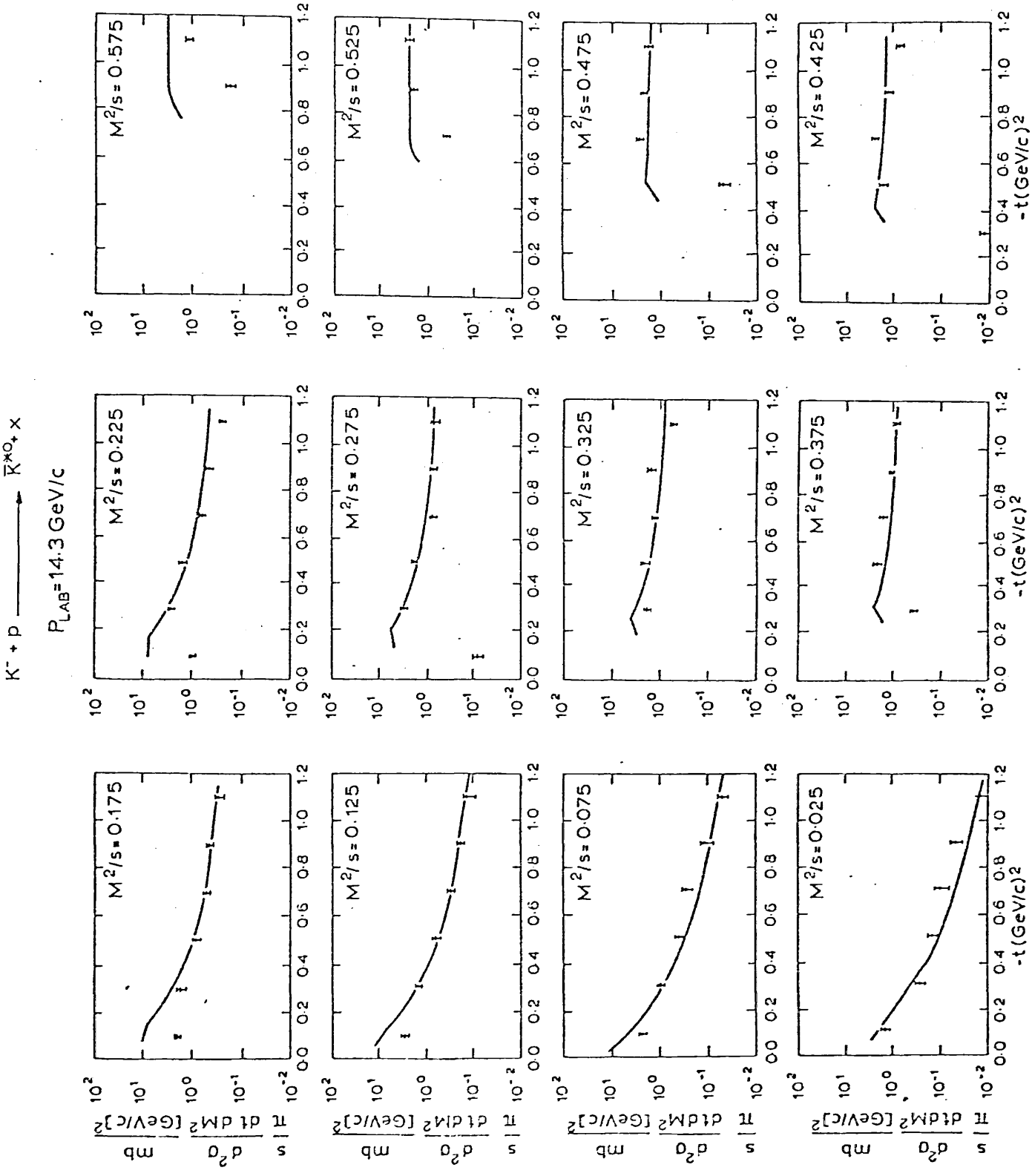
K⁻ + p → K*⁰₊ + X
P_LAB=14.3 GeV/c
M²/s=0.175
M²/s=0.225
M²/s=0.275
M²/s=0.325
M²/s=0.375
M²/s=0.425
M²/s=0.475
M²/s=0.525
M²/s=0.575
M²/s=0.025
M²/s=0.075
M²/s=0.125
π/s d²σ/dtdM² mb/[GeV/c]²
-t(GeV/c)²

Fig. 1.

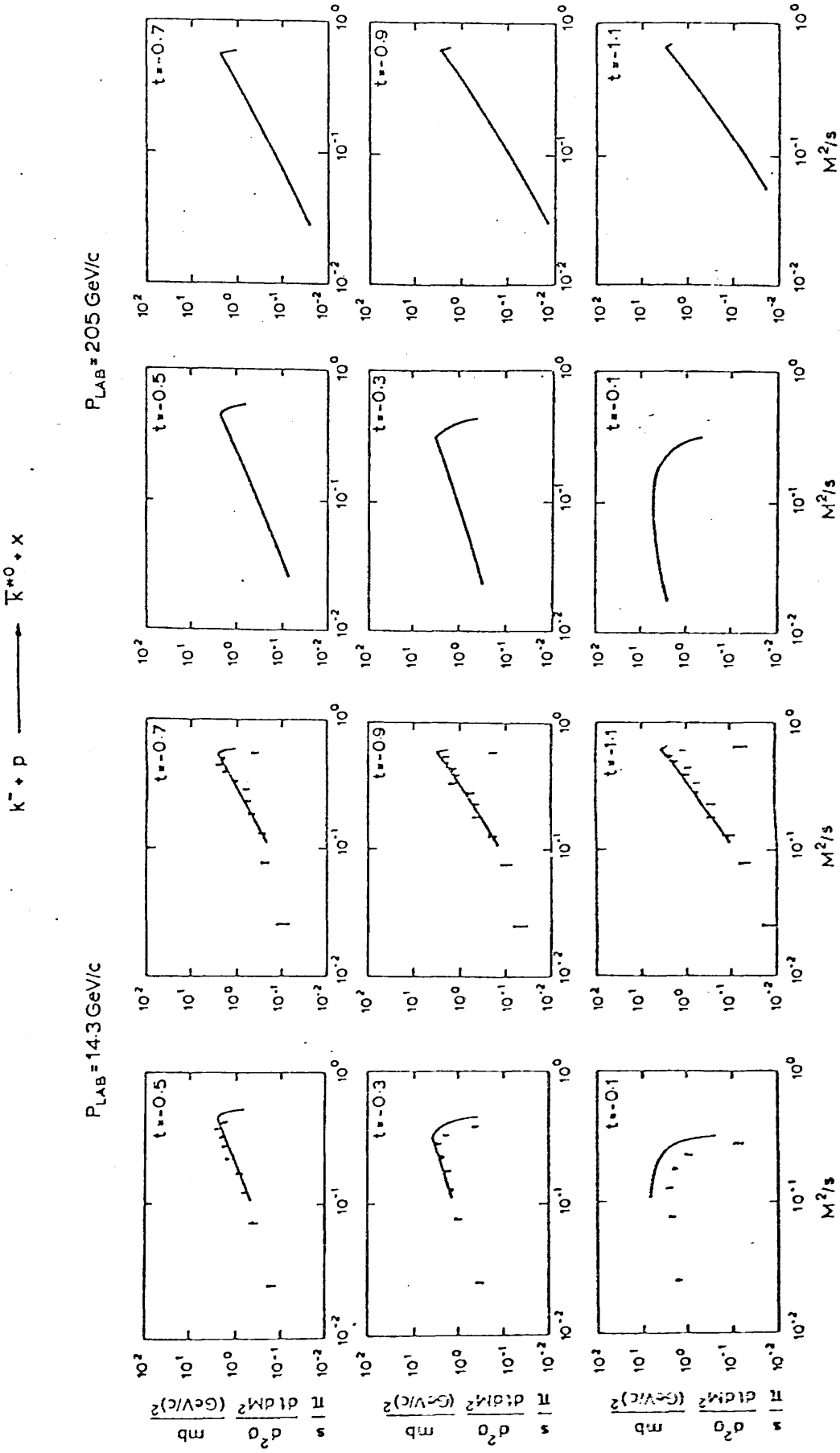
K⁻ + p ⟶ K*0 + X
P_LAB = 14.3 GeV/c
P_LAB = 205 GeV/c
t = -0.5
t = -0.7
t = -0.3
t = -0.9
t = -0.1
t = -1.1
M²/s
(a)
(b)

Fig. 2

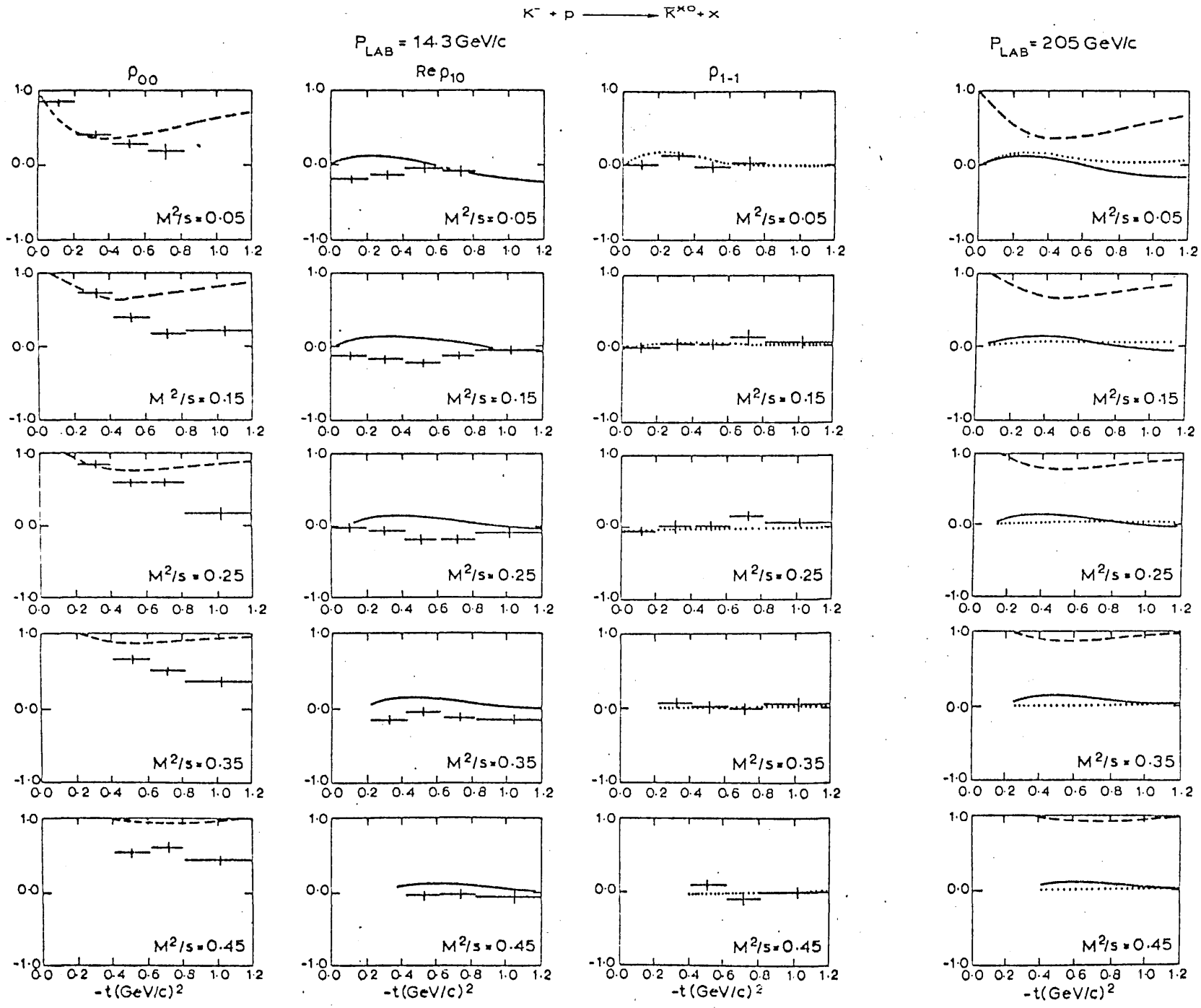
K⁻ + p ⟶ K̄⁰ + X
P_LAB = 14·3 GeV/c
P_LAB = 20·5 GeV/c
ρ00
Re ρ10
ρ1-1
M²/s = 0·05
M²/s = 0·15
M²/s = 0·25
M²/s = 0·35
M²/s = 0·45
-t (GeV/c)²
a.
b.

Fig. 3

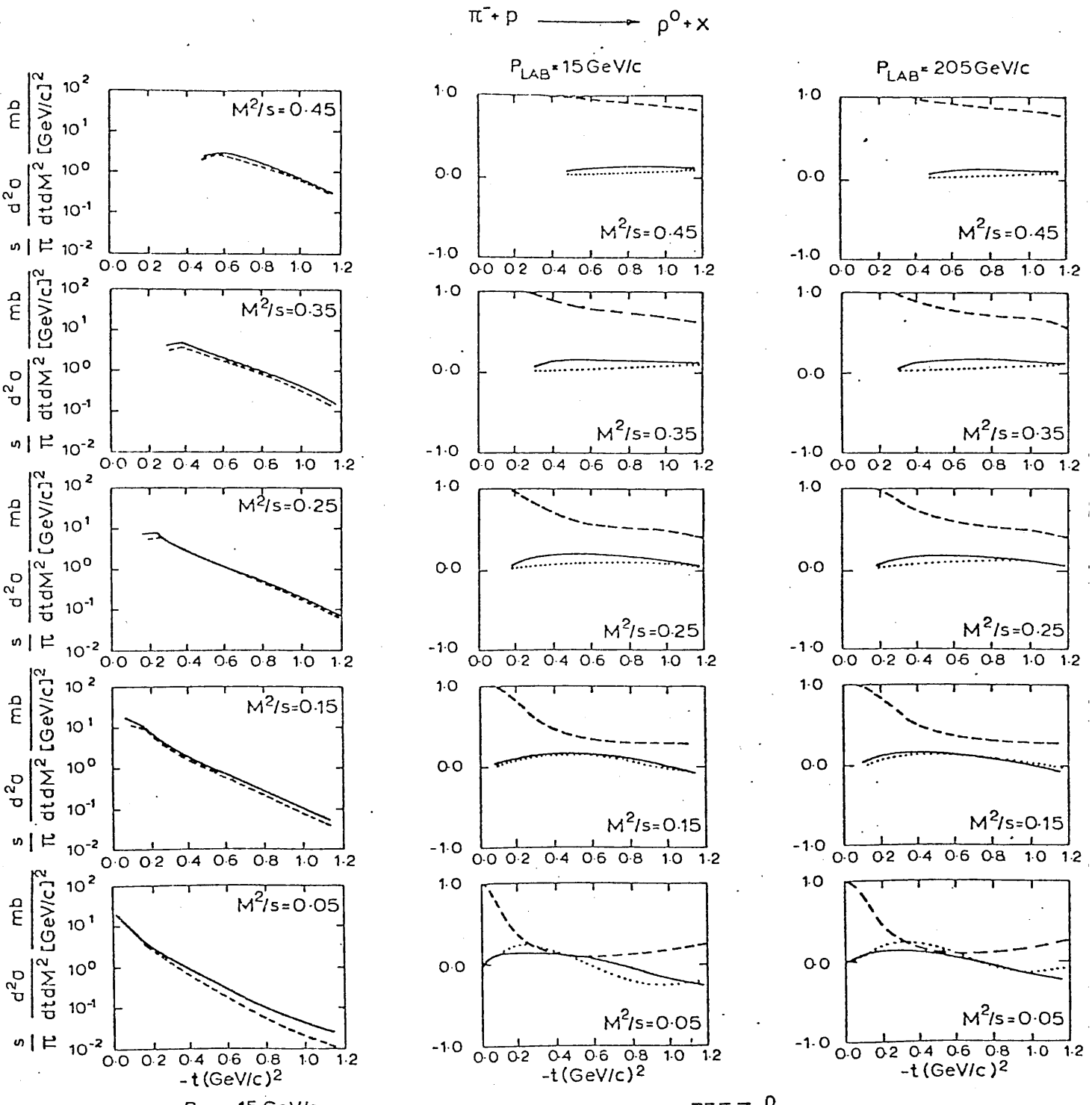
π⁻ + p ⟶ ρ⁰ + X
P_LAB = 15 GeV/c
P_LAB = 205 GeV/c
M²/s = 0·45
M²/s = 0·35
M²/s = 0·25
M²/s = 0·15
M²/s = 0·05
s/π d²σ/dtdM² mb/[GeV/c]²
-t (GeV/c)²
P_LAB = 15 GeV/c
P_LAB = 205 GeV/c.
ρ₀₀
Re ρ₁₀
ρ₁₋₁

a. b.

Fig. 4

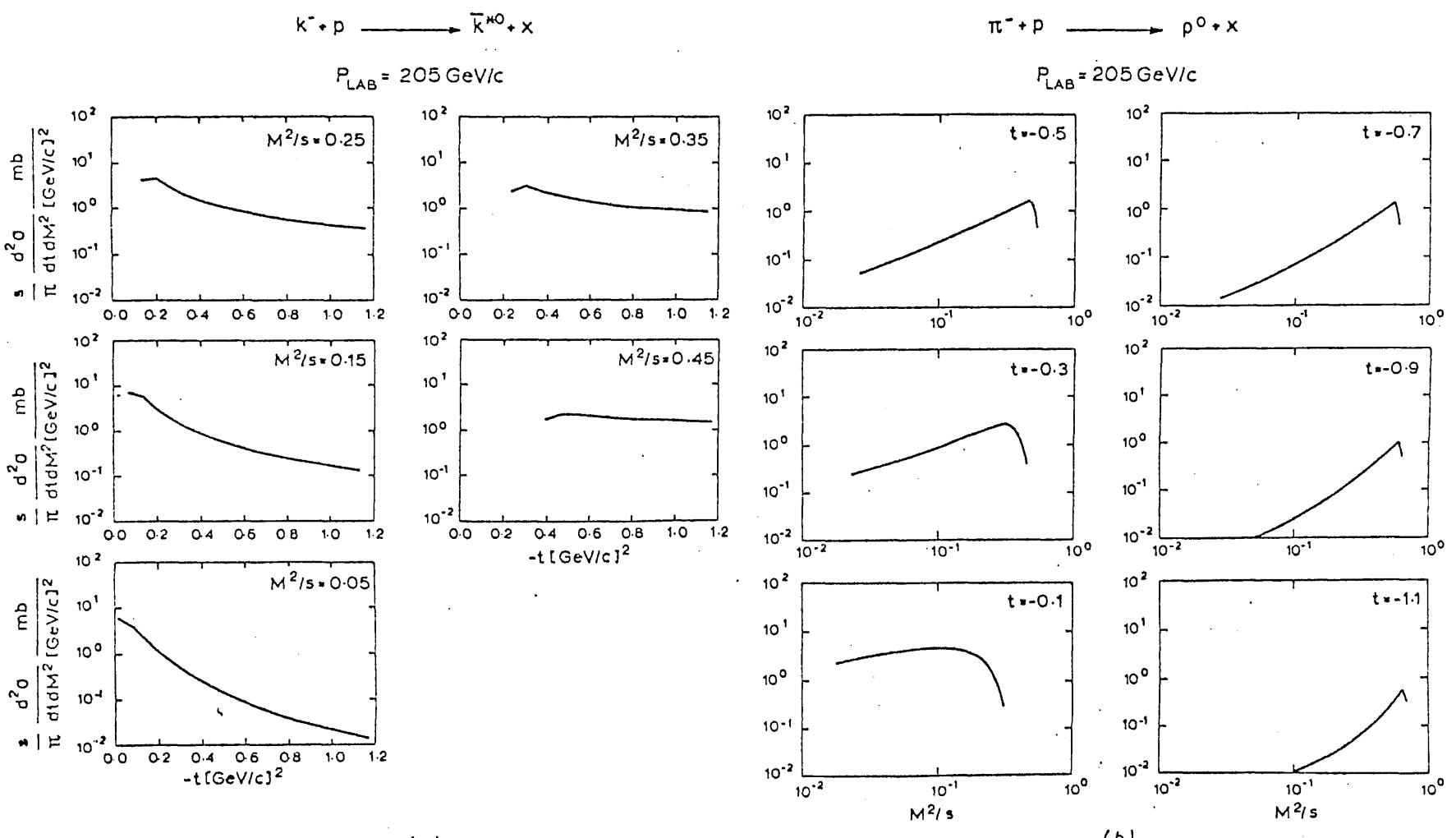
$K^- + p \longrightarrow \bar{K}^{*0} + X$
$P_{LAB} = 205$ GeV/c
$\pi^- + p \longrightarrow \rho^0 + X$
$P_{LAB} = 205$ GeV/c
$\frac{s}{\pi} \frac{d^2\sigma}{dt\,dM^2}$ mb/[GeV/c]^2
$M^2/s = 0.25$
$M^2/s = 0.35$
$M^2/s = 0.15$
$M^2/s = 0.45$
$M^2/s = 0.05$
$-t$ [GeV/c]^2
$t = -0.5$
$t = -0.7$
$t = -0.3$
$t = -0.9$
$t = -0.1$
$t = -1.1$
M^2/s
(a)
(b)

Fig. 5

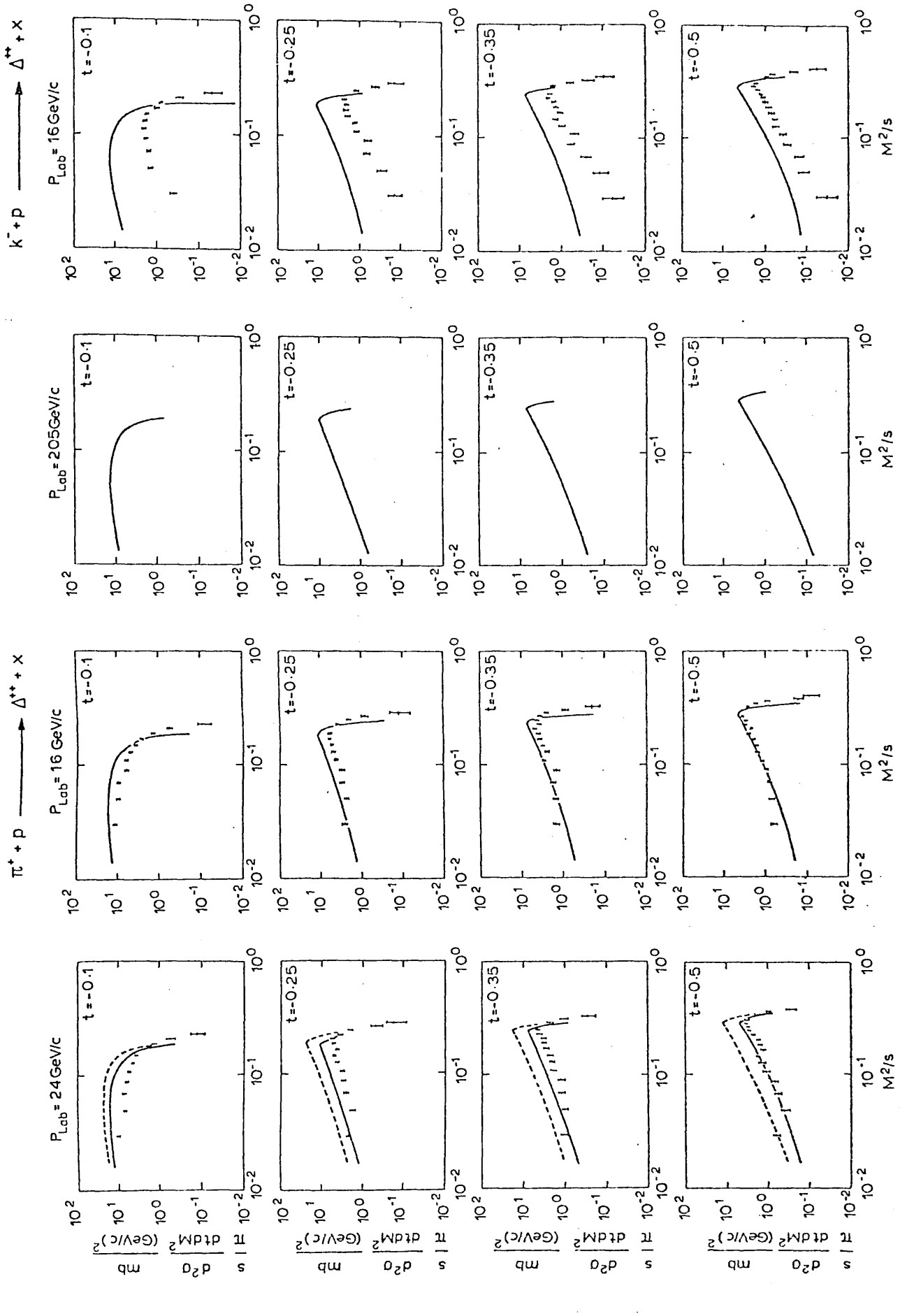
π⁺ + p ——→ Δ⁺⁺ + X
K⁻ + p ——→ Δ⁺⁺ + X
P_Lab = 24 GeV/c
P_Lab = 16 GeV/c
P_Lab = 205 GeV/c
P_Lab = 16 GeV/c
t=-0.1
t=-0.25
t=-0.35
t=-0.5
s/π d²σ/dtdM² mb/(GeV/c)²
M²/s
------ pole

Fig. 6

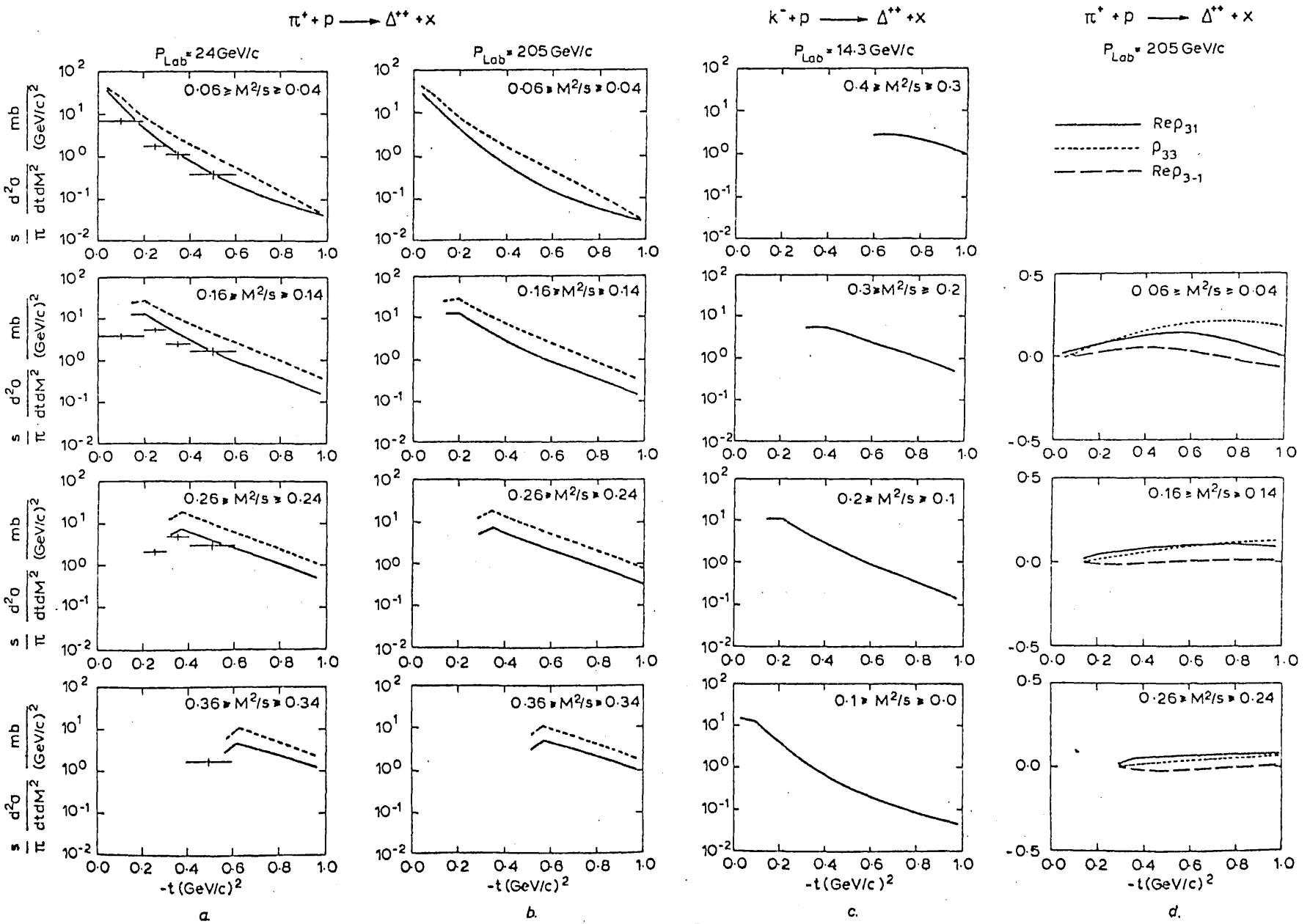
π⁺ + p ⟶ Δ⁺⁺ + X
k⁻ + p ⟶ Δ⁺⁺ + X
π⁺ + p ⟶ Δ⁺⁺ + X
P_Lab = 24 GeV/c
P_Lab = 205 GeV/c
P_Lab = 14·3 GeV/c
P_Lab = 205 GeV/c
0·06 ≥ M²/s ≥ 0·04
0·16 ≥ M²/s ≥ 0·14
0·26 ≥ M²/s ≥ 0·24
0·36 ≥ M²/s ≥ 0·34
0·4 ≥ M²/s ≥ 0·3
0·3 ≥ M²/s ≥ 0·2
0·2 ≥ M²/s ≥ 0·1
0·1 ≥ M²/s ≥ 0·0
Reρ31
ρ33
Reρ3-1
s/π d²σ/dtdM² mb/(GeV/c)²
-t (GeV/c)²
a.
b.
c.
d.
----- pole

Fig. 7

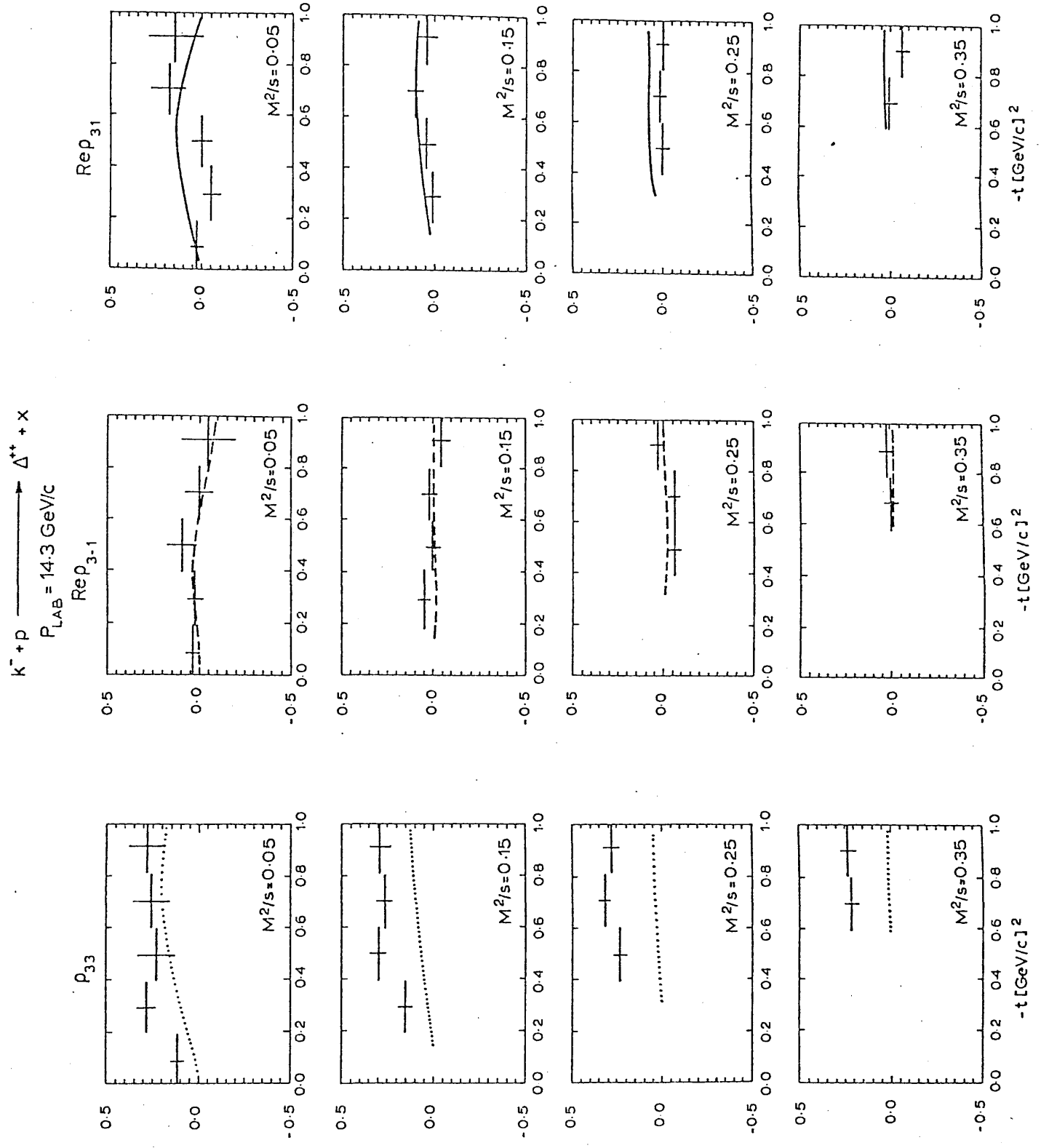
$K^- + p \longrightarrow \Delta^{++} + X$
$P_{LAB} = 14.3$ GeV/c
ρ_{33}
$\mathrm{Re}\rho_{3-1}$
$\mathrm{Re}\rho_{31}$
$M^2/s = 0.05$
$M^2/s = 0.15$
$M^2/s = 0.25$
$M^2/s = 0.35$
$-t$ [GeV/c]^2

APPENDIX I

NOTATIONS, CONVENTIONS AND NORMALIZATIONS

We adopt the metric:

$$g_{\mu\nu} = \begin{pmatrix} 1 & & & \\ & -1 & & 0 \\ & & -1 & \\ & 0 & & -1 \end{pmatrix}$$

$P_\mu = (E, \underline{p})$ denotes a 4-vector and the scalar product is given by:

$$P_\mu P_\mu = E^2 - \underline{p}^2$$

The completely antisymmetric Levi-Civita tensor is defined such that:

$$\varepsilon_{\mu\nu K\lambda} = \begin{cases} 1 & \text{for even permutation of the indices,} \\ 0 & \text{when two indices are identical,} \\ -1 & \text{for odd permutation of the indices,} \end{cases}$$

with $\varepsilon_{0123} = 1$.

The Pauli matrices are represented by:

$$\sigma_1 = \begin{pmatrix} 0 & 1 \\ 1 & 0 \end{pmatrix}, \quad \sigma_2 = \begin{pmatrix} 0 & -i \\ i & 0 \end{pmatrix}, \quad \sigma_3 = \begin{pmatrix} 1 & 0 \\ 0 & -1 \end{pmatrix}$$

and the Dirac matrices assume the form:

$$\gamma_\mu = (\gamma_o, \underline{\gamma}) \qquad \text{with}$$

$$\gamma_o = \begin{pmatrix} 1 & 0 \\ 0 & -1 \end{pmatrix}, \qquad \underline{\gamma} = \begin{pmatrix} 0 & \underline{\sigma} \\ -\underline{\sigma} & 0 \end{pmatrix}.$$

Wave functions[1]

The helicity basis is adopted for the wave functions.

i) Spinor wave functions: the normalization is given by:

$$\bar{u}(P,\lambda)\,u(P,\lambda') = 2m\delta_{\lambda\lambda'}$$

where λ and λ' are the helicity indices and $\bar{u} = u^{+}\gamma^{o}$.

The projection operator is given by:

$$2m\,\Delta(P) = \sum_{\lambda} u(P,\lambda)\bar{u}(P,\lambda) = (\not{P} + m).$$

The equation of motion is the Dirac equation

$$(\not{P} - m)\,u(P,\lambda) = 0,$$

$$\bar{u}(P,\lambda)\,(\not{P} - m) = 0.$$

ii) Vector wave functions: the normalization is such that:

$$\varepsilon_{\mu}^{*}(P,\lambda')\,\varepsilon_{\mu}(P,\lambda) = \delta_{\lambda\lambda'}$$

and the projection operator is given by:

$$\Delta_{\mu\nu}(P) = \sum_{\lambda} \varepsilon_{\mu}(P,\lambda)\;\varepsilon_{\nu}^{*}(P,\lambda) = \left(-g_{\mu\nu} + \frac{P_{\mu}P_{\nu}}{P^{2}}\right)$$

The equation of motion is written:

$$P_{\mu}\,\varepsilon_{\mu}(P,\lambda) = 0.$$

Higher spin wave functions

i) Integer spin J wave functions: for a spin J object a rank J tensor is required. It is constructed from the product of spin 1 and spin J-1 wave functions and is given by:

$$\phi_{\mu_1 \cdots \mu_J}(P,\nu) = \sum_{\lambda,\lambda'} \langle 1,J,\lambda,\lambda' | 1,J-1,J,\nu \rangle \varepsilon_{\mu_J}(P,\lambda') \, \phi_{\mu_1 \cdots \mu_{J-1}}(P,\lambda)$$

where the helicity of the spin J is bounded by $-J \leqslant \nu \leqslant J$.

It is clear that such wave functions can be constructed inductively from J spin 1 wave functions.

The equations of motion are given by:

$$(P^2-m^2)\phi_{\mu_1 \cdots \mu_J}(P,\lambda) = 0,$$

$$\phi_{\mu\mu\mu_2 \cdots \mu_J}(P,\lambda) = 0,$$

$$P_{\mu_1}\phi_{\mu_1 \cdots \mu_J}(P,\lambda) = 0,$$

and the normalization is:

$$\phi^*_{\mu_1 \cdots \mu_J}(P,\lambda)\phi_{\mu_1 \cdots \mu_J}(P,\lambda') = (-1)^J \delta_{\lambda\lambda'}$$

The projection operator is given by:

$$\Delta^J_{\mu_1 \cdots \mu_J \nu_1 \cdots \nu_J} = \sum_{\lambda} \phi_{\mu_1 \cdots \mu_J}(P,\lambda)\phi^*_{\nu_1 \cdots \nu_J}(P,\lambda)$$

ii) Half integer spin $j = J \pm \frac{1}{2}$ wave functions: the wave function is the product of a Dirac spinor and a tensor of rank J:

$$\chi_{\mu_1 \cdots \mu_J}(P,\nu) = \sum_{\lambda,\lambda'} \langle \tfrac{1}{2},J,\lambda,\lambda' \,|\, \tfrac{1}{2},J,j,\nu \rangle \phi_{\mu_1 \cdots \mu_J}(P,\lambda') u(P,\lambda)$$

The helicity of spin j obeys $-j \leqslant \nu \leqslant j$.

The Rarita-Schwinger equations[2] of motion govern the wave functions:

$$\gamma_{\mu_1} \chi_{\mu_1 \cdots \mu_J} = 0$$

$$(\not{P} - m)_{\mu_1 \cdots \mu_J} = 0.$$

The divergenceless subsidiary conditions

$$P_\mu \chi_{\mu\mu_2 \cdots \mu_J}(P) = 0$$

and the complete symmetry in the vector indices

$$g_{\mu\nu} \chi_{\mu\nu \cdots \mu_J} = 0$$

then follow.

The normalization is:

$$\bar{\chi}_{\mu_1 \cdots \mu_J}(P,\lambda') \chi_{\mu_1 \cdots \mu_J}(P,\lambda) = (-1)^{j-\frac{1}{2}} \, 2m \, \delta_{\lambda\lambda'}$$

where $\bar{\chi} = \chi^{+} \gamma^{o}$.

The projection operator is defined through:

$$2m\,\Delta^{j}_{\mu\ldots\mu_J\nu\ldots\nu_J}(P) = \sum_{\lambda} \chi_{\mu_1\ldots\mu_J}(P,\lambda)\bar{\chi}_{\nu\ldots\nu_J}(P,\lambda).$$

Note that in this formalism the wave functions for arbitrary spin can be constructed inductively from spinor and vector wave functions.

APPENDIX II

KINEMATICS AND WAVE FUNCTIONS FOR THE EVALUATION OF THE MUELLER-REGGE HELICITY AMPLITUDES

i) Kinematics:

For the evaluation of the Mueller-amplitudes we work in the centre of mass frame. The direction of particle a is taken to be along the positive z direction and the produced particle c defines the direction θ with respect to the z-axis. The reaction plane is taken to be the x-z plane after integrating over the azimuthal angles of all the particles in the M^2-cluster, X. The kinematics is shown in Fig. a, on the following page.

The momenta are denoted:

$$P_a = (E_a, 0, 0, k),$$
$$P_b = (E_b, 0, 0, -k),$$
$$P_c = (E_c, q \sin\theta, 0, q \cos\theta),$$

where k and q are, respectively, the initial and final state c.m. 3-momenta.

ii) Wave functions for the Mueller-Regge amplitudes:

a) Δ production:

We have the process $\frac{1}{2}^+(P_a) + b(P_b) \longrightarrow \frac{3}{2}^+(P_c) + X$

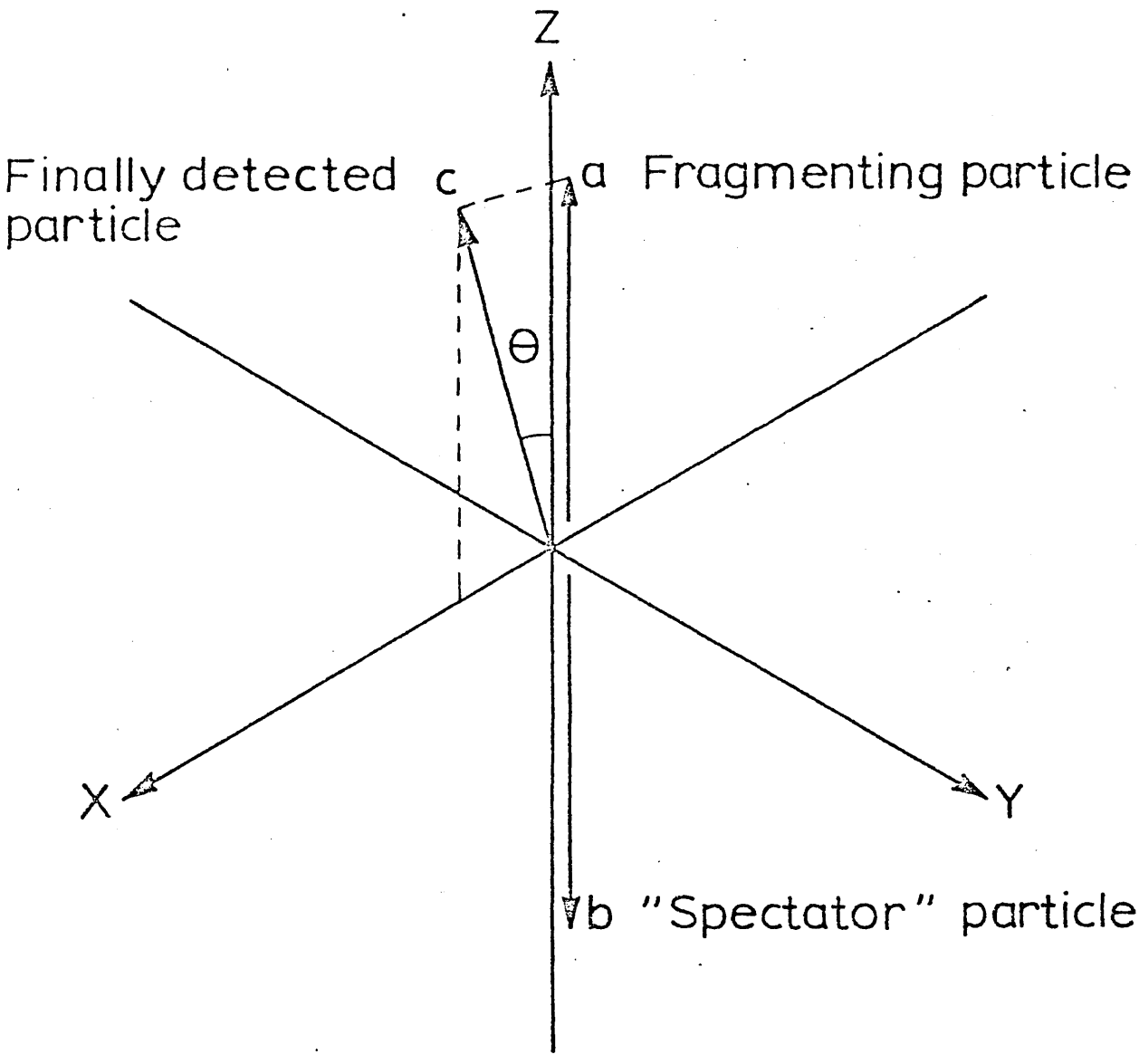

Fig. a. The kinematics for a+b ⟶ c+X in the c.m. frame.

and the relevant spin $\frac{1}{2}$ and spin $\frac{3}{2}$ wave functions are given by:

$$u(P_a,+\tfrac{1}{2}) = \frac{1}{\sqrt{E_a+m_a}}\begin{pmatrix} E_a+m_a \\ 0 \\ k \\ 0 \end{pmatrix},\quad u(P_a,-\tfrac{1}{2}) = \frac{1}{\sqrt{E_a+m_a}}\begin{pmatrix} 0 \\ E_a+m_a \\ 0 \\ -k \end{pmatrix},$$

and:

$$\chi_\mu(P_c, \pm\tfrac{3}{2}) = u(P_c, \pm\tfrac{1}{2})\,\varepsilon_\mu(P_c, \pm 1)$$

$$\chi_\mu(P_c, \pm\tfrac{1}{2}) = \frac{1}{\sqrt{3}}\left[u(P_c, \pm\tfrac{1}{2})\varepsilon_\mu(P_c, \pm 1) + \sqrt{2}\; u(P_c, \pm\tfrac{1}{2})\varepsilon_\mu(P_c, 0)\right]$$

where:

$$u(P_c, +\tfrac{1}{2}) = \frac{1}{\sqrt{E_c + m_c}} \begin{pmatrix} (E_c + m_c)\cos\theta/2 \\ (E_c + m_c)\sin\theta/2 \\ q\cos\theta/2 \\ q\sin\theta/2 \end{pmatrix},$$

$$u(P_c, -\tfrac{1}{2}) = \frac{1}{\sqrt{E_c + m_c}} \begin{pmatrix} -(E_c + m_c)\sin\theta/2 \\ (E_c + m_c)\cos\theta/2 \\ q\sin\theta/2 \\ -q\cos\theta/2 \end{pmatrix},$$

and:

$$\varepsilon_\mu(P_c, \pm 1) = \mp\frac{1}{\sqrt{2}} \begin{pmatrix} 0 \\ \cos\theta \\ \pm i \\ -\sin\theta \end{pmatrix},$$

$$\varepsilon_\mu(P_c, 0) = \frac{1}{m_c} \begin{pmatrix} q \\ E_c \sin\theta \\ 0 \\ E_c \cos\theta \end{pmatrix}.$$

b) vector meson production:

The process under consideration is $0^-(P_a) + p(P_b) \longrightarrow 1^-(P_c) + X$, and the required vector wave functions $\varepsilon_\mu(P_c, \pm 1)$ and $\varepsilon_\mu(P_c, 0)$ are given above.

c) Tensor mean production:

The reaction of interest is $0^-(P_a)+p(P_b) \longrightarrow 2^+(P_c)+X$, and the tensor wave functions are given by:

$$\phi_{\mu\nu}(P_c,\pm 2) = \varepsilon_\mu(P_c,\pm 1)\varepsilon_\nu(P_c,\pm 1),$$

$$\phi_{\mu\nu}(P_c,\pm 1) = \frac{1}{\sqrt{2}}\left[\varepsilon_\mu(P_c,\pm 1)\varepsilon_\nu(P_c,0)+\varepsilon_\mu(P_c,0)\varepsilon_\nu(P_c,\pm 1)\right]$$

$$\phi_{\mu\nu}(P_c,0) = \frac{1}{\sqrt{6}}\left[2\varepsilon_\mu(P_c,0)\varepsilon_\nu(P_c,0)+\varepsilon_\mu(P_c,-1)\varepsilon_\nu(P_c,\pm 1) + \right.$$
$$\left. + \varepsilon_\mu(P_c,+1)\varepsilon_\nu(P_c,-1)\right]$$

where the ε_μ's have been given in a).

Note that we have left the spin $\frac{3}{2}$ and spin 2 wave functions explicitly in terms of the constituent spinor and vector wave functions. In this form the evaluation of the reaction amplitudes is more straightforward, since the spinor and/or vector indices can be contracted directly with those indices of other spinor and/or vectors in the appropriate currents.

THE VECTOR STRUCTURE FUNCTIONS[3]

After squaring and averaging and summing over the helicities λ_b and $\varkappa$, the vector structure functions can be written in terms of a tensor M:

$$\sum_{\lambda_b,\varkappa} \bar{\Gamma}_{\nu}^{\lambda_b,\varkappa} \Gamma_{\nu'}^{\lambda_b,\varkappa} = \text{disc}_{M^2} M^{\nu\nu'}$$

The most general tensor compatible with gauge invariance of the vector mesons of the model is given by:

$$M^{\nu\nu'} = g^{\nu\nu'} V_1 + p_b^{\nu} p_b^{\nu'} V \quad .$$

The M function contracted with the vector wave functions for forward scattering and summed over all vector helicities is given by:

$$\text{disc}_{M^2} \sum_{\lambda} \varepsilon^{*\nu'}(Q,\lambda) M^{\nu'\nu} \varepsilon^{\nu}(Q,\lambda) = \text{Flux } \sigma_{\text{tot}}(vb)$$

through the optical theorem for vb scattering in the M^2-channel.

To evaluate the two structure functions V_1 and V in terms of invariants for vb scattering we use:

$$\sum_{\lambda} \varepsilon^{*\nu'}(Q,\lambda)\, g^{\nu\nu'}\, \varepsilon^{\nu}(Q,\lambda) = 3,$$

$$\sum_{\lambda} \varepsilon^{*\nu'}(Q,\lambda) P_b^{\nu} P_b^{\nu'} \varepsilon^{\nu}(Q,\lambda) = \sum_{\lambda} (P_b \varepsilon(Q,\lambda))^2 .$$

We work in the centre of mass system for the vb scattering where:

$$P_b = (E, -\underline{q}), \quad Q = (w, \underline{q}).$$

Then $\varepsilon(Q, \pm 1) = (0, \underline{q})$, $\varepsilon(Q,0) = (|\underline{q}|, w|\hat{\underline{q}}|)\frac{1}{m_v}$, and

and $P_b \varepsilon(Q, \pm 1) = 0$,

$$P_b \varepsilon(Q,0) = \frac{(E+w)q}{m_v} .$$

We obtain:

$$\begin{aligned} \text{disc}_{M^2} \sum_{\lambda} \varepsilon^{*\nu'}(Q,\lambda) M^{W'} \varepsilon^{\nu}(Q,\lambda) \\ = 3 \,\text{disc}_{M^2} V_1 + \frac{\Delta(M^2, m_v^2, m_b^2)}{4m_v^2} \,\text{disc}_{M^2} V \\ = 2\,\Delta^{\frac{1}{2}}(M^2, m_v^2, m_b^2)\, \sigma_{tot}(vb) \end{aligned}$$

We have made use of:

$$q = \frac{\Delta^{\frac{1}{2}}(M^2, m_v^2, m_b^2)}{2\sqrt{M^2}}$$

and the flux in the M^2 channel is simply:

$$\text{flux}(vb) = 2\,\Delta^{\frac{1}{2}}(M^2, m_v^2, m_b^2).$$

The notation V_1 and V will be taken to mean the discontinuity in M^2 of the two structure functions from here on, and in the text.

In the triple-Regge region $\sigma_{tot}(vb)$ is expected

to be independent of M^2. The upper bounds of V_1 and V can then be estimated and are given by:

$$V_1 \sim M^2,$$
$$V \sim \frac{1}{M^2}.$$

Now, in the inclusive cross section V is multiplied by an s^2 factor arising from $(P.P_b)^2$ so that effectively the terms in V behave like $\frac{s^2}{M^2}$. In contrast, the terms in V_1 behave like M^2. For our calculation we shall retain only the terms in V since in the triple-Regge and fixed M^2 regions the leading term is V.

We then have:

$$V \simeq \frac{8m_v^2}{M^2} \sigma_{tot}(vb).$$

APPENDIX IV

NORMALIZATION OF ONE PARTICLE INCLUSIVE CROSS SECTION [4]

The total inclusive cross section for $a+b \longrightarrow c+X$ can be written

$$\langle n\rangle \sigma_{tot}(ab \longrightarrow c) = \frac{1}{F}\int dM^2 \int \frac{d^3p_c}{2E_c}\frac{d^3p_x}{2E_x}\delta^4(P_a+P_b-P_c-P_x)$$

$$\cdot \sum\!\!\!\!\!\!\int |\langle c,X|A|a,b\rangle|^2 ,$$

where $\sum\!\!\!\!\!\!\int$ denotes all the summation and averaging over all the helicity states, different particle states, etc. and integration over all 3-momenta internal to the missing mass state X, and $\langle n\rangle$ is the average multiplicity of c. The differential quantity corresponding to the inclusive cross section is obtained from the above expression through the use of appropriate delta functions and is given by:

$$\langle n\rangle \frac{d^2\sigma}{dtdM^2} = \frac{1}{F}\int dM^2 \int \frac{d^3p_c}{2E_c}\frac{d^3p_x}{2E_x}\delta^4(P_a+P_b-P_c-P_x)\delta(t-(P_a-P_c)^2)$$

$$\cdot \delta(M^2-(P_a+P_b-P_c)^2)\sum\!\!\!\!\!\!\int |\langle c,X|A|a,b\rangle|^2 .$$

Evaluating this expression in the cm. frame and using the Mueller theorem we obtain:

$$\frac{s}{\pi}\frac{d^2\sigma}{dtdM^2} = \frac{1}{64\pi^2 k^2}\frac{1}{2S_a+1}\sum_{\lambda_c} H^{\lambda_c\lambda_c}$$

for the fixed-M^2 and triple-Regge regions. Note that the fixed-M^2 and triple-Regge limits correspond to the

subregion of phase space where the produced particle c is at a large rapidity gap from the rest of the produced particles (M^2-cluster). Clearly, the expectation value of n obtained from integrating the above expression over this subregion of phase space is unity, i.e. we are not likely to encounter another particle in the rapidity neighbourhood of $c^{(5)}$.

REFERENCES

1. See e.g.

   S. Gasiorowicz, Elementary Particle Physics, Wiley, New York (1966);

   P. Roman, Theory of Elementary Particles, North-Holland (1964);

   H. Pilkuhn, The Interaction of Hadrons, North-Holland (1967);

   T. Takahashi, An Introduction to Field Quantization, Pergamon Press (1969);

   V.B. Berestetskii, E.M. Lifshitz and L.P. Pitaevskii, Relativistic Quantum Theory, Pergamon Press (1971);

   I.V. Novozhilov, Introduction to Elementary Particle Theory, Pergamon Press (1975);

   R. Delbargo, Elementary Particle Symmetries, D.I.C. Lecture Notes (1972-1973).

2. W. Rarita and J. Schwinger, Phys. Rev., 60, 61 (1941).

3. K.J.M. Moriarty, J.P. Rad, J.H. Tabor and A. Ungkitchanukit, Acta Phys. Austr., 46 (1976).

4. P. Choudhoury, K.J.M. Moriarty, J.H. Tabor and A. Ungkitchanukit, A Study of Δ Production, R.H.C. Preprint (1975).

5. R.N. Cahn, Phenomenology of Inclusive Reactions, (1972 Ph.D. Thesis), LBL-1007.

TABLE I

Regge Trajectories

Trajectory	α_o	$\alpha'\|(GeV/c)^{-2}\|$
π,B	-0.013	0.665
ρ,A_2	0.470	0.905
ω,f	0.386	1.017

TABLE II

Regge Exchanges and Clebsch-Gordan Coefficients for

$0^- \overset{p}{\to} 1^-$

Reaction	Exchange	D + 2S	F
$\pi^+ \overset{p}{\to} \rho^+$	π,A_2		2
	ω	2	
$\pi^- \overset{p}{\to} \rho^-$	π,A_2		-2
	ω	2	
$\pi^- \overset{p}{\to} \rho^o$	π,A_2		2
$\pi^+ \overset{p}{\to} \rho^o$	π,A_2		-2
$\pi^+ \overset{p}{\to} \omega$	ρ,B	2	
$K^- \overset{p}{\to} K^{*o}$	π,A_2		$-\sqrt{2}$
	ρ,B	$\sqrt{2}$	
$K^+ \overset{p}{\to} K^{*o}$	π,A_2		$\sqrt{2}$
	ρ,B	$\sqrt{2}$	

TABLE III

Regge Exchanges and Clebsch-Gordan Coefficients for $0^- \overset{p}{\to} 2^+$

Reaction	Exchange	D + 2S	F
$\pi^- \overset{p}{\to} f^o$	π	2	
$\pi^+ \overset{p}{\to} f^o$	π	2	
$\pi^+ \overset{p}{\to} A_2^+$	ρ		2
	f^o	2	
$\pi^- \overset{p}{\to} A_2^-$	ρ		-2
	f^o	2	
$\pi^+ \overset{p}{\to} A_2^o$	ρ,B		2
$K^- \overset{p}{\to} K^{**-}$	π	1	
	ρ		-1
	ω		-1
	f^o	1	
$K^- \overset{p}{\to} \bar{K}^{**o}$	π	$\sqrt{2}$	
	ρ		$-\sqrt{2}$

TABLE IV

Regge Exchange and Clebsch-Gordan coefficient for $p \overset{b}{\to} \Delta^{++}$

Reaction	Exchange	G
$p \overset{b}{\to} \Delta^{++}$	π, A_2	$-\sqrt{2}$
	ρ	$-\sqrt{2}$